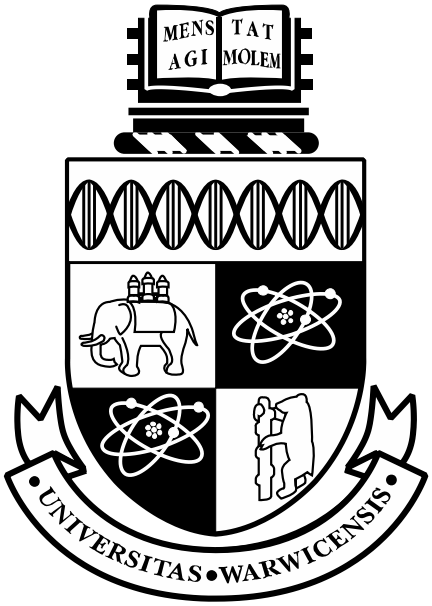

Computational Simulation of Novel Treatment Strategies for Critical Lung Disease in Adults, Children and Neonates

by

Sina Saffaran

Thesis submitted to **The University of Warwick** in fulfilment of the requirements for the degree of **Doctor of Philosophy** in Engineering

School of Engineering

April 2020

THE UNIVERSITY OF
WARWICK

Table of Contents

List of Figures

List of Tables

Acknowledgements

Firstly, I would like to pay my sincere regards to my supervisor Professor Declan Bates whose guidance, support, care and instilling skills throughout my PhD course have been completely invaluable and to whom I will always be indebted.

I owe many thanks to Dr Anup Das for all the help and support over the course of my studies. Also, I would like to express my gratitude to Prof Nadir Yehya, Prof Jonathan Hardman and Dr Don Sharkey, without whom I would not have been able to complete this research.

From the bottom of my heart, I would like to say a big thank you to my family for their love, understanding, care, encouragement and support over the last four years and all of the years previously. I would like to dedicate this thesis to my mother, Farah, who showed me the genuine meaning of unconditional love and kindness; my father, Mahdi, who is a fountain of patience and strength; and my sister, Setareh, whose love has been a source of inspiration throughout my life.

Last but not least, I would like to thank Hoda, Yashar and Yousef for all the friendship, help, kindness and support during the last years. All the gatherings, fun chats and cooking sessions we had together were really helpful and motivating. There is not much I have not shared with you along the way. We shared the same joys and sadness and grew up together. Going through this journey would be painful without you and I will be always thankful.

Declaration

This thesis is submitted to the University of Warwick in support of my application for the degree of Doctor of Philosophy. It has been composed by myself and has not been submitted in any previous application for any degree.

The work presented in this thesis was carried out by the author in collaboration with

- Prof Nadir Yehya (Children's Hospital of Philadelphia);
- and Dr Don Sharkey (University of Nottingham)

All novel modelling, computational design and analysis was carried out by the author while all patient data collection was carried out by Prof Nadir Yehya and Dr Don Sharkey.

Parts of this thesis have been published by the author. Full details of all papers arising from the work described in the thesis are given in Chapter 1, Section 1.2.

Abstract

Critical lung diseases such as acute respiratory distress syndrome (ARDS) and chronic obstructive pulmonary disease (COPD) are one of the leading causes of death worldwide. The most important component of treatment for patients with such conditions is mechanical ventilation. However, mechanical ventilation can also cause ventilator induced lung injuries (VILI). Consequently, clinicians have for many years been conducting extensive investigations using experimental studies in animal models and clinical trials in human patients in order to find safer and more effective ventilation strategies. To assist these efforts, engineering approaches such as computational modelling can also be employed to investigate and develop novel treatment strategies, with fewer ethical, practical and cost constraints than in vivo experiments.

In this thesis, a state-of-the-art computational simulator of cardio-pulmonary physiology is used to investigate novel treatments including ventilatory strategies and drug interventions for critical lung disease in adults, paediatrics and neonates. First, the impact of a novel compound on gas exchange is evaluated in virtual patients with COPD and pulmonary hypertension (PH) as a complication, considering both systemic administration of the drug and dry powder inhalation. Next, the ability to simulate paediatric subjects is incorporated into the model, and a new dataset of paediatric ARDS patients is analysed to investigate whether, and how, more lung protective ventilation could be achieved in clinical practice. Subsequently, the utility of two recently proposed measures of VILI, mechanical power (MP) and driving pressure (ΔP), as targets to derive maximally protective ventilator settings is tested on two cohorts of virtual adult and paediatric ARDS patients. Finally, initial results on the adaptation of the computational simulator to investigate neonatal pathophysiology are presented.

Abbreviations

ΔP	–	Driving Pressure
ABG	–	Arterial Blood Gases
ARDS	–	Acute Respiratory Distress Syndrome
BE	–	Base Excess
C_{CO2}	–	Carbon Dioxide Content of the Blood
C_{O2}	–	Oxygen Content of the Blood
CO	–	Cardiac Output
CO_2	–	Carbon Dioxide
COPD	–	Chronic Obstructive Pulmonary Disease
CPAP	–	Continuous Positive Airway Pressure
DC	–	Duty Cycle (Inspiratory-to-total time ratio)
DI	–	Deep Inhalation
DPI	–	Dry Powder Inhalation
DS	–	Dead Space
EL_{rs}	–	Elastance of the Respiratory System
F_{insp}	–	Inspiratory Flow into The Lung from The Ventilator
F_IO_2	–	Fraction of Oxygen in Inspired Gas
Hb	–	Haemoglobin
HCO_3	–	Bicarbonate Concentration
HPV	–	Hypoxic Pulmonary Vasoconstriction
I:E	–	Inspiratory-to-Expiratory Time Ratio
iNO	–	Inhaled Nitric Oxide
minV	–	Minute Ventilation
$minV_{alv}$	–	Alveolar Minute Ventilation
MMP	–	Modified Mechanical Power
MP	–	Mechanical Power
mPAP	–	Mean Pulmonary Artery Pressure

mPaw	–	Mean Airway Pressure
MPCWP	–	Mean Pulmonary Capillary Wedge Pressure
N_2	–	Nitrogen
O_2	–	Oxygen
OI	–	Oxygenation Index
$PaCO_2$	–	Partial Pressure of Carbon Dioxide in Arterial Blood
PaO_2	–	Partial Pressure of Oxygen in Arterial Blood
PARDS	–	Paediatric Acute Respiratory Distress Syndrome
$P_E'CO_2$	–	Partial Pressure of Carbon Dioxide at the End of Exhalation
PEEP	–	Positive End-Expiratory Pressure
PH	–	Pulmonary Hypertension
pH	–	Ph Level in Blood
PIP	–	Peak Inspiratory Pressure
P_{plat}	–	Plateau Pressure
PVR	–	Pulmonary Vascular Resistance
R_{aw}	–	Airway Resistance
RDS	–	Respiratory Distress Syndrome
RQ	–	Respiratory Quotient
RR	–	Respiratory Rate
sGC	–	Soluble Guanylate Cyclase
SO_2	–	Oxygen Saturation
TOP	–	Threshold Opening Pressure
V_{PEEP}	–	Volume of Gas in the Lung due to PEEP
V/Q	–	Ventilation-Perfusion Ratio
V_D	–	Volume of Anatomical Dead Space
V_{frc}	–	Volume of Functional Residual Capacity
VILI	–	Ventilator Induced Lung Injury
VO_2	–	Oxygen Consumption
V_T	–	Tidal Volume
ZEEP	–	Zero End-Expiratory Pressure

Chapter 1:

Introduction

1.1. Thesis outline and main contributions

Computational simulation offers a new approach to traditional medical research that is particularly well suited to investigating treatment of critical illness. Critically ill patients are routinely monitored in great detail, providing extensive, high quality data-streams for model design & configuration and patient-matching. Models based on these datasets can incorporate very complex representations of cardiorespiratory pathophysiology that may be validated against responses of individual patients, for use as investigational surrogates. This thesis develops a number of such models and uses them to perform "virtual" clinical trials of novel treatment strategies in a number of different clinical scenarios.

Chapter 2 consists of an introduction to respiratory system modelling and presents the key concepts and background material used in this thesis. The important role of mechanical ventilation in managing critically ill patients in the intensive care unit is discussed. Previous models of the respiratory system are reviewed and the computational simulation platform that forms the basis for the studies conducted in this thesis is described.

In Chapter 3, the efficacy of a modulator of soluble guanylate cyclase (sGC) in COPD patients with pulmonary hypertension (PH) is investigated by using computer simulation. In this study, close matching of the simulator to data from a clinical trial on three COPD patients was demonstrated. The study showed that administering an sGC via dry powder inhalation can reduce PH without deteriorating oxygenation, particularly when administration is combined with exercise.

In Chapter 4, computational modelling is used to analyse an extensive new database on paediatric acute respiratory distress syndrome (PARDS) patients collected by medical collaborators at The Children's Hospital of Philadelphia. The results of this study suggest that these patients may be being routinely over-ventilated (i.e. excessive ventilation (low CO_2) which may not be necessarily injurious, however, it increases the risk of ventilator induced lung injury (VILI)), and that there is scope for achieving more protective ventilation without compromising safe gas exchange. The results suggest that interventions based on (a) progressively lowering tidal volume (V_T) while maintaining constant minute ventilation, and (b) adjusting positive end-expiratory pressure (PEEP) and V_T to reduce driving pressure (ΔP), can produce significant reductions in multiple key parameters associated with ventilator induced lung injury (VILI) without compromising safety.

In Chapter 5, computational modelling is used to identify novel ventilatory strategies that minimize driving pressure, mechanical power (MP), and modified mechanical power (MMP) in clinical datasets from adults and children with acute respiratory distress syndrome (ARDS). The identified strategies were consistent within each patient group, and were similar in both adults and children, suggesting that protective ventilatory strategies derived from studies in adults may have utility in children with ARDS. This analysis also revealed potential problems with some currently proposed measures of VILI, at least in terms of their use as direct targets for optimizing ventilator settings.

In Chapter 6, the development of the first detailed computational simulator of neonatal respiratory physiology in the ARDS disease state is presented. Results of matching the model to new patient data collected by medical collaborators at the Queen's Medical

Centre in Nottingham indicate that the responses of individual neonatal patients to a range of different ventilator settings are accurately reproduced by the model, confirming its potential usefulness for investigating new therapeutic strategies.

Chapter 7 summarises the main findings from the work conducted in this thesis and suggests additional work that could be performed to further develop the models and exploit them in future studies of novel treatment strategies for acute respiratory illness.

1.2. Publications arising from this research

The work contained in this thesis has been published in the following peer-reviewed research papers:

1. Saffaran S, Das A, Hardman JG, Yehya N and Bates D (2017) "Development and validation of a computational simulator for pediatric acute respiratory distress syndrome patients", in the *Proceedings of 39th Annual International Conference of the IEEE Engineering in Medicine and Biology Society (EMBC)*, Jeju Island, South Korea.
2. Saffaran S, Wang W, Das A, Schmitt W, Becker-Pelster E, Hardman JG, Weimann G and Bates D (2018) "Inhaled sGC modulator can lower PH in patients with COPD without deteriorating oxygenation." *CPT Pharmacometrics and Systems Pharmacology* 2018; 7:491–498.
3. Saffaran S, Das A, Hardman JG, Yehya N and Bates D (2019) "High-fidelity computational simulation to refine strategies for lung-protective ventilation in paediatric acute respiratory distress syndrome." *Intensive Care Medicine* 2019; 1:10–12.
4. Saffaran S, Das A, Algarni S, Laviola M, Niklas C, Hardman JG, Sharkey D and Bates D (2019) "Computational simulation of mechanically ventilated neonatal patients in the intensive care unit" in the *Proceedings of 41st Annual International Conference of the IEEE Engineering in Medicine and Biology Society (EMBC)*, Berlin, Germany.
5. Saffaran S, Das A, Laffey JG, Hardman JG, Yehya N and Bates D (2020) "Utility of driving pressure and mechanical power to guide protective ventilator settings in two cohorts of adult and pediatric patients with acute respiratory distress syndrome." *Critical Care Medicine 2020*; doi: 10.1097/CCM.0000000000004372.

Chapter 2:

Background

2.1. Pulmonary physiology

The human pulmonary system comprises all organs and structures within the body that play a significant role in the process of respiration i.e. the exchange of oxygen (O_2) and carbon dioxide (CO_2) with the environment in order to facilitate the production of energy. Lungs are surrounded by respiratory muscles which assist airflow into and out of the body and the pulmonary artery, vein and capillary network which transports blood to and from the lungs to allow for gas exchange between blood and air. Lung volumes and capacities describe how much air normally fills the lungs. Lung volumes fluctuate during the breathing cycle, as the alveoli expand and contract. There are various terms that are used to characterize the lung volumes and capacities in different points in the breathing cycle. Some of the most common lung volume terms are:

- Total Lung Capacity (TLC) – The volume of air in the lungs upon the maximum effort of inspiration;
- Residual Volume (RV) – The volume remaining in the lungs after maximal exhalation;
- Tidal Volume (V_T) – The amount of air a person inhales during a normal breath;

- Functional Residual Capacity (FRC) – The volume remaining in the lungs following normal expiration.

Respiration begins at the nose or mouth, where oxygenated air is brought in. The trachea is the starting point to transfer the gas. It is the largest of all the airways and at its distal end branches into two bronchi leading to the left and right lung. Each bronchus progressively branches into shorter, narrower airways called bronchioles.

Bronchioles subsequently branch into elastic cavities called alveoli. The lungs consist of approximately 300 million alveoli, where different gasses are transferred into and out of the bloodstream. The factors that determine the gas flow to and from the alveolar units are the airway resistances and the pressure gradient between the mouth and the lungs. Each alveolus has a thin surface surrounded by a network of capillaries. From this point, O_2 is diffused to the blood and CO_2 is diffused to the alveolar units. Inhaling oxygenated gas provides higher partial pressure of oxygen (PO_2) inside alveolar compartments than in the corresponding capillaries. This pressure gradient moves O_2 across the alveolar membrane into the blood. The same process happens for CO_2 in the opposite direction since the partial pressure of carbon dioxide (PCO_2) is higher in the capillaries than alveoli. The diffusion of gasses continues until the partial pressures in both environments are in equilibrium. The rate of diffusion is different for different types of gas due to their individual properties. The pulmonary capillaries with oxygenated blood mix into the pulmonary vein and consequently converge to the heart where oxygenated blood is pumped into systemic circulation.

Due to higher solubility of CO_2, blood carries it in dissolved form while only a relatively small portion of the total blood oxygen content is dissolved (reduced solubility of O_2). Consequently, O_2 is mostly carried in the blood as oxyhaemoglobin which is formed by the combination of haemoglobin with oxygen. As CO_2 is more soluble and more chemically reactive, it is present in a higher quantity in blood. Moreover, the dissolved CO_2 reacts with water to form H_2CO_3 which accordingly can be dissociated to H^+ and bicarbonate (HCO_3), this reaction is reversible. This makes CO_2 a major regulatory factor for controlling pH in the blood. An elevated level of CO_2 in the blood leads to higher

amounts of H^+ ions which subsequently makes the blood more acidic (reducing the pH). Raised amounts of HCO_3^- cause a reduction in the available H^+ ions, which increases pH (making the blood more alkaline). The kidneys also play a role in regulating and maintaining the pH balance in the human body by absorbing HCO_3^- and producing H^+ ions.

Information regarding the distribution of gas exchange in the lung can provide substantial insight regarding any underlying pathology. Adequate ventilation in the presence of sufficient perfusion results in efficient gas exchange. This matched occurrence of ventilation and perfusion can be represented by the V/Q (ventilation/perfusion) distribution. A V/Q ratio of 1 denotes that the ventilation and perfusion are matched whereas values higher than 1 indicate areas of the lung with good ventilation but poor perfusion, and values less than 1 indicate areas with low ventilation but adequate perfusion. Extreme cases are where there is ventilation with no perfused blood (dead space); and where there is perfusion but no ventilation (shunt). Important information about the state of the lungs can thus be extracted from the levels of V/Q mismatch. However, the involved time-varying parameters such as cardiac output and minute ventilation complicate accurate measurement of the V/Q imbalance.

2.2. Mechanical ventilation

Since the appearance of the very first satisfactory mechanical ventilator in 1929 (i.e. the "Iron Lung" [1]), mechanical ventilation has been one of the most frequent life support therapeutic intervention for critically ill patients. It is also the most important therapeutic intervention for patients with respiratory failure in intensive care units (ICU's) [2, 3].

A number of different studies have indicated that mechanical ventilation along with suitable ventilator settings and interventions (i.e. protective ventilation) can reduce length of ICU stay, mortality, and associated healthcare costs in patients with acute lung injury (ALI) and acute respiratory distress syndrome (ARDS) [2, 4–7]. However, clinicians administering mechanical ventilation encounter many challenges in determining the safest and most effective ventilator management strategy due both to a

lack of comprehensive guidelines and the fact that the settings for each patient should ideally be set based on their individual characteristics and disease state [3, 8]. State-of-the-art advanced mechanical ventilators can aid clinicians in this task by providing decision support capabilities and taking advantage of automatic feedback to adjust mechanical ventilator settings based on patient data [9, 10]. It should be noted, however, that these systems rely solely on measured patient outputs and consider predefined ranges of mechanical ventilator settings, and not the individual patient physiology and underlying disease [9, 10]. Currently, clinicians in the ICU aim to keep the patient within a respiratory comfort region while maintaining adequate oxygenation based on general available guidelines [11, 12]. Also, the physicians' personal experience often plays an important role in choosing the best set of ventilator settings [13].

Inappropriate ventilation strategies could result in potentially unsafe treatment and cause ventilator-induced lung injuries (VILI). The concept of VILI was first introduced by Mead et al. in 1970 [14]. The term VILI refers to the lung injury arising due to exposure to injurious ventilation contributions such as high airway pressures resulting in barotrauma, over-distension of alveoli, repeated alveolar collapse and expansion (atelectotrauma) and localised injury and inflammation due to intubation. These high pressures and volumes adversely impact the operation of the respiratory system. As a result, in spite of its important life-saving role in intensive therapy unit, mechanical ventilation can potentially cause prolonged ICU stay, a range of lifelong lung injuries and even multiple organ failure and death [13, 15, 16]. A study on a total of 5183 mechanically ventilated patients by Anzueto et al. [17] revealed that VILI was diagnosed in 154 patients (2.9%). Furthermore, another study by Tejerina et al. [18] showed a higher rate of incidence (15%) in a larger cohort (2897 patients). Considering the sizeable number of patients undergoing mechanical ventilation (e.g. more than 69k patients in the UK in 2012 according to the Case Mix Programme), thousands of patients are potentially suffering from VILI each year.

Therefore, the main challenge when mechanically ventilating critically ill patients can be summarised as maintaining adequate gas exchange whilst avoiding VILI [19, 20]. Over recent years, numerous clinical trials have been conducted aimed at exploring

mechanical ventilation strategies that could reduce the risk of VILI. Different approaches including the use of low tidal volumes, high PEEP, high-frequency oscillatory ventilation, etc. have been investigated to reduce the risk of lung injury for mechanically ventilated patients [4, 6, 14, 20–24]. However, although considerable progress has been made, there is still significant uncertainty about which strategy will minimize VILI for any given clinical scenario, and the mortality rate for ARDS and ALI patients receiving mechanical ventilation remains high (30-40%) [14, 25]. Further improvements in minimising VILI could potentially be achieved by incorporating tailored strategies based on an individual patient's pathophysiology. However, many challenges such as the lack of accurate comprehensive patient data at the bedside and the complexity of the underlying pathophysiology hinder clinicians from considering individual patient information when making decisions for ventilator management [14, 25–29].

2.3. Previous models of the pulmonary system

Engineering approaches such as computational modelling can be employed in order to create an easier route to development of bespoke treatments, with fewer constraints than in vivo experiments. The real-life processes can be reproduced and better understood by means of modelling. It also can be engaged in testing and evaluating hypotheses [30]. However, the enormous requirements made on the capability of the models designed to be used in clinical environments has raised high-maintenance expectations on validation of such models with safety-critical applications. Consequently, the models need to be validated by means of promising methods to guarantee the essential robustness and earn the required reliability, stability and credibility in this field. [31–33].

Formulating the theoretical principles of the respiratory system such as relationships in gas exchange and ventilation paved the way for the mathematical and computational modelling. The efforts began by studies of acidosis as well as the equilibrium between oxygen and carbonic acid in the blood [34–36]. The work continued in this area resulting in a deeper theoretical understanding of the underlying physiology and

introducing different relations and equations such as Henderson-Hasselbalch equation, Van Slyke equation, etc. which are the cornerstone of the present-day studies of pulmonary physiology [37–45].

Computational modelling of respiratory system has been involved in different studies over the past years, improving the research outcome in the field [46–52]. It was not until the middle of the twentieth century that the advances in engineering methodologies along with the developed mathematics of respiration resulted in the development of the first simple models of the respiratory system. The model established by Grodins and colleagues [53, 54] uses differential equation to illustrate the relationship among a single-compartmental lung with constant volume, blood and tissue. The model describes the effect on O_2-CO_2 interaction by the chemoreceptors, chemical buffering etc. In spite of its simplicity and deficiencies such as missing dead space (DS), this model has been the base of many other works [55–58].

Multi-compartmental models are able to describe the respiratory system in more details. A detailed model is more effective when studying features such as compliance, resistance, ventilation-perfusion distribution and delivery of gas across the whole lung. It also offers the ability to consider inhomogeneity in the lung. Accordingly, many studies in the literature have taken advantage of this feature in their models. In such a model by Hinds [59, 60], ventilation/perfusion distribution and variations of volume and pressure within the lung were illustrated. The effect of series dead space and its role in ventilation is explored by another work by Petrini [61].

Likewise, the combined effect of recruitment and de-recruitment was studied in a model with 27k parallel alveolar units which shed light on the pressure-volume relationship of these alveolar compartments [62]. The effects of ventilation-perfusion inequality on the lung, gas exchange and pulmonary ventilation were analysed using a model by JB West [63]. Moreover, this study also examined the efficiency of the model under a different number of alveolar compartments and proposed that, in a multi compartmental model, a minimum of 100 compartments are essential to provide the optimal trade-off between accuracy and computational complexity. However, this model does not take into

consideration the individual alveolar compliances, inflow resistances and vascular resistances.

In another work by Dickinson [64], a model called "MacPuf" was developed. This cardiorespiratory simulator takes into account the ventilation control, pulmonary circulation, gas exchange and tissue metabolism. Each stage of modelling has been carefully designed, considering critical aspects like dissociation curves for O_2 and CO_2, shunt, dead space etc. Furthermore, the model can represent mechanical ventilation with PEEP.

On the other hand, there are many studies utilising single or two-compartmental models. These models offer less computational complexity while providing better insight into poorly understood physiological behaviour. In a study, Swanson and colleagues [65] propose a two-compartmental model to investigate alveolar gas exchange under exercise. Other examples of studies using single/two-compartmental models of the respiratory system include Hotchkiss et al. [66], Vidal Melo et al. [67, 68], Joyce et al. [69], Farmery et al. [70] and Liu et al. [71]. Yet, single/two-compartmental respiratory models do not deliver enough accuracy for simulating lung injury under pathological conditions and modelling treatments. They are also incompetent when it comes to representing ventilation/perfusion distribution, tidal breathing, series or parallel resistances etc.

"VentSim" is a respiratory model introduced by Rutledge [72], which is an expanded version of his previous work "VenPlan" [18]. The three chief model components, comprising ventilator component, an airway component and a circulation component, have been wisely embedded into the model by dint of linked first-order differential equations. Yet, the simulator has not been validated with actual ventilated patients' data. "VO2.htm" is an interactive computer simulation of pulmonary gas exchange by Kapitan [73] that is web based and indicates the final effect on the arterial blood gas composition caused by simultaneous change in multiple factors. For more details on the literature of respiratory system modelling over the past years the reader is referred to [74, 75].

2.4. A high-fidelity computational simulator of integrated cardiorespiratory pathophysiology

The simulator used as the basis for the studies described in this thesis is a multi-compartmental computational model that uses an iterative technique to simulate integrated respiratory and cardiovascular pathophysiological scenarios. The simulator has been developed over the past several years and has been applied and validated on a number of previous studies [76–84].

In contrast to previous models of pulmonary pathophysiology that included only two or three alveolar compartments, this model allows the user to define up to several hundred individual compartments (each with its own individual mechanical characteristics) to be implemented in the simulation. An alveolar compartment in the model represents a cluster of alveoli in the lungs (different lung segments) rather than one alveolus, so that the total number of compartments comprises the whole lung. Each of these alveolar compartments has a unique and configurable bronchiolar resistance, pulmonary vascular resistance, stiffness index, and extrinsic pressure. The ability to adjust these parameters individually across all alveolar compartments allows the model to recreate the heterogeneous effects of disease, e.g. COPD, on the overall physiology of the lung.

The model also includes specific equations to represent the effects of alveolar collapse, threshold opening pressure, alveolar stiffening, and airway obstruction. The net effect of these components of the simulation is that defining, clinical features of acute lung injury may be observed in the model, e.g. alveolar gas trapping, collapse-reopening of alveoli, pulmonary oedema, etc. However, the model does not currently consider the spatial arrangement of different lung regions (i.e. from the top to the bottom of the lung) and its effect on V/Q mismatch.

Moreover, the model includes representations of multiple interacting organ systems (cardio-pulmonary-vascular) and incorporates an unprecedented level of physiological detail including multiple alveolar compartments, multi-compartmental gas-exchange, viscoelastic compliance behaviour, interdependent blood-gas solubility and haemoglobin behaviour and heterogeneous distributions of pulmonary ventilation and perfusion.

Each model component is described as several mass conserving functions and solved as algebraic equations, obtained or approximated from the published literature, experimental data and clinical observations. These equations are solved in series in an iterative manner, so that solving one equation at the current time instant determines the values of the independent variables in the next equation. At the end of the iteration, the results of the solution of the final equations determine the independent variables of the first equation for the next iteration.

The pulmonary model consists of the mechanical ventilation equipment, anatomical and alveolar dead space, anatomical and alveolar shunts, ventilated alveolar compartments and corresponding perfused capillary compartments. The model simulates all relevant aspects of pulmonary dynamics and gas exchange such as the transport of air from mouth to airway and alveoli, the gas exchange between alveoli and their corresponding capillaries, and the gas exchange between blood and peripheral tissue compartment. The pressure differential created by the mechanical ventilator drives the flow of gas through the system. The model includes series dead space to represent the trachea, bronchi and the bronchioles. The volume of dead space is split into 50 stacked layers of equal volumes. No mixing between the compartments of the series dead space is assumed. The lung model incorporates up to several hundred independently configurable alveolar compartments, implemented in parallel, allow the model to accurately simulate alveolar shunt and alveolar dead space.

Figure 1 shows a simplified, diagrammatic representation of the model. The inhaled air is initially assumed to consist of five gases: oxygen, nitrogen, carbon dioxide, water vapour and a 5th gas (α) used to model additives. The atmospheric pressure is fixed at 101.3kPa and body temperature is fixed at 37.2°C. During an iteration of the model, the flow (f) of air to or from i^{th} alveolar compartment is determined by the following equation:

$$f_i = \frac{(\mathrm{P_v} - \mathrm{P}_i)}{(\mathrm{R_u} + \mathrm{R}_{\mathrm{A},i})} \qquad \text{for } i = 1, \ldots, \mathrm{N_A} \tag{1}$$

where P_v and P_i are the pressure supplied by the mechanical ventilator and the pressure in the i^{th} alveolar compartment respectively. R_u represents the constant upper airway resistance and $R_{A,i}$ is the bronchial inlet resistances of the alveolar compartment i. N_A is the total number of alveolar compartments (for the studies in this thesis, N_A=100). The rationale for choosing 100 compartments in this case is based on both a study on COPD patients employing the same simulator which found 100 alveolar compartments as the optimal trade-off between model accuracy and complexity, and another study in the literature which evaluated the efficiency of a multi compartmental model under a different number of alveolar compartments [63].

The total flow of air entering the series dead space is the sum of all flows to/from the alveoli. The volume of gas "x" in the i^{th} alveolar compartment ($v_{i,x}$), is updated as follows:

$$v_{i,x} = \begin{cases} v_{i,x} - f_i \cdot \dfrac{v_{i,x}}{v_i} & \text{Exhaling} \\ v_{i,x} + f_i \cdot F_{N_{SD}} & \text{Inhaling} \end{cases} \quad (2)$$

where x is any of the five gases and v_i is the total volume of the i^{th} alveolar compartment (sum of the volume of the five gases in the compartment.) $F_{N_{DS}}$ is the fraction of gas in the last layer of the dead space.

Hypoxic Pulmonary Vasoconstriction (HPV) is the intrinsic reaction of the respiratory system to low levels of oxygen in blood. This mechanism restricts the blood flow in the pulmonary blood vessels where there is not enough oxygen. This is modelled as a simple function, resembling the stimulus response curve suggested by [85], and is incorporated into the simulator to gradually constrict the blood vessels as a response to low alveolar oxygen tension.

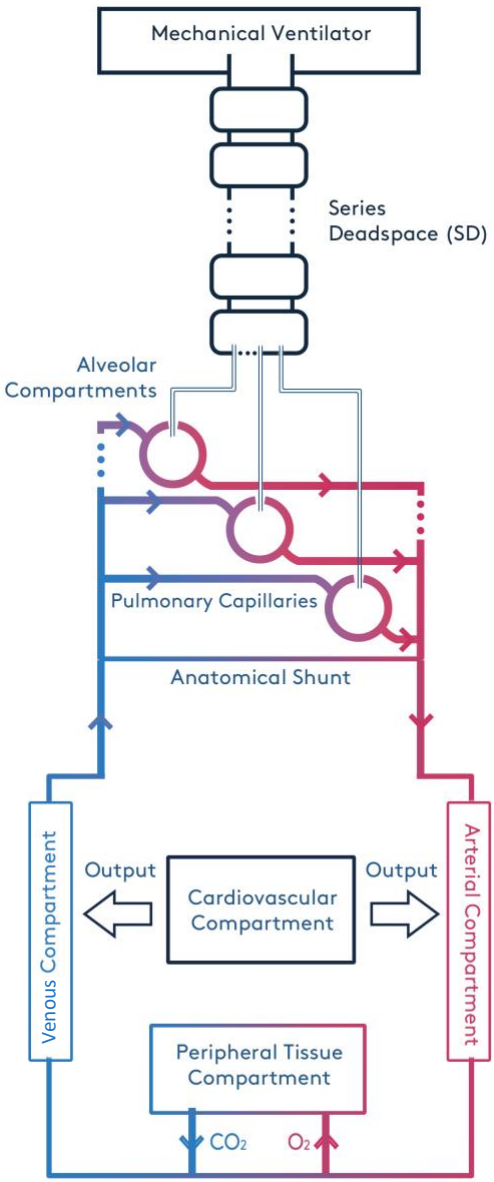

Figure 1. Diagrammatic representation of the model and its main features.

To model the equilibration process between the alveolar compartment and the corresponding capillary compartment, small volumes of each gas (O_2 and CO_2) is moved between the compartments until there are identical partial pressures of these gases in both compartments (i.e. they differ by <1%). In blood, the total O_2 content (C_{O2}) is carried in two forms, as a solution and as oxyhaemoglobin (saturated haemoglobin):

$$C_{O2} = S_{O2} \cdot \mathrm{Huf} \cdot \mathrm{Hb} + PO_2 \cdot O_{2_{sol}} \tag{3}$$

In this equation, S_{O2} is the haemoglobin saturation, Huf is the Hufner constant, Hb is the haemoglobin content and $O_{2_{sol}}$ is the O_2 solubility constant. In order to describe the O_2 dissociation curve, the following pressure-saturation relation is used in the model, as proposed in [45]:

$$S_{O2} = \left(\left(\left(PO_2{}^3 + 150 \cdot PO_2\right)^{-1} \times 23400\right) + 1\right)^{-1} \tag{4}$$

PO_2 is the partial pressure of oxygen in the blood. In view of the appropriate correction factors in base excess (BE), temperature (T) and pH [44], PO_2 is calculated as:

$$PO_2 = 7.5006168 \cdot PO_2 \cdot 10^{[0.48(\mathrm{pH}-7.4)-0.024(\mathrm{T}-37)-0.0013\cdot \mathrm{BE}]} \tag{5}$$

pH is the blood pH level and the constant '7.5005168' is the pressure conversion factor from kPa to torr.

Using the Henderson-Hasselbach logarithmic equation, the plasma CO_2 content can be calculated (Eq.6). Next, the CO_2 content of the blood (C_{CO2}) is deduced from Eq.7, [41].

$$C_{CO2plasma} = 2.226 \cdot CO_{2_{sol}} \cdot P_{CO2} \cdot \left(1 + 10^{(\mathrm{pH}-\mathrm{pK}')}\right) \tag{6}$$

$$C_{CO2} = C_{CO2plasma} \cdot \left[1 - \frac{0.0289 \cdot \mathrm{Hb}}{(3.352 - 0.456 \cdot S_{O2}) \cdot (8.142 - \mathrm{pH})}\right] \tag{7}$$

where $CO_{2_{sol}}$ is the plasma CO_2 solubility coefficient, pK' is the apparent pK, PCO_2 is the partial pressure of CO_2 in plasma, and '2.226' is the conversion factor from miliMoles·L^{-1} to mL·100mL^{-1}. Values for $CO_{2_{sol}}$ and pK' can be deduced from, [86]:

$$CO_{2_{sol}} = 0.0307 + 0.0057 \cdot (37 - T) + 0.00002 \cdot (37 - T)^2 \quad (8)$$

$$pK' = 6.086 + 0.042(7.4 - pH) + (38 - T)\left(0.00472 + \left(0.00139 - (7.4 - pH)\right)\right) \quad (9)$$

PCO_2 is consequently determined by incorporating the standard Henry's law and $CO_{2_{sol}}$. For pH, the Henderson-Hasselbach and the Van Slyke equations [87] are combined, resulting in the following equation:

$$pH = 6.1 + \log\left(\frac{HCO_3}{0.225 \cdot P_{CO2}}\right) \quad (10)$$

and bicarbonate concentration (HCO_3) can then be calculated by, [87]:

$$HCO_3 = \left((2.3 \times Hb + 7.7) \times (pH - 7.4)\right) + \frac{BE}{(1 - 0.023 \times Hb)} + 24.4 \quad (11)$$

In order to update the arterial blood gas "x" content, the non-shunted blood from pulmonary capillaries ($C_{cap,x}$) as well as the anatomical shunt (Sh) are mixed with arterial blood using the equation below:

$$C_{a,x} = \frac{CO \cdot \left(Sh \cdot C_{v,x} + (1 - Sh) \cdot C_{cap,x}\right) + C_{a,x} \cdot (v_a - CO)}{v_a} \quad (12)$$

In the above, CO is cardiac output and v_a is the arterial volume. The shunt fraction (Q_S/Q_T) in the model is calculated as:

$$Q_S/Q_T = \frac{C_{cap,O2} - C_{a,O2}}{C_{cap,O2} - C_{v,O2}} \quad (13)$$

In the simulator, the peripheral tissue is incorporated as a single compartment. Similar to alveolar equilibration, the peripheral capillary and tissue equilibrium is modelled by

removing the consumed O_2 (VO_2) from blood and adding the produced CO_2 (VCO_2). Metabolic production of acids, other than carbonic acid via CO_2 production, is not modelled. After peripheral tissue equilibration of gases, the venous calculations of partial pressures, concentrations and pH calculations are performed using comparable equations to those above.

The total compliance ($\mathrm{E_{dyn}}$) of the lung in the model is calculated using the standard equation:

$$\mathrm{E_{dyn}} = \frac{\mathrm{V_{max}} - \mathrm{V_{min}}}{\mathrm{P_{max}} - \mathrm{P_{min}}} \tag{14}$$

where the end-inspiratory lung volume ($\mathrm{V_{max}}$), end-expiratory lung volume ($\mathrm{V_{min}}$), maximum pressure in lung ($\mathrm{P_{max}}$) and the minimum pressure in lung ($\mathrm{P_{min}}$) are obtained directly from the model at the end of every breath. The simulated patient is assumed to be under complete mechanical ventilation. Consequently, the effects of ventilatory autoregulation by the patient are not currently incorporated into the models.

For the i^{th} alveolar compartment, the pressure of the compartment (P_i) is determined by:

$$\mathrm{P}_i = \mathrm{S}_i(\mathrm{V}_i - \mathrm{V_c})^2 - \mathrm{P_{ext},}_i \tag{15}$$

where

$$\mathrm{S}_i = \frac{10^{\mathrm{k}_i} \cdot {\mathrm{N_A}}^2}{200000} \tag{16}$$

$$\mathrm{V_c} = \frac{0.2\mathrm{V_{FRC}}}{\mathrm{N_A}} \tag{17}$$

V_i is the given volume of alveolar compartment in millilitres. $\mathrm{V_c}$ is defined as a "collapsing volume" at which the alveolus tends to empty. The parameter $\mathrm{P_{ext}}$ is an extrinsic pressure which is representative of the net pressure generated outside each alveolus, such as the outward pull of the chest wall (positive component indicating

distend) and the compressive effect of interstitial fluid in the alveolar wall (a negative component indicates compression from outside the alveolus tending to cause collapse). S_i is a scalar that determines the alveolar compliance. A higher S_i suggests a stiffer compartmental behaviour, which requires a larger pressure from the mechanical ventilator to drive air into the compartment. The unit of S_i is "$cmH_2O\ mL^{-2}$". All of the abovementioned parameters ($P_{ext,i}$, S_i and V_c) are different yet essential components for representing a diseased lung.

The alveolar compartments in the model are placed in a parallel arrangement and interact with the series dead space with respect to the movement of gases. The total airway resistance R_{aw} is determined by the following equation for N_A parallel compartments:

$$\frac{1}{R_{aw}} = \frac{1}{R_{B,1}} + \frac{1}{R_{B,2}} + \cdots + \frac{1}{R_{B,N_A}} \tag{18}$$

where $R_{B,i}$ is the bronchial inlet resistance of the i^{th} compartment given as:

$$R_{B,i} = m_i \cdot R_{B0} \tag{19}$$

and R_{B0} corresponds to the default bronchial inlet resistance of an alveolar compartment. R_{B0} is set to $10^{-5} \cdot N_A$ kpa ml^{-1} min^{-1} (6 $cmH_2O\ L^{-1}\ s^{-1}$) for adults; the inlet resistance is higher for a model with more compartments as the volume of each compartment decreases; giving, for example, a resistance of 0.001 kpa ml^{-1} min^{-1} in each compartment for 100 compartments. m_i is a coefficient representing a dynamic change in airway resistance and is determined by the following equation:

$$m_i = \begin{cases} 1 & P_{trachea} \geq TOP_i \\ 10^5 & P_{trachea} < TOP_i \end{cases} \tag{20}$$

where $P_{trachea}$ is the pressure in the trachea and TOP_i is defined as the threshold opening pressure of the i^{th} alveolar compartment with a value between 5 and 60 cmH_2O [88]. TOP_i indicates a pressure that a collapsed alveolar unit must attain to

reopen. Moreover, in order to model recruitment as a time dependant process where different airways recruit at different times, the condition $P_{trachea} \geq TOP_i$ has to stay satisfied for a specific period of time ($\tau_{c,i}$) for a compartment to be recruited. Otherwise, m_i is set to 10^5 again.

Finally, the pulmonary vascular resistance (PVR) is determined by:

$$\frac{1}{PVR} = \frac{1}{R_{V,1}} + \frac{1}{R_{V,2}} + \cdots + \frac{1}{R_{V,N_A}} \tag{21}$$

where the resistance for each compartment $R_{V,i}$ is defined as:

$$R_{V,i} = \delta_{Vi} R_{V0} \tag{22}$$

R_{V0} is the default vascular resistance for the compartment with a value of $160 \cdot N_A$ dynes s cm^{-5} min^{-1} for adults, and δ_{Vi} is a coefficient that can be used in order to modify the vascular resistance.

Chapter 3:

Investigating different administration mechanisms for a novel compound to lower pulmonary hypertension in COPD

3.1. Summary

In this chapter, a highly fidelity computational simulator of pulmonary physiology is employed to evaluate the impact of a soluble guanylate cyclase (sGC) modulator on gas exchange in patients with chronic obstructive pulmonary disease (COPD) and pulmonary hypertension (PH) as a complication. Three virtual COPD patients were configured in the simulator based on clinical data. In agreement with previous clinical studies, modelling systemic application of a sGC modulator results in reduced partial pressure of oxygen (PaO_2) and increased partial pressure of carbon dioxide ($PaCO_2$) in arterial blood, if a drug-induced reduction of pulmonary vascular resistance (PVR) equal to that observed experimentally is assumed. In contrast, for administration via dry powder inhalation (DPI), the performed simulations suggest that the treatment results in no deterioration in oxygenation. For patients under exercise, DPI administration lowers PH while oxygenation is improved with respect to the baseline values.

3.2. Introduction

Chronic obstructive pulmonary disease is one of the leading causes of morbidity and mortality in most countries [89, 90]. The World Health Organization (WHO) estimates that COPD was the fifth leading cause of death in high-income countries in 2002, and it was the sixth leading cause of death in nations of low and middle income [91]. Moreover, according to WHO, COPD is predicted to become the third leading cause of death in 2030 [92]. COPD has been identified as a major global health burden based on its high prevalence and significant health-care costs [93, 94].

A serious complication of COPD is pulmonary hypertension (PH), a progressive and debilitating condition associated with a sustained increase in mean pulmonary artery pressure (mPAP) that results from excessive vasoconstriction and remodelling of the pulmonary arteries [95]. It is associated with shorter survival and has been seen as a predictive factor for worse clinical outcomes and frequent use of health resources [96, 97]. Accordingly, there has been significant interest in exploring PH-specific therapies in patients with COPD. Various vasodilating drugs with different modes of action have been investigated in clinical studies [98]. Most of these studies considered systemic applications (oral administration), although some also considered administration via inhalation. Generally, these studies aimed for a dilation or relaxation of the pulmonary arterial vessels, thus lowering pulmonary vascular resistance. On the other hand, unselective vasodilation of pulmonary vessels may also lead to a relief of hypoxic vasoconstriction in low-/non-ventilating areas of the lung, and consequently to increased ventilation-perfusion (V/Q) mismatch and a deterioration of oxygenation.

One of the most extensively investigated drugs in COPD-PH is the phosphodiesterase-5 (PDE-5) inhibitor Sildenafil (Pfizer) [99–104]. When given systemically, i.e. oral or intravenous administration, in acute studies Sildenafil (Pfizer) consistently resulted in a reduction of mPAP and an improvement of exercise capacity and six-minute walking distance [101, 102, 104]. While during exercise there seems to be no adverse reaction, at rest the hemodynamic changes occurred at the expense of worsening gas exchange due to increased V/Q mismatching [101]. In chronic studies no clear positive effect of the

treatment with Sildenafil (Pfizer) as compared to placebo could be observed, with positive [100] as well as negative outcomes being reported [99, 103].

Trials have also been undertaken with Bosentan (Actelion), an oral endothelin receptor antagonist, in treating PH in COPD. Stolz et al. found in severe COPD patients that those treated with Bosentan (Actelion) suffered from a decreased quality of life, worsening arterial oxygen saturation and an increased alveolar-arterial gradient with no change in exercise capacity [105]. In another study the treatment group benefited from significant improvements in mPAP, pulmonary vascular resistance (PVR) and six-min walk distance without a significant decline in oxygenation [106].

Inhalation therapy was investigated in COPD-PH patients with inhaled nitric oxide (iNO) [107–114] and the prostacyclin analogue Iloprost (Schering/Bayer)[115–117]. The trials with iNO consistently demonstrated a considerable and concentration dependent reduction of PVR [107, 109–114]. The response of gas exchange, in particular of oxygenation, to iNO therapy is however heterogeneous. Though, clear concentration dependence cannot be derived from the different studies, there is at least evidence that at lower iNO concentrations arterial oxygenation is improved or remains unchanged with iNO inhalation [107, 109, 111, 114], while at higher concentrations (>20 ppm) there is no gain in oxygenation [110] or even a deterioration [112, 113]. The latter response is presumably the result of increased V/Q mismatch caused by nitric oxide releasing hypoxic vasoconstriction in poorly ventilated regions of the lung. However, the opposite effect was also observed in another study, where an improvement of PaO_2 was recorded with high nitric oxide concentrations [114].

An inconsistent picture also emerges from the studies with inhaled Iloprost (Schering/Bayer). While Boeck and colleagues did not find positive effects but instead a worsening of gas exchange for two different Iloprost (Schering/Bayer) doses in a cross-over study [115], two other studies reported improvements in V/Q matching, gas exchange and exercise tolerance [116, 117].

Recently Riociguat (Bayer), a stimulator of soluble guanylate synthase (sGC) has been approved for treatment of pulmonary arterial hypertension and chronic

thromboembolic PH after it showed improved six-minute walk distance, compared with placebo, and also improved PVR, functional class, dyspnoea, and health-related quality of life in these diseases [118, 119]. Riociguat (Bayer) was also investigated in a single dose study with COPD patients with borderline or manifest PH (mPAP >= 23 mmHg) [120]. Similar as for other therapies, significant reductions of mPAP and PVR could be demonstrated in this patient population. Although some reduction in oxygenation occurred with orally administered Riociguat (Bayer) in these studies, this was not at levels which were judged to be clinically relevant.

Overall, the results from the different studies discussed above indicate that:

- The pharmacological principle of vasodilation is generally appropriate for improving pulmonary hemodynamic and exercise tolerance of COPD-PH patients
- Systemic administration of drugs bears a high risk of deterioration of V/Q mismatch due to relief of hypoxic vasoconstriction
- Inhaled administration shows positive effects and may, in contrast to systemic administration, lead to improved V/Q mismatching, although also the opposite can happen if the distribution of the drug is not strictly limited to well ventilated regions of the lung, or if alveolar absorption is high and considerable systemic exposure occurs after inhalation.

One potential limitation to consider is the fact that inhalation with a metered dose or dry powder inhaler, typically used in lung diseases such as COPD and asthma [121, 122], is associated with a deep breath. This could, however, deteriorate the advantage of inhaled administration, as a deep breath may result in drug particles being deposited in lung areas that are not ventilated at rest.

The complexity of the findings summarized above highlights the fact that the role of different therapies and corresponding administration methods in COPD related PH needs further exploration. In this study, simulation approaches employing a high-fidelity

simulation model were adopted to evaluate the effects of a vasodilator, in terms of hemodynamic and oxygenation, in COPD patients with PH.

In the following, the ability of the simulation model to recapitulate observed changes in gas exchange after systemic administration of the sGC stimulator Riociguat (Bayer) is demonstrated, based on the experimentally determined reductions of pulmonary vascular resistance. Thus validated, the model is then used to evaluate the effects of alternative administration methods (dry powder inhalation via a deep breath and inhalation via normal breathing e.g. using a ventilator) of the drug. Also, the consequences of administering the drug to patients while under exercise is quantitatively investigated.

3.3. Materials and Methods

3.3.1. Model matching to patient data

Over the past years, Genetic Algorithms (GA) has been widely used as a robust search and optimisation approach. The method is effective for problems with both large and small parameter search spaces. Lately, many studies have also employed GA in a range of different problems in physiological modelling [123, 124]. Inspired by the evolutionary process concepts observed in nature such as selection, mutation, recombination etc., this technique produces a set of fittest candidates from the initial population. The randomly sourced initial population of candidates undergoes a repetitive evolutionary process of reproduction through selection for mating according to a fitness function, and recombination via crossover with mutation. A complete repetitive sequence of these genetic operations is called a generation. The performance of each candidate is evaluated by means of a fitness function defined from the knowledge domain and specific to the problem.

Global optimisation methods such as GA are more likely to converge to a global optimal because of their stochastic nature. However, this improved performance comes with the price of higher computation time compared with local methods. The reader is referred to [125] for more details of different operators, binary coding schemes and the

theory of genetic search. Many different termination criteria can be used to stop the process of GA seeking for the best fit. In the current study, an adaptive termination criterion is used where the GA terminates the search when there is no improvement on the best solution achieved over a specified number of successive generations.

To speed up the optimization process, a parallelised computer code implementation of a genetic algorithm was employed in this study. The cost function evaluation process associated with a population can be accelerated hugely by distributing the tasks to multiprocessors (multiple cores and/or multiple machines). Optimization of the model to patient data was performed using the "Tinis" high performance computing cluster provided by the University of Warwick (3488 x Intel Xeon E5-2630 v3 2.4 GHz Haswell cores; 16 cores per node; 203 nodes; 64 GB DDR4 memory per node / 4 GB per core) running Matlab (2017b) and utilizing the global optimization and parallel computing toolboxes. An adaptive termination strategy, which allows the optimization algorithm to run as long as necessary, was applied for each case to ensure the global optimal was reached.

For the present work the pulmonary simulator is matched to the characteristics of three COPD-PH patients with differing gas exchange properties which were included in the previous study with Riociguat (Bayer) [120]. The respective data on PaO_2, $PaCO_2$, dead space fraction and V/Q at baseline (see Table 1) were taken from the study report. The optimization problem is formulated to find the configuration of model parameters that minimize the cost function J given below:

$$\min_x \mathrm{J} = \sqrt{\sum_{i=1}^{5} \frac{\widehat{\mathrm{Y}}_i - \mathrm{Y}_i}{\mathrm{Y}_i}} \tag{23}$$

with

$$\mathrm{Y} = [\mathrm{P_aO_2}, \mathrm{P_aCO_2}, \mathrm{DSV}, \mathrm{VQ_1}, \mathrm{VQ_2}] \tag{24}$$

where Y is the vector of data values and $\hat{Y}$ is the vector of model estimated values for arterial partial pressures of oxygen and carbon dioxide (PaO_2 and $PaCO_2$ respectively), dead space to ventilation fraction (DSV), $0.001<V/Q<0.1$ (VQ_1) and $0.1<V/Q<10$ (VQ_2). The best set of model parameters which gives the minimum value for J is selected as the best match. In case of multiple solutions with similar cost, no difference in the performance of different solutions were observed.

The three example data sets where chosen in order to cover a wide spectrum of COPD pathophysiology. For two of the patients, multiple inert gas elimination technique (MIGET) was applied in order to determine data on V/Q mismatch, and thus for these patients a comparison of data and model outputs on V/Q is also presented. The PVR of individual patients were set based on the provided individual data. As there was no available data indicating if the patients suffered from alveolar loss or not, this was not modelled. Also, the overall high airway resistance of COPD patients is taken into account by means of modelling the obstructed airways (i.e. airways with very high resistance values).

Table 1 reports the matching results for all three COPD patients considered. From the table, it is clear that the models are closely matched to the data with percentage errors below or around 1%. In order to assess the robustness of subsequent findings, 100 random parameter sets within ±5% of the best fit for each patient were also generated. All the analyses described below were applied to the best-fit model, and findings were subsequently checked for consistency on all 100 parameter sets around each optimal patient parameter set.

3.3.2. Modelling of drug effects and application methods

The change from baseline of PVR after drug administration was used as an input for the model. In order to specifically simulate the behaviour of Riociguat, the respective mean relative PVR curve as measured for a dose of 2.5 mg Riociguat (Bayer) [120] was considered for the present simulations (see Figure 2). Individual data on PVR changes after treatment with Riociguat (Bayer) were not published in [120] and therefore the same mean profile was used for all simulated patients.

Table 1. Patient matching results

	Patient 1		**Patient 2**		**Patient 3**	
	data	model	data	model	data	model
PaO_2 (mmHg)	129.2	129.3	76.8	76.69	66.0	65.5
$PaCO_2$ (mmHg)	44.1	44.12	49.8	49.85	32.5	32.3
Dead space (%)	45.8	45.8	39.9	39.8	-	40.0
0.001<V/Q<0.1 (%)	33.1	33.2	13.6	13.61	-	22.4
0.1<V/Q<10 (%)	63.7	64.4	84.9	84.29	-	75.1

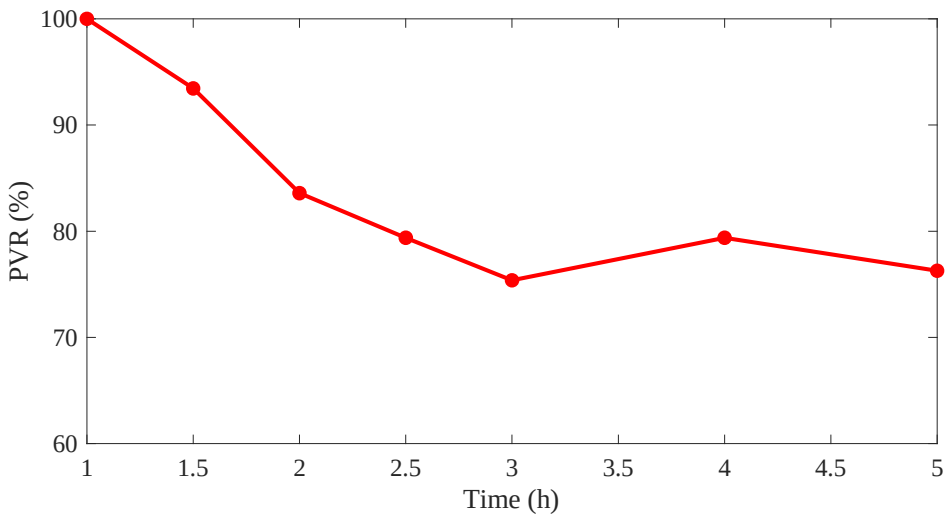

Figure 2. Mean change of PVR from baseline over time in patients receiving a single dose of Riociguat 2.5mg [120].

In the simulator, the pulmonary vessels are modelled as a parallel network with 100 compartments. Each compartment has a vascular resistance denoted as PVR_i and the total pulmonary vascular resistance is defined as:

$$\mathrm{PVR_{tot}} = \frac{1}{\frac{1}{\mathrm{PVR_1}} + \frac{1}{\mathrm{PVR_2}} + \cdots + \frac{1}{\mathrm{PVR_{100}}}} \tag{25}$$

Reduction of PVR is thus captured by changing the resistances of individual compartments due to drug administration. For a given temporal profile of the drug induced change of PVR (see Figure 2) the temporal changes of PVR_i in the individual compartments are calculated as follows.

After systemic application the drug substance is delivered to the lung through the blood circulation. The assumption in this case is that the drug will act equally on all compartments with blood going through them, and produce the same amount of vascular resistance reduction:

$$\overline{\mathrm{PVR_i}}(\mathrm{t}) = \mathrm{PVR}_i^{\mathrm{baseline}} - \alpha(\mathrm{t}) \cdot \Delta_{\mathrm{PVR}} \tag{26}$$

Where Δ_{PVR} is a fixed value denoting the equal reduction in resistance for all compartments, and α(t) is a time dependent variable reflecting the variability of the drug effects over time. Combining Eqs. 25 and 26, the desired PVR reduction shown in Figure 2 can be straightforwardly implemented by adjusting α.

In the case of inhaled application of an aerosol, for example, containing the drug, it is assumed that deposition of the drug in different compartments of the lung is proportional to the extent of ventilation in these compartments. This means that the drug only reaches compartments of the lung which are ventilated under normal breathing conditions. Also, it is assumed that an inhaled application will not lead to systemic exposure causing any systemic effect, nor any effect in the parts of the lung not directly addressed via inhalation.

Despite the assumption that the drug reaches only ventilated areas, and thus only in a part of the lung will a vasodilatory effect be induced, a similar reduction of total PVR is

assumed to be achievable as observed with the systemic application (Figure 2). This assumption is supported by the fact that for inhaled iNO, PVR reductions in the range of 25-30% were observed [109, 110, 114]. Yet, as there is no data on the inhaled reduction level of PVR with Riociguat, the possibility that the inhaled effect may overall be lower when given systemically cannot be ruled out. Furthermore, it is assumed that the inhalation process is short, compared to the absorption and induction effect and thus the time course of the PVR reduction would be the same as the one observed after oral administration (Figure 2). Furthermore, it is assumed that the drug effect is proportional to the amount of drug deposited. Accordingly, the changes in vascular resistance due to treatment with the drug for each compartment is proportional to the ventilation reaching that compartment, and consequently the changed resistance $\overline{\mathrm{PVR_i}}$ is given by:

$$\overline{\mathrm{PVR_i}}(\mathrm{t}) = \mathrm{PVR}_i^{\mathrm{baseline}}(1 - \beta(\mathrm{t}) \cdot \Delta_{\mathrm{PVR}i}) \tag{27}$$

where $\Delta_{\mathrm{PVR}i} = \frac{\mathrm{V_{T_{alv(}}}_{i)}}{\mathrm{V_T}}$, β(t) reflects the temporal effect of the drug, $\mathrm{V_{T_{alv(}}}_{i)}$ is the ventilation of alveolar compartment i and $\mathrm{V_T}$ is the total tidal volume. Combining Eqs.25 and 27, the desired PVR reduction in Figure 2 can be implemented straightforwardly by adjusting β.

Independent of the application device, dry powder inhalation always needs a deep breath for inhaling the drug dose. Deep inhalation (DI) causes a rapid increase of lung volume which results in dilating of the airway and a temporary reduction of airway resistance [126, 127], which will affect how the drug is delivered. The effect of this reduction of airway resistance is modelled, with the underlying assumption that compartments with larger initial volumes will exhibit smaller reductions in airway resistance. Given that total parallel airway resistance $\mathrm{R_{aw}}$ is given by:

$$\mathrm{R_{aw}} = \frac{1}{\frac{1}{\mathrm{R_{aw1}}} + \frac{1}{\mathrm{R_{aw2}}} + \cdots + \frac{1}{\mathrm{R_{aw100}}}} \tag{28}$$

the new airway resistance for compartment i is then given by:

$$\bar{R}_{awi} = R_{awi} \cdot \Delta_{awi} \qquad \text{where} \quad \Delta_{awi} = \frac{1}{1 + \frac{X_{aw}}{Vol_i}} \tag{29}$$

Where Vol_i is the volume of compartment i, and X_{aw} is a scaling parameter related to tidal volume. It can be seen that a smaller Vol_i will lead to a bigger reduction of airway resistance. For example, setting $X_{aw} = 20$, then: i) if $Vol_i = 20$ml, $\Delta_{awi} = 0.5$, ii) if $Vol_i = 80$ml, $\Delta_{awi} = 0.8$. DI is replicated in the virtual patients by applying a threefold increase in tidal volume for a period of five respiratory cycles.

In COPD patients, oxygen consumption is more restrained by impaired pulmonary ventilation than by oxygen delivery, which imposes exercise limitations upon these patients. Under exercise, VO_2 for COPD patients has been shown to increase to 0.7 $L.min^{-1}$ (SD=0.25) on average [128, 129]. In response to the elevated VO_2, minute ventilation and cardiac output rise accordingly to deliver more oxygen to the tissues [129, 130]. In our model, the physiological effects of initiating exercise were simulated by progressively increasing VO_2 every minute to 0.35, 0.5, 0.6, 0.65 and 0.7 $L.min^{-1}$ in the virtual patients. Minute ventilation was subsequently increased as required to maintain the arterial blood gases (ABG) at their pre-exercise values, using the exponential relation between tidal volume and respiratory rate (RR) in [131]. Cardiac output was raised to 8.2 $L.min^{-1}$ according to the average change observed in [129], and following the increase in CO an additional 10% reduction in PVR to that caused by the drug was applied [132]. Exercise was simulated to start 30 minutes after administration of the drug by inhalation with deep breath and continues for 90 minutes. The at-rest and under-exercise values for tidal volume and respiratory rate as well as the corresponding changes to PaO_2 and $PaCO_2$ due to exercise are presented in Figure 3.

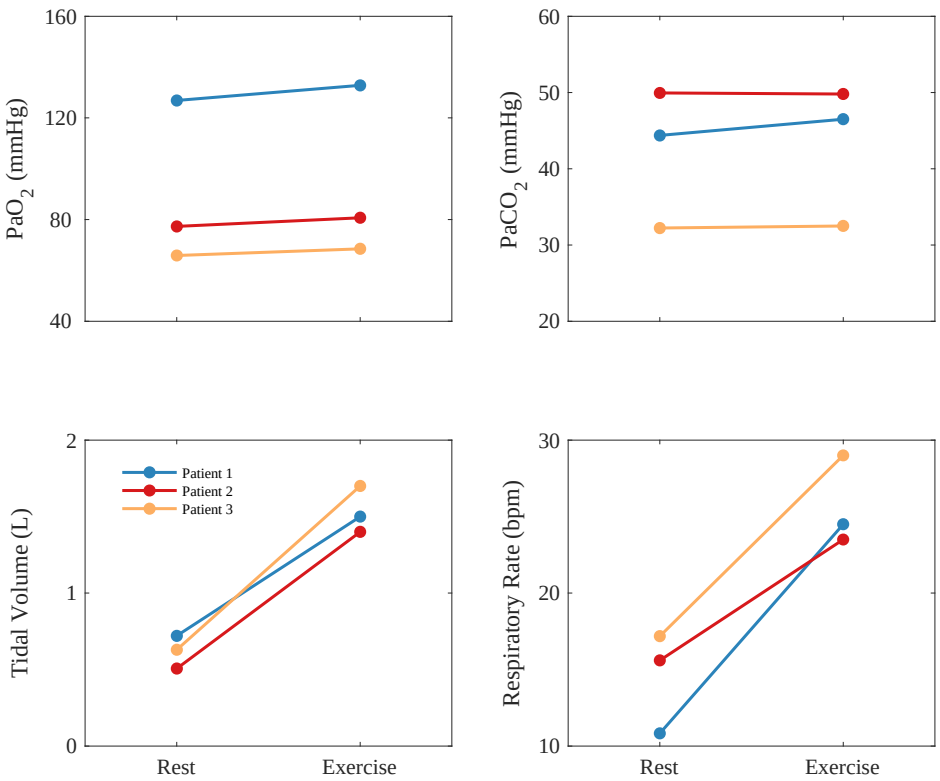

Figure 3. Values for tidal volume and respiratory rate as well as the corresponding changes to PaO_2 and $PaCO_2$ at-rest and under-exercise.

Minute ventilation was subsequently increased as required to maintain the arterial blood gases (ABG) at their pre-exercise values, using the exponential relation between tidal volume and respiratory rate (RR) in [131].

3.4. Results

3.4.1. Systemic application

The average PVR reduction profile observed with 2.5 mg Riociguat (Bayer) was applied to the three configured virtual COPD patients, for each of the three application methods (systemic, inhaled and DPI). The changes in gas exchange parameters, PaO_2 and $PaCO_2$ over time were then recorded, and are shown for each patient in Figure 4 (A) and (B). In the case of systemic application, reductions in PaO_2 and increases in $PaCO_2$ were observed for all 3 patients. For systemic application, the average percentage change for PaO_2 is -24.1% and for $PaCO_2$ is +9.2%, which are consistent with results reported in a previous clinical study with Riociguat (Bayer) [120].

3.4.2. Inhaled application

In contrast to the systemic application, an inhaled administration leads to considerable improvements in oxygenation, as shown in Figure 4 (G) and (H). The maximum increases of PaO_2 are 11%, 4% and 4% with an average of 6.33%, while the maximum decreases of $PaCO_2$ are -11%, -6% and -5%, respectively, with an average of -7.33%. This is as expected, since in this case no deep breaths are required on the part of the patients and thus the entire compound is delivered only to the normally ventilated regions of the lung.

3.4.3. Dry powder inhaler application at rest and under exercise

Figure 4 (C) and (D) shows the effects of application of the same compound using dry powder inhalation via a deep breath at rest, which is a more realistic scenario for an inhaled therapy in COPD. With the same PVR reduction profile, changes of blood gas values are in between those calculated for the systemic and continuous inhaled applications. In fact, it can be seen that PaO_2 is slightly increased and $PaCO_2$ is slightly reduced for all 3 patients. The maximum increases of PaO_2 are 2%, 1% and 1% with an average of 1.33%. The maximum decreases of $PaCO_2$ are -2%, -1% and -1%, respectively, with an average of -1.33%. Figure 4 (E) and (F) show that undertaking exercise for one hour after application by DPI produces further improvements in

oxygenation, with maximum increases of PaO_2 of 5.1%, 0.8% and 2.5% with an average of 2.8%, and maximum decreases of $PaCO_2$ of -2%, -3.3% and -2.5%, respectively, with an average of -2.6%.

3.4.4. Robustness analysis

To test the robustness of our results, for each patient, all simulations (i.e. systemic application, inhalation with deep breath at rest and under exercise and inhalation with normal breath) were repeated on 100 parameter sets randomly chosen within bounds of ±5% of the optimal parameter set found by means of global optimization. Figure 5 compares the maximum change in PaO_2 and $PaCO_2$ observed for each patient and each application method using the optimal parameter set (squares) with the average maximum change in PaO_2 and $PaCO_2$ calculated using 100 random parameter sets (circles with one standard deviation (SD) as error bars). The outcomes confirm the consistency of the observed responses to the different methods of drug administrations, i.e. the average maximum change from baseline for PaO_2 and $PaCO_2$ across all random sets for each patient closely matches the maximum changes reported when employing the optimal parameter set during our previous analysis. Figure 6 to Figure 8 show time-response plots for the performed robustness analysis.

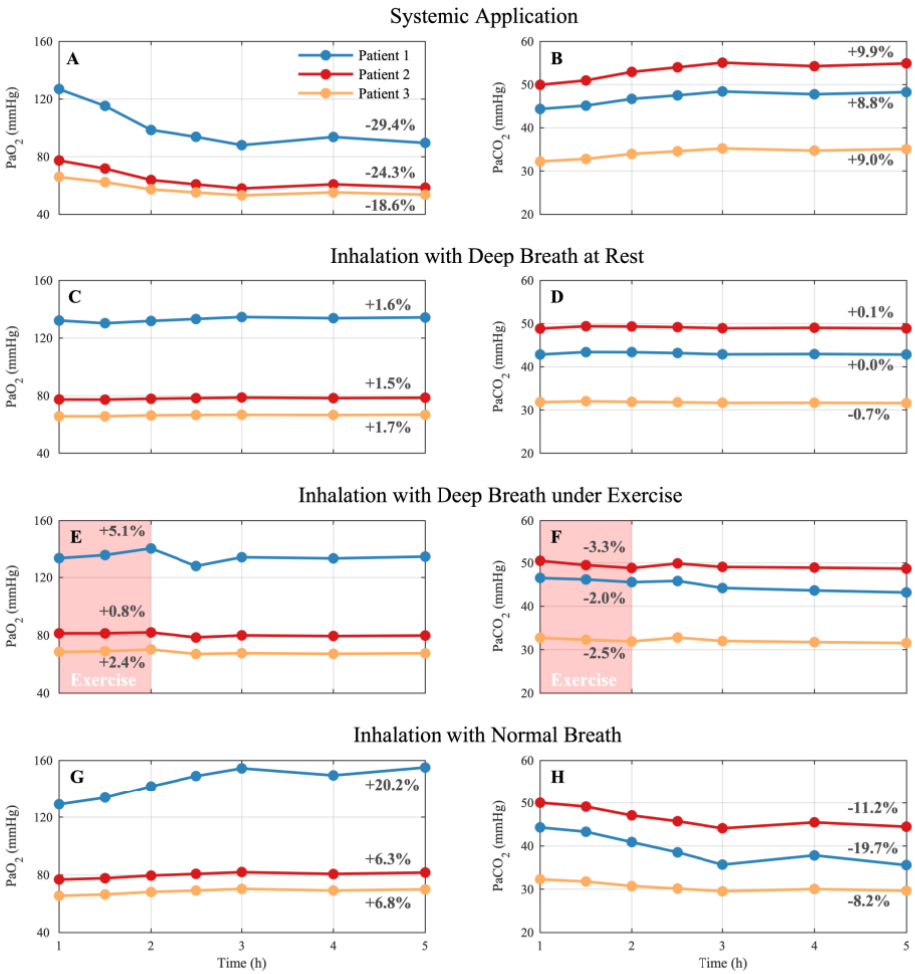

Figure 4. Simulation results for patients using different drug administration methods.

The systemic administration deteriorates oxygenation while inhalation with normal breath improves oxygenation. Inhalation with deep breath had a minimal effect on oxygenation when at rest, however, under exercise it improved oxygenation.

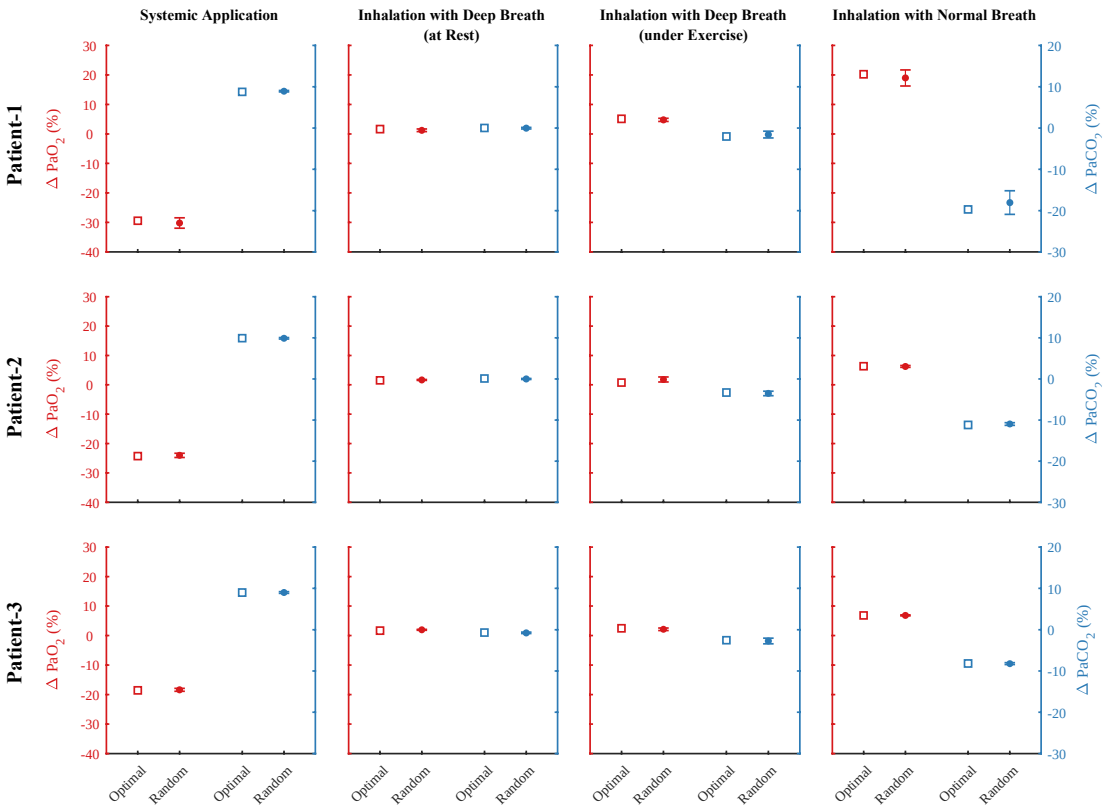

Figure 5. Comparison of the maximum change in PaO_2 and $PaCO_2$ observed for each patient and each application method using the optimal parameter set (squares) with the average maximum change in PaO_2 and $PaCO_2$ calculated using 100 random parameter sets (circles with one standard deviation as error bars).

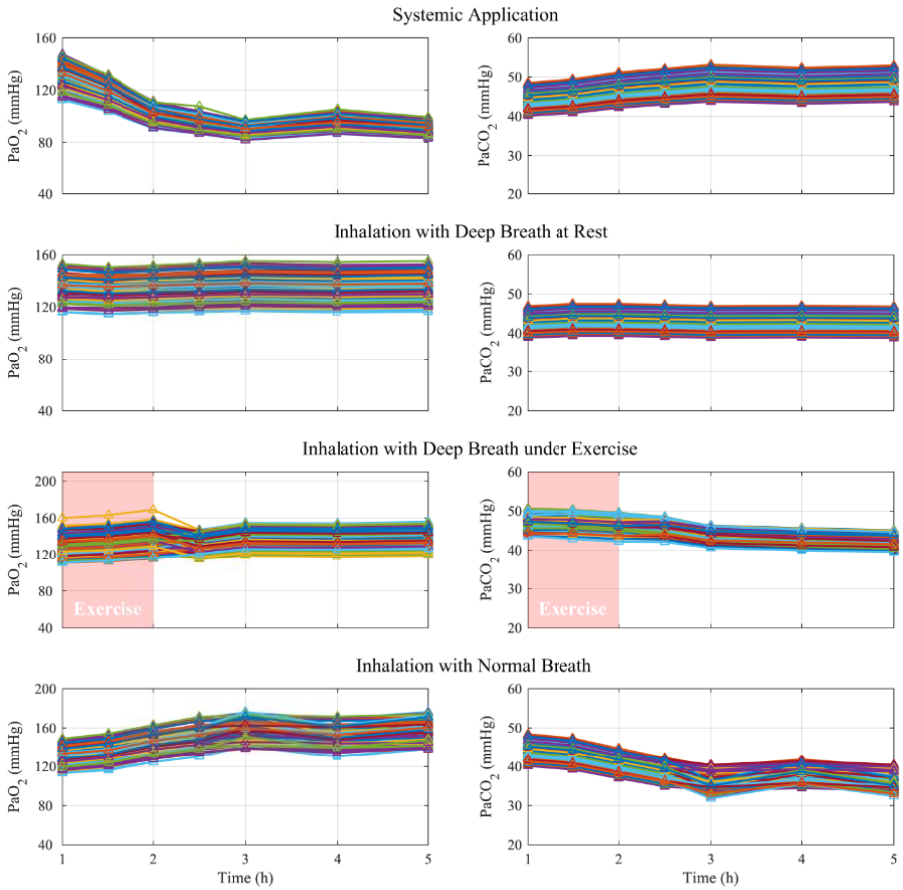

Figure 6. Patient 1 - The Results of the simulations for 100 random parameter sets within ±5% of the best fit.

The outcomes confirm the consistency of the observed responses to the different methods of drug administrations.

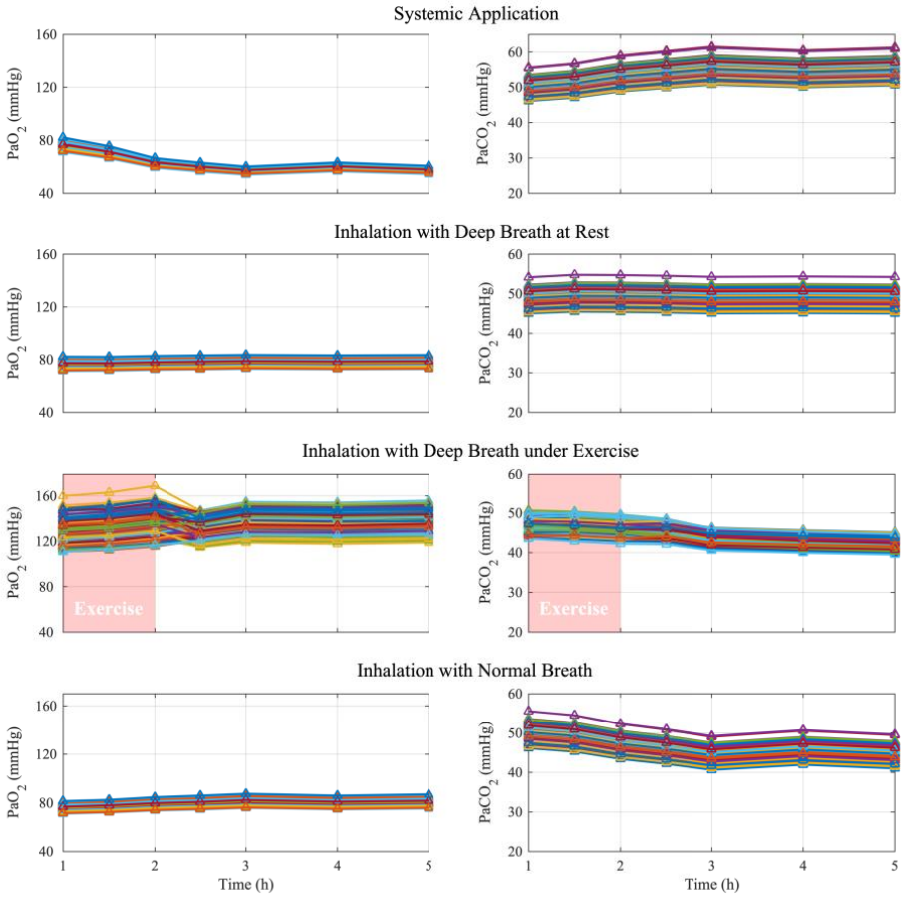

Figure 7. Patient 2 - The Results of the simulations for 100 random parameter sets within ±5% of the best fit.

The outcomes confirm the consistency of the observed responses to the different methods of drug administrations.

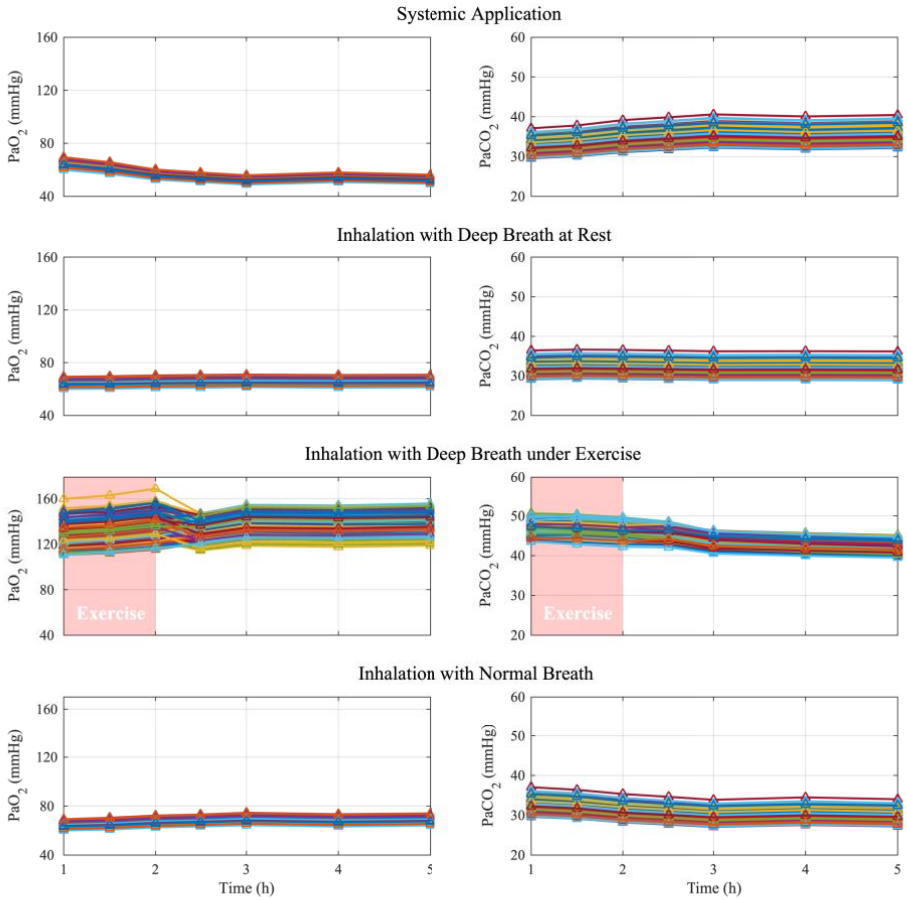

Figure 8. Patient 3 - The Results of the simulations for 100 random parameter sets within ±5% of the best fit.

The outcomes confirm the consistency of the observed responses to the different methods of drug administrations.

3.5. Discussion

This is the first study to investigate the efficacy of sGC modulators in COPD patients with PH by using computer simulation. The capability of the simulator to accurately describe the pathophysiological characteristics of gas exchange in COPD patients has already been demonstrated in a previous study [83]. That study showed that by including sufficient numbers of alveolar compartments in the model, accurate representations of both steady-state blood gases and ventilation-perfusion mismatch via V/Q curves could be obtained. In this study, close matching of the simulator to data on three patients whose hemodynamic was invasively monitored in the study reported by Ghofrani is further demonstrated [120]. Calculations of blood gas concentrations for these virtual patients, considering the observed temporal profile of average PVR changes after oral administration of Riociguat (Bayer), resulted in predictions of changes in O_2 and CO_2 partial pressures that were consistent with those observed in the previous clinical study. These results can be considered as a validation of the capability of the pulmonary simulator to reliably describe the effects on gas exchange of compounds acting on the vascular resistance, in particular those stimulating sGC activity.

As already discussed in previous publications, the systemic application of vasodilating drugs may lead to a worsening of V/Q mismatch and in consequence to an impairment of blood gas concentrations which limits their clinical use. This arises due to the non-selective distribution of the drug to all parts of the lung, which together with inhibition of hypoxic pulmonary vasoconstriction leads to an excess of blood flowing to poorly ventilated parts of the lung.

One potential way to avoid increases of V/Q mismatch is via inhaled administration, as long as the drug can be expected to only reach the ventilated parts of the lung. This avoids increasing the perfusion of non-ventilated lung compartments, provided systemic exposure stays low enough after inhalation not to be effective. Our results from simulations based on this scenario with inhalation of a hypothetical sGC modulating drug, which can be applied to act on the lung selectively, supports this hypothesis when it is administered by normal breathing. In contrast to the findings from systemic

administration, the inhaled application led to improved oxygenation, because perfusion of ventilated lung compartments was improved and effects on less well/non ventilated areas were limited. However, if the drug is formulated as a dry powder, its inhalation will usually be connected with a deep breath, which could cause a certain proportion of the compound to be deposited in regions of the lung that are not, or poorly, ventilated when returning to normal breathing at rest. To quantitatively investigate the trade-offs involved, the effect of inhaled administration of a compound inducing the same effect on total PVR as 2.5 mg oral Riociguat (Bayer) in COPD-PH with a deep breath is also modelled, causing the temporary recruitment of less well-ventilated areas. The resulting simulations reveal that although administering the drug by a deep breath may not improve oxygenation to the same extent as inhalation with normal breathing, it does avoid the potential deterioration in gas exchange associated with systemic drug administration. Moreover, when administered under exercise, most of the non/poorly ventilated parts of the lung in which the drug is deposited due to deep breathing become ventilated again as a result of increased minute ventilation, leading to further improvements in oxygenation. Interestingly, these findings are also in agreement with the results of a clinical trial on the systemic administration of the phosphodiesterase-5 (PDE-5) inhibitor Sildenafil, which produced a worsening of gas exchange due to increased V/Q mismatching at rest, but not under exercise [101]. If lower effect on PVR is assumed during dry powder inhalation, the inhaled administration of the drug can still be more effective by trading off a lower effect on PVR with better preservation of V/Q matching in comparison to the systemic route of administration.

A robustness analysis of these results performed by means of randomly selecting 100 model parameter sets around the optimal values for each patient produced results that were uniformly consistent with the above findings. Our results highlight the potential advantages of administering sGC's to patients via dry powder inhalation, rather than systemically, particularly when drug administration is combined with exercise.

Chapter 4:

Evaluating strategies for lung-protective ventilation in paediatric acute respiratory distress syndrome using high-fidelity computational simulation

4.1. Summary

There have been no randomized trials to determine or evaluate lung-protective ventilation strategies in paediatric acute respiratory distress syndrome (PARDS), and the available observational studies are inconclusive. In this chapter, a new patient dataset is analysed to investigate whether, and how, more protective ventilation could be achieved in clinical practice. A novel high-fidelity computational simulator of PARDS was calibrated against individual patient data from an ongoing observational prospective cohort of PARDS from the Children's Hospital of Philadelphia and used to investigate alternative strategies for achieving more protective ventilation without breaching safety limits on gas exchange. An initial cohort of 30 PARDS patients (age 3.1 ± 0.4 years ventilated via 5.0 mm internal diameter tracheal tubes under neuromuscular blockade) was selected for model and strategy development. Two additional cohorts were

subsequently selected to test the utility and generalisability of our results: 28 patients between 1 and 2 years of age, and 19 patients aged between 1 month and 18 years with tidal volumes >10 $mL.kg^{-1}$. Interventions based on progressive reductions in tidal volume or driving pressure produced significant average reductions in multiple parameters associated with ventilator induced lung injury (tidal volumes, dynamic strain, mechanical power and driving pressure) in all three cohorts without compromising safety limits on gas exchange. Our results indicate that there may be general scope for implementing more protective ventilation in PARDS, suggest strategies for achieving this at the bedside, and demonstrate the utility of high-fidelity computational simulations in intensive care research.

4.2. Introduction

Mechanical ventilation in paediatric acute respiratory distress syndrome (PARDS) is less studied than in adults. After introducing the concept of ARDS in 1967 [133], neither the subsequent American-European Consensus Conference [134] nor the Berlin definition [135] considered differences between adult and paediatric patients when introducing definitions and guidelines. Consequently, current guidelines for mechanical ventilation in PARDS have largely been adapted from developments in the treatment of adult ARDS. In 2015, a paediatric-specific definition for PARDS was proposed by the Paediatric Acute Lung Injury Consensus Conference (PALICC) [136], which showed improved performance for PARDS, relative to adult ARDS definitions [137, 138]. However, recommendations for mechanical ventilation for children from both PALICC and the Paediatric Mechanical Ventilation Consensus Conference (PEMVECC)[139] largely rely on adult trials, with some contribution from paediatric observational data.

Convincing evidence from clinical trials suggest that lower tidal volumes can reduce mortality in adult ARDS [4, 6, 140]. Recent research has highlighted the potential of other lung-protective strategies based on reducing driving pressure and MP to reduce ventilator induced lung injury (VILI) [141–144]. To date, there has been no randomized trial to determine the appropriate application of protective ventilation in PARDS. Observational studies are unclear, with conflicting results [145–148]. Concerns about

hypercapnia or increased ventilatory dead space in paediatrics may also contribute to the hesitancy to lower V_T. There is therefore an urgent need for studies that can provide additional evidence regarding how lung-protective ventilation could be safely implemented during treatment of PARDS patients. It is hypothesized that analysis of a large-scale PARDS dataset using a computational simulator would allow us to (a) determine the scope (in terms of lowering V_T, ΔP and MP) for safely implementing more protective ventilation, and (b) develop, test and directly compare alternative strategies for achieving this in practice.

4.3. Materials and Methods

4.3.1. Patient selection

Development cohort

Patients were selected from an ongoing (since 2011) observational prospective cohort [149] of intubated children meeting Berlin criteria for ARDS from the Children's Hospital of Philadelphia (CHOP). The study was reviewed by the CHOP Institutional Review Board, and requirement for informed consent was waived. As the cohort was initiated prior to publication of the PALICC definition of PARDS [136], they were not screened based on oxygenation index; however, all patients met PALICC criteria. Thirty subjects between 2.5 and 4 years of age ventilated via a 5.0 mm cuffed endotracheal tube during neuromuscular blockade were selected. The initial cohort is restricted to this age/size range to limit some of the variability during model development: e.g. subjects are selected with 5.0 mm internal diameter tracheal tubes, allowing consistency when calculating ventilatory resistance. Furthermore, this age range was close to the median age (4 years) of the overall cohort. Finally, paralyzed subjects are used to ensure reproducibility of the associations between ventilator changes and gas exchange, which would be confounded by spontaneous effort. Arterial blood gases and ventilator changes during the first 72 hours of PARDS were recorded. The respiratory variables of peak inspiratory pressure (PIP), PEEP, and exhaled V_T were collected at the ventilator for patients with $V_T \geq 100$ mL using

integrated software provided by the manufacturer (Dräger, Inc., Lübeck, Germany), and using a sensor proximate to the endotracheal tube for $V_T < 100$ mL. Ventilator management and use of ancillary therapies were not protocolized.

Test cohorts

To test the utility and generalisability of the model and associated ventilation strategies, the analyses are repeated in a separate cohort of children aged 1 to 2 years. This age group was selected because larger V_T are commonly used to overcome perceived increases in dead space in younger lungs. Finally, analyses were repeated in a cohort of 19 children between 1 month and 18 years of age with $V_T > 10$ mL.kg^{-1}, as this is identified as a subgroup in which lung-protective strategies may have the greatest impact. The subjects in the test cohort 2 (high tidal volume) are not a subgroup of any other two cohorts.

4.3.2. Simulator development and calibration to patient data

The paediatric simulator was developed by performing a detailed revision of both the structure and parameters of the baseline simulator described in Chapter 2, Section 2.4, in light of the key differences between paediatric and adult physiology, as described below.

There are a number of other respiratory physiology simulators for ARDS patients available in the literature [27, 64, 72–74, 150, 151], each of varying degrees of complexity and proven validity. Of these, only the model reported in [64, 74] can be applied to study paediatric patients. However, this model suffers from a number of significant limitations. These include the fact that (a) the model simulates the entire lung as a single compartment, (b) little justification/explanation is given for selection of model parameters, (c) the model specifies a lower age limit of 8 years, (d) the model cannot represent the pathophysiology of individual patients or disease states, and (e) no attempt has been made to validate its responses against real patient-data. To the authors' knowledge, the results reported here represent the first application of a validated computational simulator to investigate novel ventilation strategies for PARDS.

There are a number of important differences between adult and paediatric pulmonary physiology. Some physiological features such as lung volume, cardiac output, oxygen consumption, airway resistance and pulmonary vascular resistance are highly variable in children depending on their age and weight. Thus, these different physiological parameters are required to be adaptively set in the model based on the age or weight of the target population. On the other hand, the stiffer lungs of paediatric subjects need to be taken into account when adjusting the volume-pressure equation of single alveolar compartments. The corresponding modifications applied to the model are fully described in this section.

Cardiac output and the volume of functional residual capacity are estimated in the model using the following equations (The study population fro CO was composed of normotensive individuals 1 day to 85 years old and the study population for V_{frc} included subjects aged 0.1-11.2 years old) [152, 153]:

$$\mathrm{CO} = 933 \times \mathrm{weight}_{(\mathrm{kg})}^{0.38} \qquad (\mathrm{ml.min^{-1}}) \tag{30}$$

$$\mathrm{V_{frc}} = 9.51 \times \mathrm{weight}_{(\mathrm{kg})}^{1.31} \qquad (\mathrm{ml}) \tag{31}$$

The total airway resistance and pulmonary vascular resistance are greater in children than in adults, decreasing as they grow older. The specific airway resistance can be estimated by [154]:

$$\mathrm{sR_{tot}} = 1.3083378 - 0.00016486 * \mathrm{age}^3 - 0.03670306 * \mathrm{sex} \qquad (\mathrm{kPa.s}) \tag{32}$$

where sex is set to 1 for males and 0 for females (The equation was extracted from data on healthy paediatric subjects aged 2-11 years old). The total resistance is calculated as:

$$\mathrm{R_{tot}} = \frac{\mathrm{sR_{tot}}}{\mathrm{V_{frc}}} \qquad (\mathrm{kPa.s.l^{-1}}) \tag{33}$$

and is distributed between the main airway and 100 parallel alveolar compartments in the model. Every alveolar compartment also has two resistances placed in series, namely

the alveolar inlet resistance and the upper bronchial resistance. The pulmonary vascular resistance is calculated by means of the following equation [155]:

$$\mathrm{PVR} = \frac{80(\mathrm{MPAP} - \mathrm{MPCWP})}{\mathrm{CO}} \qquad (\mathrm{dyn.s.cm^{-5}}) \tag{34}$$

Note that the difference in values for mean pulmonary arterial pressure (MPAP) and mean pulmonary capillary wedge pressure (MPCWP) is virtually identical in children and adults. Hence, lower cardiac output plays the main role in generating higher PVR values for paediatric subjects. Furthermore, to characterize the stiffer nature of paediatric lungs at baseline the denominator of Eq.16 is reduced to 2000, 5000, 12000 and 50000 $cmH_2O\ mL^{-2}$ for patients younger than 1, 1 to 2, 3 to 5 and 8 to 10 years old respectively.

The simulator was matched to individual patient data using advanced global optimisation algorithms already described in Chapter 3 (see Section 3.3.1). The optimization problem is formulated to find the configuration of model parameters that minimize the cost function J given below:

$$\min_{x} \mathrm{J} = \sqrt{\sum_{i=1}^{7} \frac{\widehat{\mathrm{Y}}_i - \mathrm{Y}_i}{\mathrm{Y}_i}} \tag{35}$$

with

$$\mathrm{Y} = [\mathrm{PaO_2}, \mathrm{PaCO_2}, \mathrm{P_E'CO_2}, \mathrm{PIP}, \mathrm{mPaw}, \mathrm{TOP_{mean}}, \mathrm{V_{frc}}] \tag{36}$$

where Y is the vector of data values and $\widehat{\mathrm{Y}}$ is the vector of model estimated values. $P_E'CO_2$ is partial pressure of carbon dioxide at the end of an exhaled breath. The average threshold opening pressure of all the compartments (TOP_{mean}) is optimized to be 20 cmH_2O [88].

4.3.3. Strategies for achieving lung-protective ventilation

After matching the model to each individual patient, the potential for achieving lung-protective ventilation in these patients was investigated by evaluating four different strategies on each of the virtual patients. The primary objective of the ventilation strategies was to progressively lower the risk of VILI without violating the following safety constraints:

- $PaO_2 \geq 8$ (60) kPa (mmHg)
- $PaCO_2 \leq 8$ (60) kPa (mmHg)
- PIP $\leq$ 35 cmH_2O
- RR $\leq$ 40 bpm

PaO_2, $PaCO_2$ and RR are partial pressure of oxygen in arterial blood, partial pressure of carbon dioxide in arterial blood and respiratory rate, respectively. These constraints are based on those used in clinical trials in adult ARDS, adapted to match the requirements of paediatrics [4, 156]. Also, the clinicians validated these ranges and the upper limits were observed in the current dataset. In cases where the data indicated that a patient's initial settings did not comply with one or more of the aforementioned safety criteria, an attempt to reduce VILI was only made if it led to an improvement in the patient's safety parameters (e.g. reducing $PaCO_2$ or PIP). The four strategies were designed using volume control mode (VC-CMV) and based on physiological equations that are widely used in clinical practice, as follows:

Strategy 1: V_T was reduced in steps of 0.5 $mL.kg^{-1}$ with each step lasting for 30 minutes. ABG and PIP were checked at the end of each phase until any further reduction violated one of the above constraints. RR was simultaneously adjusted at each step to maintain a constant minute ventilation (MinV) using:

$$\mathrm{MinV} = \mathrm{V_T} \times \mathrm{RR} \tag{37}$$

Strategy 2: Alveolar minute ventilation ($MinV_{alv}$) was kept constant instead of the general MinV. To do this, the amount of anatomical dead space (V_D) must be taken into account, and thus $MinV_{alv}$ was calculated from the equation [157–159]:

$$\mathrm{MinV_{alv}} = (\mathrm{V_T} - \mathrm{V_D}) \times \mathrm{RR} \tag{38}$$

Strategy 3: Here, a strategy previously employed in [49, 160] was implemented in the simulator. In this approach, the $\mathrm{MinV_{alv}}$ was kept constant using Eq.38, and the inspiratory flow kept constant using the equation:

$$\mathrm{F_{insp}} = \frac{\mathrm{V_T} \times \mathrm{RR}}{60 \times \mathrm{DC}} \tag{39}$$

where F_{insp} is the square inspiratory flow into the lung from the ventilator (no pause time used), and DC is duty cycle. As V_T and RR had already been determined (same as strategy 2), F_{insp} could only be manipulated by varying DC in Eq.39. Thus, the difference between strategies 2 and 3 is that DC is set as constant for the former, while DC is adjusted to maintain a constant F_{insp} in the latter.

Strategy 4: A recent study of adult ARDS [141] suggested that reductions in V_T are most advantageous in terms of lowering mortality when this leads to a corresponding decrease in driving pressure (ΔP), defined as the difference between plateau pressure (P_{plat}) and PEEP.

$$\Delta\mathrm{P} = \mathrm{P_{plat}} - \mathrm{PEEP} \tag{40}$$

P_{plat} is calculated directly from the simulator and represents the end inspiratory lung pressure. The employed strategy for decreasing ΔP works by increasing the applied PEEP and then adjusting V_T to keep the plateau pressure constant. For this purpose, PEEP was increased by 1 cmH_2O (causing a rise in P_{plat}) and then V_T was reduced in steps of 0.5 mL kg^{-1} until P_{plat} returned to its initial value. The procedure was then repeated until one of the safety constraints was violated.

4.3.4. Additional variables collected

Strain, strain rate, and mechanical power were also calculated. Dynamic and static strain are markers of mechanical load during ventilation and can assist with understanding how the whole lung is affected by ventilation [161–163]. Although it is not possible to

measure exact values of strain in clinical practice, in the simulator they can be estimated as [161]:

$$\text{Dynamic Strain} = \frac{V_T}{V_{frc(ZEEP)}} \quad (41)$$

$$\text{Static Strain} = \frac{V_{PEEP}}{V_{frc(ZEEP)}} \quad (42)$$

where V_{PEEP} is the volume of gas in the lung due to PEEP and $V_{frc(ZEEP)}$ is the volume of functional residual capacity when PEEP is zero. Strain rate is strain divided by inspiratory time (T_i).

$$\text{Strain Rate} = \frac{\text{Strain}}{T_i} \quad (43)$$

Mechanical power is calculated using the below equation [142]:

$$MP = 0.098 \times RR \times \left\{ {V_T}^2 \times \left[0.5 \times EL_{rs} + RR \times \frac{(1 + I{:}E)}{60 \times I{:}E} \times R_{aw} \right] + V_T \times PEEP \right\} \quad (44)$$

where EL_{rs} is the elastance of the respiratory system, I:E is the inspiratory-to-expiratory time ratio, and R_{aw} is the airway resistance. The unit for MP is J min^{-1}.

4.3.5. Statistical analysis

Data are presented as mean ± SD, or shown graphically using median, interquartile and total ranges. Data for all subjects, even those in whom VILI reductions could not be performed without violating safety constraints, is presented. To avoid violation of underlying distribution assumptions, variables were compared using nonparametric statistics when appropriate, including Spearman's rho, Wilcoxon signed-rank test, Mann–Whitney U test and Kruskal–Wallis H test. A two-sided p-value of < 0.05 was considered to represent significance.

4.4. Results

4.4.1. The simulator accurately represents individual patient data

The ability of the simulator to accurately reproduce patient data was first verified by comparing its responses against data on the responses (PaO_2 and $PaCO_2$values) of 30 patients (37% mild, 30% moderate, 33% severe per PALICC; 24% mild, 48% moderate, 28% severe per Berlin) in the development cohort to mechanical ventilation. No strong correlation was observed between the reported values of V_T (Kruskal-Wallis $p = 0.7$), PEEP ($p = 0.4$) and RR ($p = 0.3$) and PARDS severity category. Inspired oxygen fraction (F_IO_2) increased significantly with PARDS severity (Mann–Whitney $p < 0.05$). Average data across the cohort are shown in Table 2, while data for each individual patient are presented in Table 3 to Table 5. At baseline, 2 patients in the development cohort had V_T > 10 mL.kg^{-1}, 10 patients had V_T 8–10 mL.kg^{-1}, 16 had V_T 6–8 mL.kg^{-1}, and 2 had V_T < 6 mL.kg^{-1}.

After model calibration, each individual patient in the cohort was simulated for 30 minutes (or until reaching steady state) under mechanical ventilation with constant flow in the supine position. Figure 9 (A) and (B) compare the outputs of the simulator with the original data, expressed as median, interquartile range and actual range. Figure 10 (A) and (B) shows the Bland-Altman plots for data points versus simulator outputs. To further test the reliability of the simulator, an additional validation procedure was performed in which PIP or mPaw were left out of the model calibration step, and the predicted model responses for these parameters were then checked against the data after the model matching stage. Figure 11 illustrates the results of the extended model validation on the development cohort by comparing the patient data against simulator predicted values expressed as median, interquartile range and actual range. The largest difference between the data and estimated values were observed when working with large pressure values which are considered unsafe in the clinical practice and violates the safety limits of this study as well (i.e. PIP > 35 cmH_2O). These results confirm the capability of the simulator to accurately replicate multiple output values of the patients included in the cohort dataset across a range of different ventilator settings.

Table 2. Patient characteristics and mechanical ventilator settings presented as mean ± SD across the cohorts.

	Patient Data & Ventilator Settings							
Parameters	**Age**	**Weight**	**F_IO_2**	**RR**	**V_T**	**PEEP**	**PF**	**OI**
	y	kg		bpm	mL.kg^{-1}	cmH_2O		
Development Cohort	3.1±0.4	14.7±3.2	0.6±0.2	25.9±6.0	7.8±1.6	9.8±2.6	154.7±76.7	13.0±7.1
Test Cohort 1	1.4±0.3	10.3±1.9	0.6±0.2	26.6±4.4	8.1±1.2	8.7±1.9	178.4±61.6	9.4±4.5
Test Cohort 2	5.3±6.0	18.2±15	0.6±0.3	23.7±8.0	11.1±1.0	10.8±2.6	157.4±67.8	15.7±12.9
	Blood Gases & Airway Pressures							
	PaO_2		**$P_E'CO_2$**	**$PaCO_2$**		**PIP**		**mPaw**
	kPa (mmHg)					cmH_2O		
Development Cohort	10.1±2.0 (75.5±15.2)		6.0±1.6 (44.8±12.2)	7.2±1.8 (53.9±13.6)		30.2±7.7		15.9±4.2
Test Cohort 1	12.3±3.3 (92.4±24.8)		5.4±0.9 (40.4±7.1)	6.4±1.0 (47.7±7.6)		28.7±5.5		14.5±2.5
Test Cohort 2	11.2±4.6 (84.4±34.4)		4.6±1.0 (34.8±7.2)	5.6±1.6 (41.9±11.9)		32.0±6.5		17.8±4.2

Table 3. Patient characteristics and mechanical ventilator settings for each individual patient in the development cohort.

ID	Age	Weigh	F_IO_2	RR	V_T	PEEP	PF	OI	PaO_2	$P_E'CO_2$	$PaCO_2$	PIP	mPaw
	(y)	(kg)		(bpm)	($mL.kg^{-1}$)	(cmH_2O)			(mmHg)			(cmH_2O)	
# 1	2.8	15	0.45	28	6.7	6	137	8	62	39	46	20	11
# 2	2.8	14	0.5	20	6.3	14	152	14.5	76	54	72	34	22
# 3	2.8	14.5	0.6	25	6.8	10	97	15.5	58	42	60	25	15
# 4	2.8	17	0.5	20	4.5	10	236	5.9	118	37	53	26	14
# 5	2.8	20	0.21	26	7	10	295	5.1	62	32	32	26	15
# 6	3	9.5	1	40	8.9	8	78	16.7	78	62	65	22	13
# 7	3	15	0.5	30	8.7	5	118	6.8	59	37	40	20	8
# 8	3	13.6	0.5	16	7.4	10	178	7.3	89	43	59	21	13
# 9	3	15	0.3	24	5.3	10	266	6.4	80	50	56	28	17
# 10	3	13	0.4	28	7.8	12	230	7	92	59	60	25	16
# 11	3.3	15	0.5	25	7.5	8	178	7.3	89	43	46	26	13
# 12	3.5	14	0.35	34	10.3	8	274	5.1	96	54	56	28	14
# 13	4	17.5	0.55	20	6.9	10	149	10.1	82	43	72	29	15
# 14	4.3	19	0.6	24	7.2	14	111	18	67	41	56	41	20
# 15	2.5	12.2	0.3	26	8.9	12	343	5.2	103	60	63	32	18
# 16	3.7	15	0.4	22	6.7	6	170	5.9	68	48	51	24	10
# 17	3.3	14	0.55	35	6.5	15	118	21.2	65	55	74	47	25
# 18	2.8	27	0.8	24	6.7	12	73	24.7	59	33	42	32	18
# 19	2.9	12	1	32	7.5	10	72	23.6	72	42	48	34	17
# 20	3	9.5	1	37	8.9	12	78	29.5	78	50	79	42	23
# 21	3	15	0.8	21	8.7	8	79	17.7	63.2	39	45	31	14
# 22	3	13.6	1	20	9.6	8	57	26.3	57	30	39	24	15
# 23	3	15	0.7	30	8	12	130	18.5	91	30	33	46	24
# 24	3	13	0.4	27	7.5	12	150	12.7	60	72	75	41	19
# 25	3.1	13	0.55	27	8.1	12	129	14.0	70.95	59	65	36	18
# 26	3.1	13	0.75	21	8.8	8	112	10.7	84	62	64	20	12
# 27	3.25	13	1	23	7.7	7	59	18.6	59	20	34	28	11
# 28	3.3	15.5	0.35	23	8.4	8	237	6.8	82.95	47	59	36	16
# 29	3.33	15	0.6	24	7.5	6	108	11.1	64.8	26	38	26	12
# 30	3.5	14	0.35	20	13.6	12	226	8.4	79.1	35	36	37	19
Mean	3.1	14.7	0.6	25.9	7.8	9.8	154.7	13.0	75.5	44.8	53.9	30.2	15.9
SD	0.4	3.2	0.2	6.0	1.6	2.6	76.7	7.1	15.2	12.2	13.6	7.7	4.2

Table 4. Patient characteristics and mechanical ventilator settings for each individual patient in test cohort 1.

ID	Age	Weigh	F_IO_2	RR	V_T	PEEP	PF	OI	PaO_2	$P_E'CO_2$	$PaCO_2$	PIP	mPaw
	(y)	(kg)		(bpm)	($mL.kg^{-1}$)	(cmH_2O)			(mmHg)			(cmH_2O)	
# 1	1.7	12	0.35	30.5	30.6	5	274	4.4	95.9	39	41	26	12
# 2	1.5	9.8	0.5	23.5	23.3	8	230	4.8	115	47	48	20	11
# 3	1.4	10	0.4	25	24.8	8	262	5.0	104.8	40	46	28	13
# 4	1.67	8.8	0.35	25.5	25.7	8	274	5.1	95.9	39	52	30	14
# 5	1.67	12	0.4	23	22.9	5	195	5.1	78	42	44	21	10
# 6	2	10	0.5	20.5	20.6	10	226	5.3	113	39	44	17	12
# 7	1.5	12	0.4	28.5	28.5	8	260	5.4	104	39	47	26	14
# 8	2	14	0.5	20	20	8	236	5.9	118	39	41	22	14
# 9	1.4	12.7	0.4	25	25.2	10	242	6.6	96.8	24	33	31	16
# 10	1.1	10	0.4	29.5	29.4	12	246	7.3	98.4	35	41	37	18
# 11	1.5	10.5	0.4	29	29	10	200	8.0	80	43	49	32	16
# 12	1	6.5	0.65	28	28	8	160	8.1	104	54	57	26	13
# 13	1.4	10	0.4	25.5	25.7	10	197	8.6	78.8	30	41	28	17
# 14	1.33	8.8	0.45	39	39	8	169	8.9	76.05	39	51	30	15
# 15	1.5	11	0.5	29	29	8	154	9.1	77	54	55	31	14
# 16	1.75	11	0.5	23.5	23.4	11	197	9.1	98.5	36	54	39	18
# 17	1.25	10	0.5	28	28.2	8	146	9.6	73	40	50	29	14
# 18	1.4	7.5	0.8	22	21.9	8	124	9.7	99.2	46	47	23	12
# 19	1	7.5	1	35	34.9	12	190	10.0	190	29	39	35	19
# 20	1.8	12.3	0.7	24.5	24.6	8	135	10.4	94.5	45	58	25	14
# 21	1.1	11.6	0.5	24	24.2	10	172	10.5	86	43	54	35	18
# 22	1	8.2	0.8	31	31.2	5	93	10.8	74.4	51	57	24	10
# 23	1.6	13	0.5	25.5	25.3	8	130	10.8	65	33	37	30	14
# 24	1.5	10	0.65	21.5	21.7	10	123	12.2	79.95	50	54	29	15
# 25	1.75	12.7	0.8	21.5	21.7	8	85	14.1	68	37	40	25	12
# 26	1.1	10	0.9	26	26.1	10	105	16.2	94.5	34	37	35	17
# 27	1.25	9	0.6	30.5	30.5	12	105	17.1	63	44	57	35	18
# 28	1.25	7.7	1	30	30.2	8	65	24.6	65	41	61	34	16
Mean	1.4	10.3	0.6	26.6	26.6	8.7	178.4	9.4	92.4	40.4	47.7	28.7	14.5
SD	0.3	1.9	0.2	4.4	4.4	1.9	61.6	4.5	24.8	7.1	7.6	5.5	2.5

Table 5. Patient characteristics and mechanical ventilator settings for each individual patient in test cohort 2.

ID	Age	Weigh	F_IO_2	RR	V_T	PEEP	PF	OI	PaO_2	$P_E'CO_2$	$PaCO_2$	PIP	mPaw
	(y)	(kg)		(bpm)	($mL.kg^{-1}$)	(cmH_2O)			(mmHg)			(cmH_2O)	
# 1	0.2	5.4	0.5	25	11.7	15	224	9.8	112	40	41	40	22
# 2	0.5	6	0.35	35.5	11.1	7	194	6.2	67.9	24	31	28	12
# 3	0.5	7.6	0.4	38.5	10	8	127	11.8	50.8	31	39	26	15
# 4	0.6	6.8	0.5	39	10.4	6	156	10.3	78	35	63	37	16
# 5	0.7	7	0.3	32	13	12	250	7.6	75	21	25	36	19
# 6	0.8	8.5	0.4	23.5	10.4	12	197	8.6	78.8	39	40	25	17
# 7	0.9	10	0.45	25.5	10.2	10	146	11.6	65.7	50	71	30	17
# 8	1.25	7.7	1	24.5	10.4	8	65	24.6	65	41	61	34	16
# 9	2	10	0.5	20.5	11.4	10	226	5.3	113	39	44	17	12
# 10	3.2	14	0.6	20	10.7	12	148	10.8	88.8	36	38	30	16
# 11	3.5	14	0.35	20.5	13.6	12	226	8.4	79.1	35	36	37	19
# 12	3.5	13	1	28.5	10.8	12	59	50.8	59	48	49	42	30
# 13	4.6	16.4	0.35	20.5	12.1	10	251	5.7	87.9	34	40	26	14
# 14	8	14	0.45	16.5	11.9	12	153	11.8	68.9	31	35	27	18
# 15	9.25	40	1	12	11.3	12	199	10.1	199	32	33	37	20
# 16	10.2	45	1	13.5	10	12	59	33.9	59	30	36	40	20
# 17	16.33	30	1	22	10	16	55	41.8	55	35	48	32	23
# 18	17.1	55	0.7	12.5	10.9	12	180	10	126	27	30	28	18
# 19	17.7	35	1	22	11.1	8	75	20	75	33	37	36	15
Mean	5.3	18.2	0.6	23.7	11.1	10.8	157.4	15.7	84.4	34.8	41.9	32.0	17.8
SD	6.0	15.0	0.3	8.0	1.0	2.6	67.8	12.9	34.4	7.2	11.9	6.5	4.2

4.4.2. Evaluating strategies for implementing protective ventilation

Figure 12 to Figure 13 show the effect of each strategy for implementing protective ventilation, in terms of its impact on V_T, MP and ΔP. Similar reductions in average V_T across the patient cohort were achieved using strategies 1-3 (15% (1.3 mL.kg^{-1}), 12% (1 mL.kg^{-1}) and 14% (1.2 mL.kg^{-1}), respectively). RR needed to be increased by a smaller amount (15%) for strategy 1, (versus 33% and 37% on average for strategies 2 and 3, respectively). After implementing any of the three strategies, the number of patients being ventilated using V_T > 10 mL.kg^{-1} fell to zero. There were also reductions in the number of patients receiving V_T in the ranges of 8–10 mL.kg^{-1} (-30 % for all strategies) and 6–8 mL.kg^{-1} (-18.8% for strategies 1 and 3, -12.5% for strategy 2). Correspondingly, the number of patients receiving V_T in the range 4-6 mL.kg^{-1} rose from 6.7% to 33.3% in strategy 1 and to 30% in strategies 2 and 3, respectively. These average reductions were achieved despite the fact that there were 8 patients (4 severe PARDS, 4 moderate PARDS) whose baseline values of $PaCO_2$ and PIP did not allow any of the strategies to be implemented without violating constraints.

Figure 14 shows significant reductions in dynamic strain for strategies 1 to 3 (-20%, -19% and -19%, respectively) with corresponding increases in static strain (+9%, +17% and +35%, respectively). The rise in static strain indicates larger lung volumes at end-expiration. In strategy 3, the change in DC (shorter exhalation time) explains the higher static strain compared to the other two approaches. To rule out the possibility that higher static strains are due to breath-stacking, the difference between the inhaled tidal volume (V_{Ti}) and exhaled tidal volume (V_{Te}) were examined in all strategies to detect possible incomplete exhalation. The change in end-expiratory lung volume was also monitored over a 3-hour time period. The results of both investigations confirm (see Figure 17) that the higher static strains are not a result of breath-stacking. Likely due to the higher RR, static and dynamic strain rates were higher in strategies 1 to 3 – Figure 15 (A) and (B).

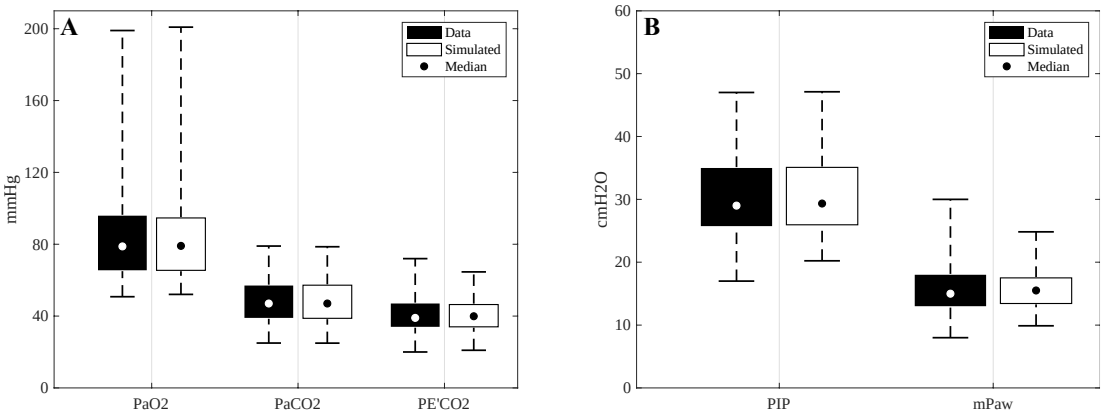

Figure 9. A comparison of the simulator outputs with the original patient data in panels (A) and (B), expressed as median, interquartile range and actual range.

The ability of the simulator to accurately reproduce patient data was first verified by comparing its responses against data on the responses.

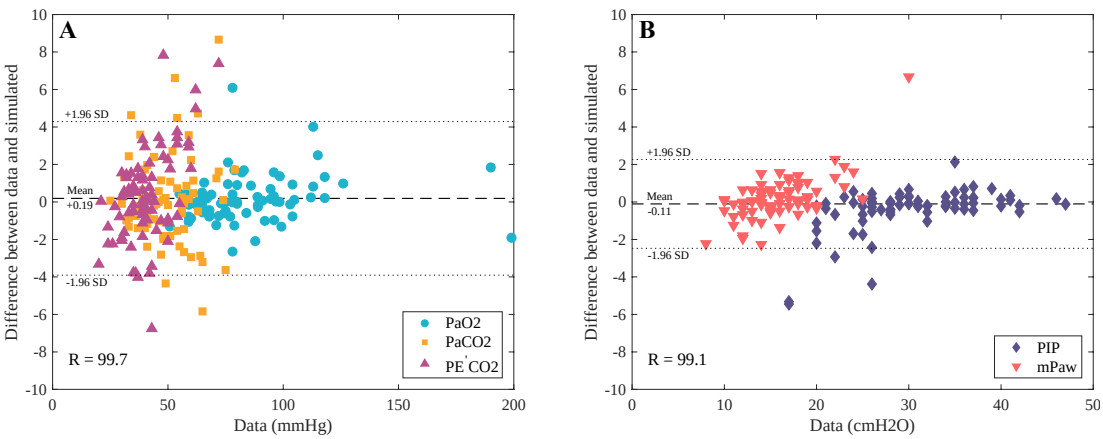

Figure 10. Panels (A) and (B) show the Bland-Altman plots for simulator outputs and original patient data. "R" represents the correlation coefficient of the data and the simulated values.

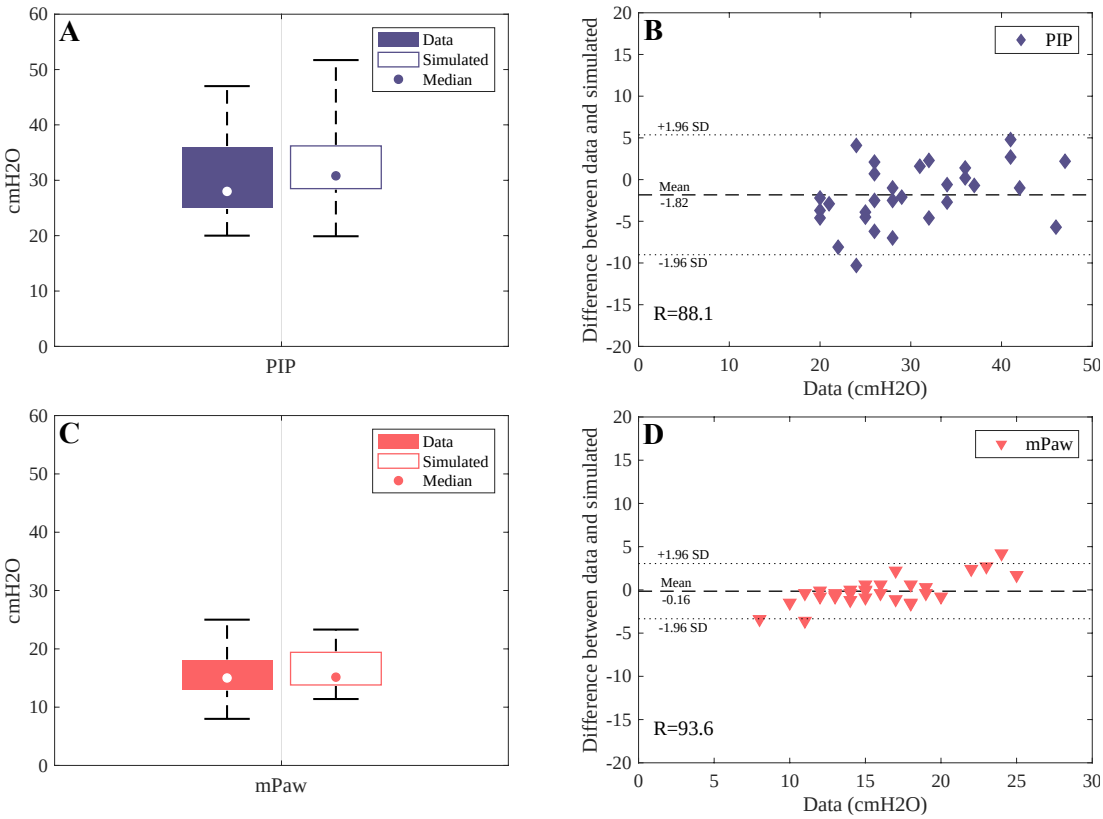

Figure 11. Results of the extended model validation on the development cohort by comparing the patient data against simulator estimated values

Panels (A) and (B) show the results for leaving PIP out of the model matching step and subsequently predicting its value. Panels (C) and (D) show the results for leaving mPaw out of the model matching step and subsequently predicting its value. In (A) and (C) data are expressed as median, interquartile range and actual range whilst (B) and (D) present the Bland-Altman plots, and "R" is the correlation coefficient of the data and the simulated values.

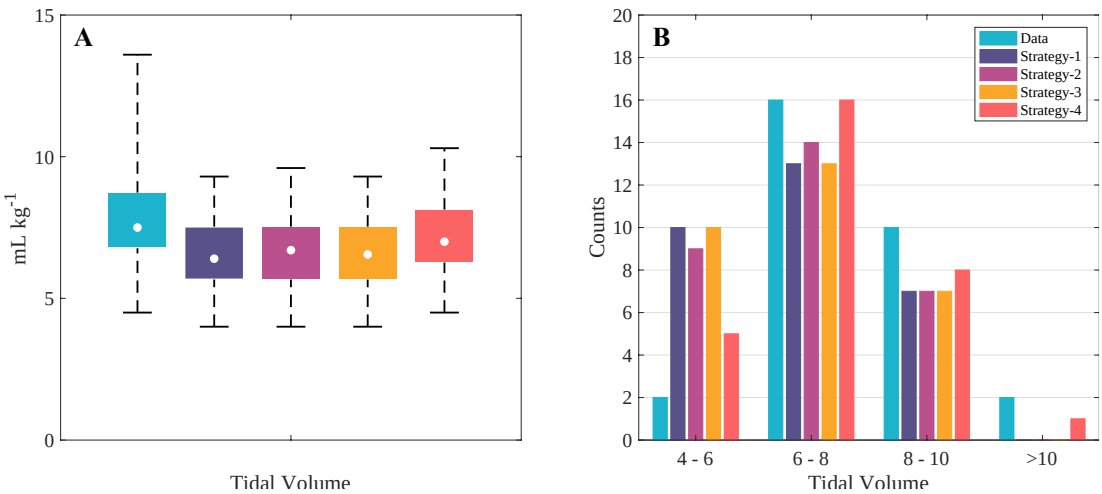

Figure 12. Development Cohort, panels illustrate the amount of tidal volume reduction.

Box plot on the left (A) shows data as median, interquartile range and actual range while histogram on the right (B) demonstrates the distribution of all patients' data before and after implementing different strategies. Similar reductions in average V_T across the patient cohort were achieved using strategies 1-3 (15% (1.3 mL.kg^{-1}), 12% (1 mL.kg^{-1}) and 14% (1.2 mL.kg^{-1}), respectively).

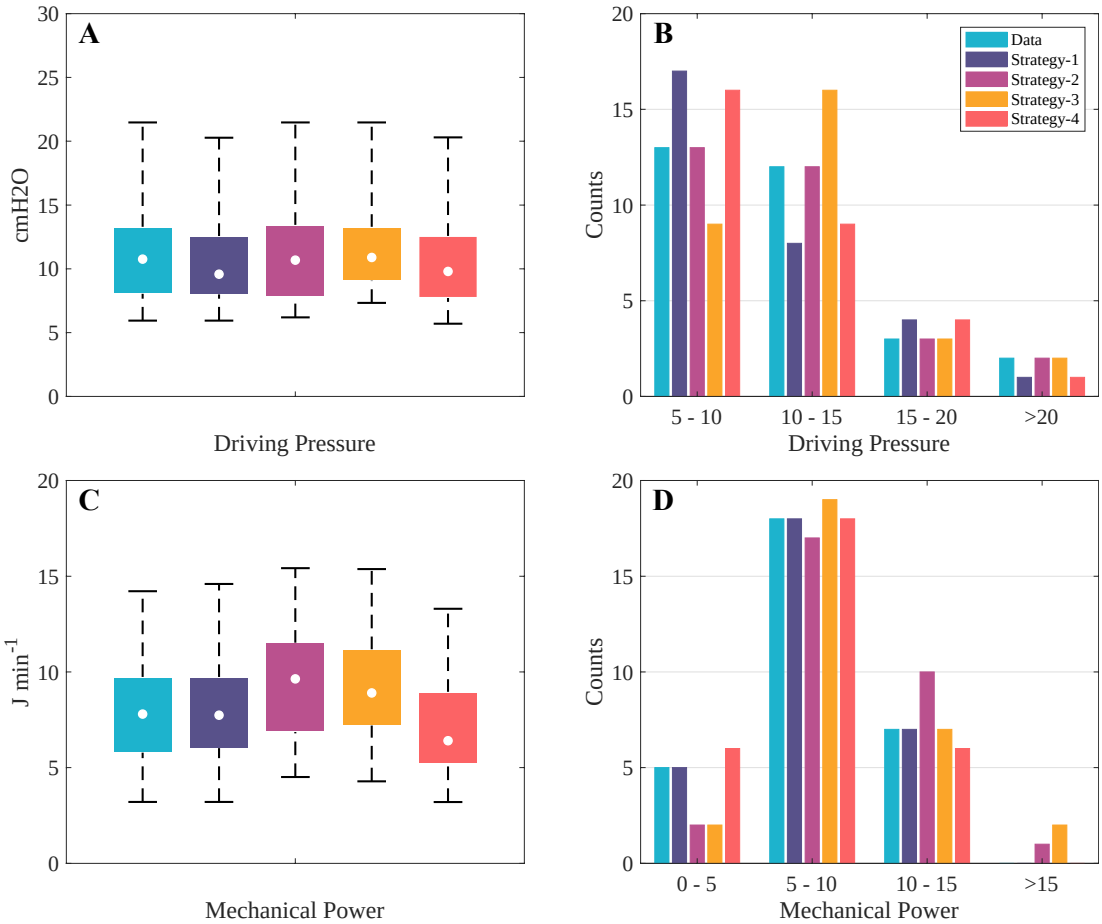

Figure 13. Development Cohort, panels illustrate the change in driving pressure (A)-(B) and mechanical power (C)-(D) before and after implementing different strategies.

Box plots on the left (A)-(C) show data as median, interquartile range and actual range while histograms on the right (B)-(D) demonstrate the distribution of all patients' data. Both ΔP and MP were reduced the most in strategies 1 and 4 and raised the most in strategies 2 and 3.

Differences emerged when considering the effect of each strategy on mechanical power. Strategy 1 produced no significant change (+1%; p=0.2, signed-rank test) but both strategies 2 and 3 resulted in large increases (+22% and +19%, respectively; both $p<0.05$).

Amongst the four safety constraints, limits on $PaCO_2$ and RR played the main role in restricting further reduction of V_T. Limits on PaO_2 were never reached. The changes in gas exchange, $P_E'CO_2$, PIP and mPaw caused by the V_T reductions are presented in Figure 16. The values that are outside of the determined safety constrains represent those patients whose initial status violated one or other of the safety constraints. Figure 15 (C) and (D) compares the levels of ventilatory dead space and dead space fraction (Eq.45) respectively, for all applied strategies.

$$\text{Dead Space Fraction} = \frac{\text{Dead Space}}{V_T} \tag{45}$$

When strategy 4 (adjusting PEEP and V_T to reduce ΔP) was applied, the $PaCO_2$ limit was the only constraint precluding further reductions due to the strategy not compensating for MinV. Maintaining MinV is not possible using this strategy, as it requires increasing RR, leading to a rise in P_{plat} which in turn impedes reduction of ΔP. Consequently, this approach was only able to reduce ΔP in the 13 patients with the lowest initial $PaCO_2$ levels. The average reduction in ΔP was -6% for all 30 patients in the dataset and -17% for the 13 patients on which this strategy could be applied. The corresponding changes in V_T and PEEP were -7% and +10% respectively. This compares with changes in ΔP of -4%, +1% and +8% for strategies 1-3, respectively. Strategy 4 was the only approach that produced a significant reduction in mechanical power (-8%, versus +1%, +22% and +19% for strategies 1-3).

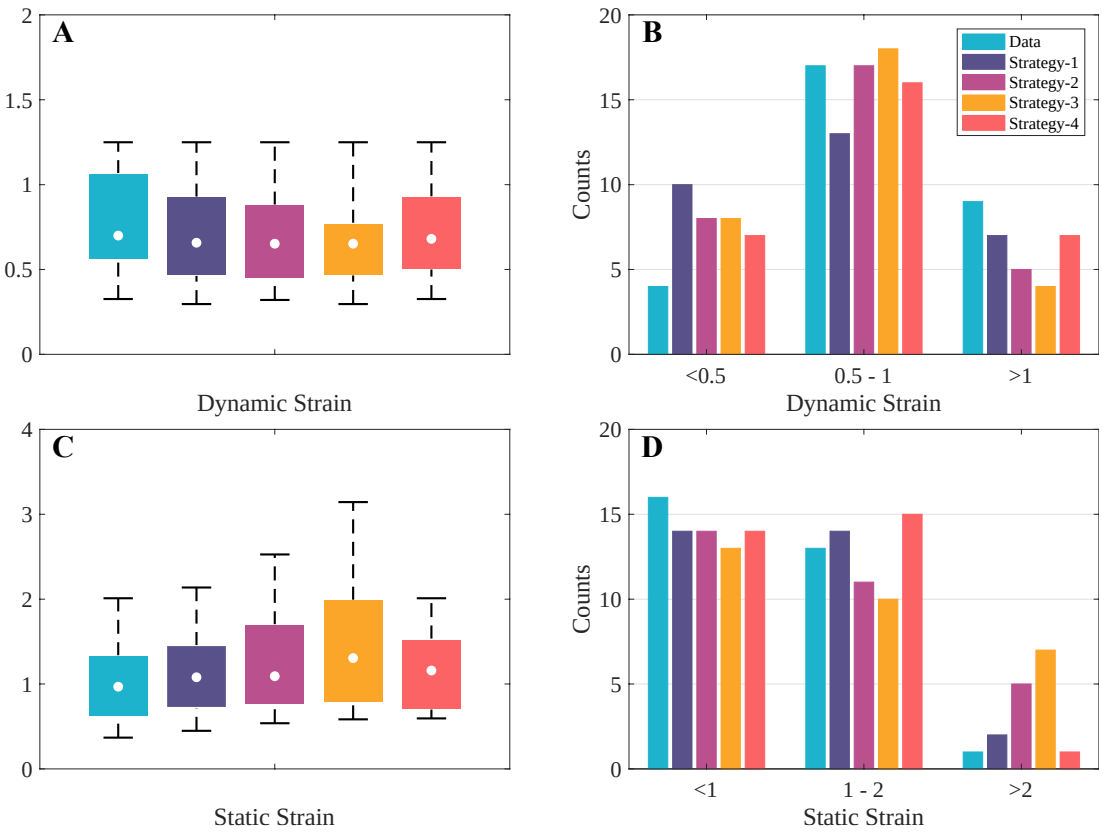

Figure 14. Development Cohort, panels compare the dynamic strain (A)-(B) and static strain (C)-(D) before and after implementing different strategies.

Box plots on the left (A)-(C) show data as median, interquartile range and actual range while histograms on the right (B)-(D) demonstrate the distribution of all patients' data. Strategy 3 had the most impact on static and dynamic strain.

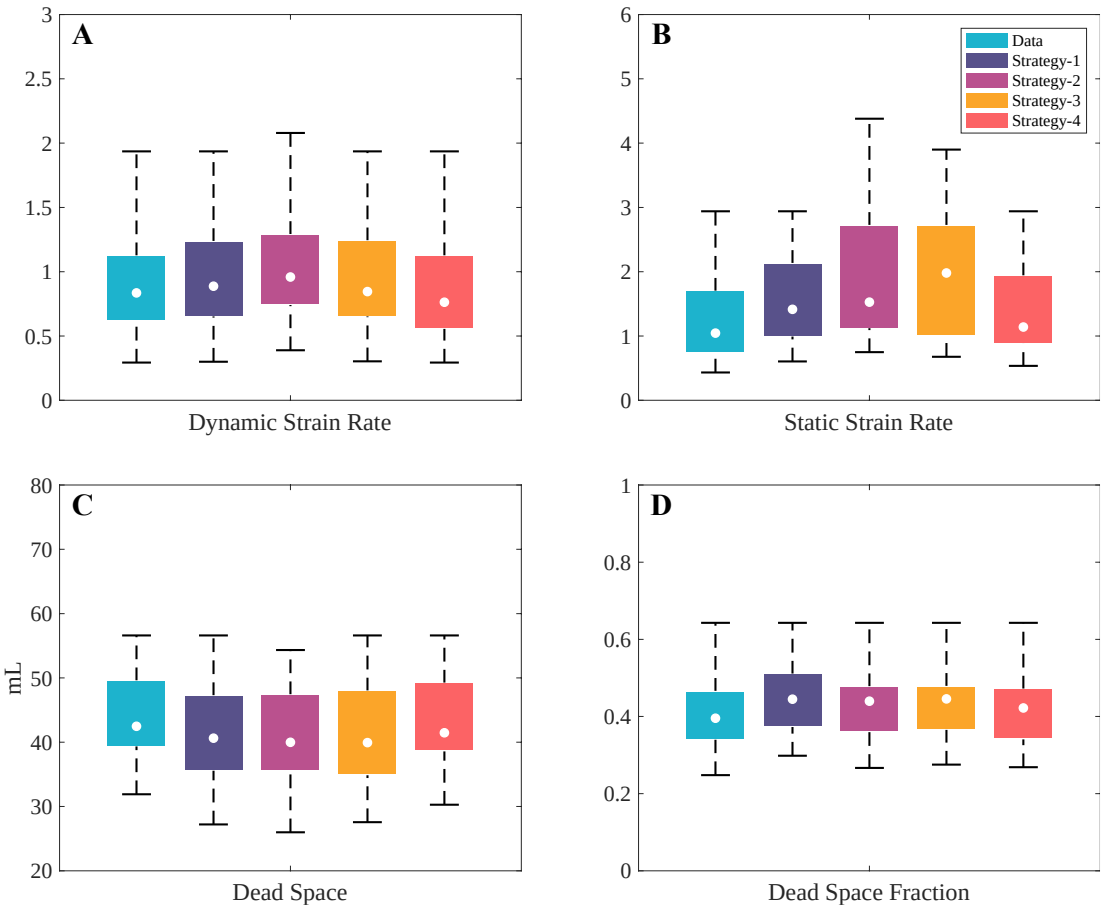

Figure 15. Development Cohort, panels compare the dynamic strain rate (A), static strain rate (B), dead space (C) and dead space fraction (D) before and after implementing different strategies.

Box plots show data as median, interquartile range and actual range. All strategies increased dead space fraction as they had little effect on dead space while reducing V_T.

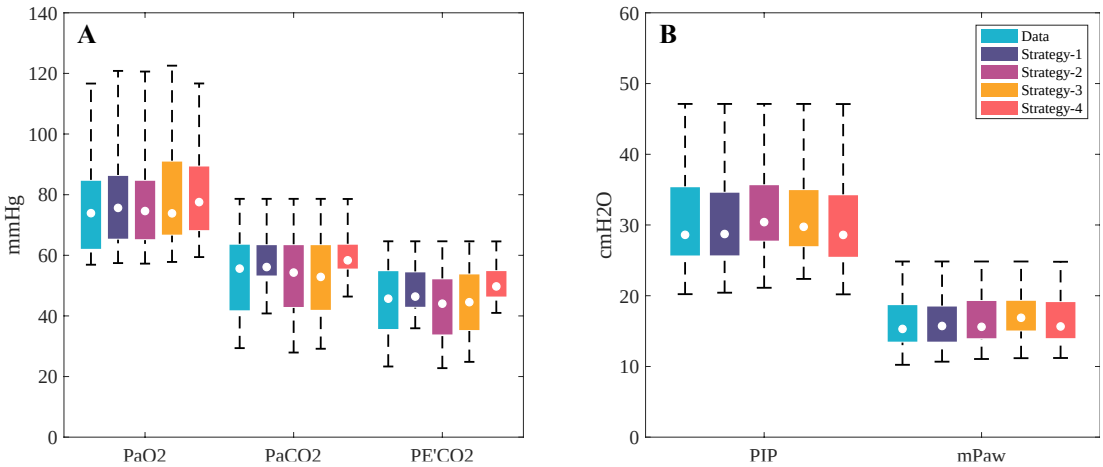

Figure 16. Panels (A) and (B) represent the variations in patients' responses to tidal volume reduction strategies.

The values that are outside the specified safety constraints are from those patients who had such values at baseline. Box plots show data as median, interquartile range and actual range. Amongst the four safety constraints, limits on $PaCO_2$ and RR played the main role in restricting further reduction of V_T. Limits on PaO_2 were never reached.

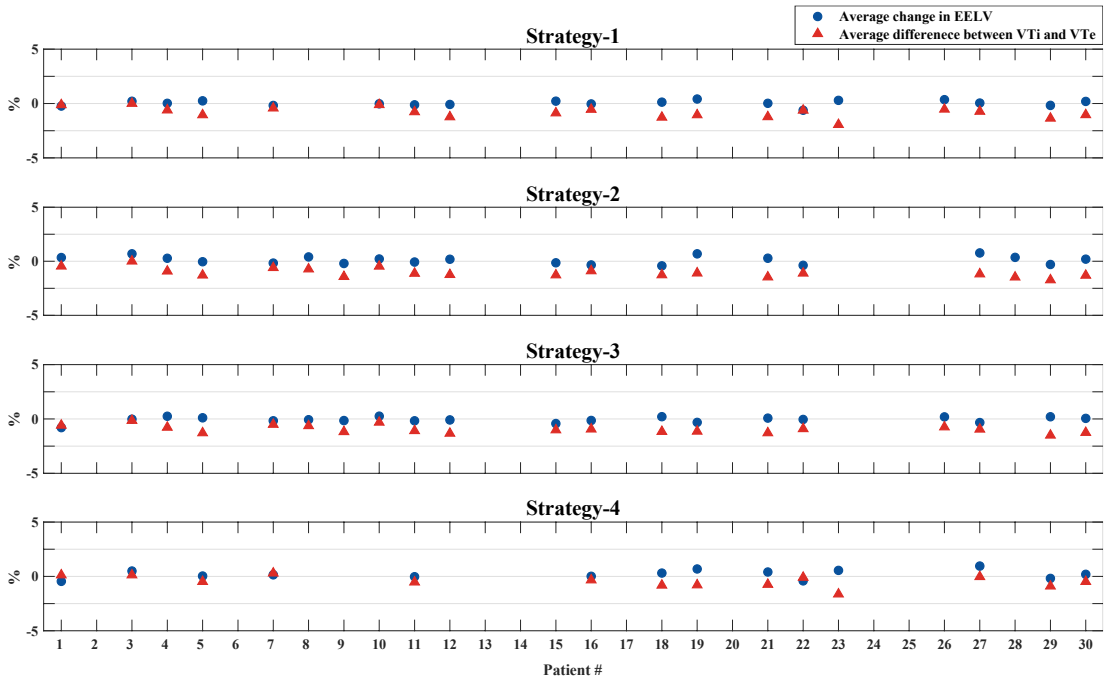

Figure 17. Figure shows the difference between the average inhaled tidal volumes (V_{Ti}) and exhaled tidal volumes (V_{Te}) (red triangles) as well as the change in end-expiratory lung volume (EELV) (blue circles) over a 3h time period.

The results of both investigations confirm that the higher static strains are not a result of breath-stacking.

4.4.3. Additional test cohorts

To test the utility and generalisability of our results, the same 4 strategies are applied to two separate test cohorts of PARDS patients from the CHOP dataset. For both test cohorts, the same fidelity in matching simulated outputs to patient data was observed as with the initial development cohort. Two patients in Test Cohort 1 and three patients in Test Cohort 2 had baseline values of $PaCO_2$ and PIP that would not allow any of the proposed strategies to be implemented.

Similar trends emerged in terms of achieving more protective ventilation for all 4 strategies with these additional datasets (Figure 18 and Figure 24). Strategy 1 produced the largest average reductions in V_T (-22% in Test Cohort 1, -28% in Test Cohort 2) and dynamic strain (-20% in Test Cohort 1, -27% in Test Cohort 2), with the lowest corresponding increase in static strain (+1% in Test Cohort 1, +3% in Test Cohort 2). Strategy 1 produced a small reduction in mechanical power (-4% in both cohorts) and significant reductions in ΔP (-13% and -16%). Although strategies 2 and 3 achieved reductions in V_T, ΔP and dynamic strain; this came at the cost of higher increases in static strain than required by strategy 1. Both strategies 2 and 3 also produced large increases in mechanical power. Finally, strategy 4 produced significant decreases in V_T, dynamic strain and ΔP in both cohorts, and the largest decreases in mechanical power (-10% in Test Cohort 1, -23% in Test Cohort 2). Over the three cohorts analysed, Test Cohort 2 (initial V_T > 10 $mL.kg^{-1}$) showed the greatest potential for improvements in terms of achieving more protective ventilation.

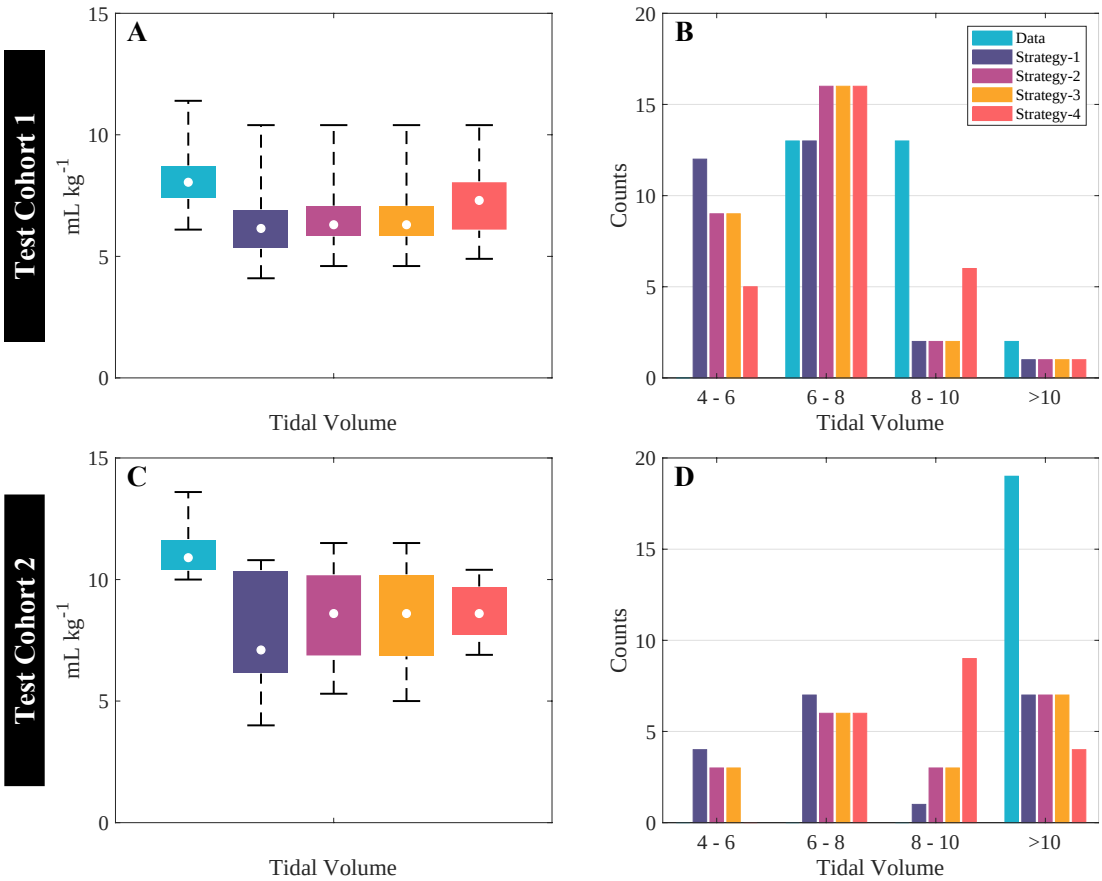

Figure 18. Test Cohort 1&2, panels illustrate the amount of tidal volume reduction.

Box plots on the left (A)-(C) show data as median, interquartile range and actual range while histograms on the right (B)-(D) demonstrate the distribution of all patients' data before and after implementing different strategies. All strategies significantly reduced V_T. Strategy 1 produced the largest average reductions in V_T (-22% in Test Cohort 1, -28% in Test Cohort 2).

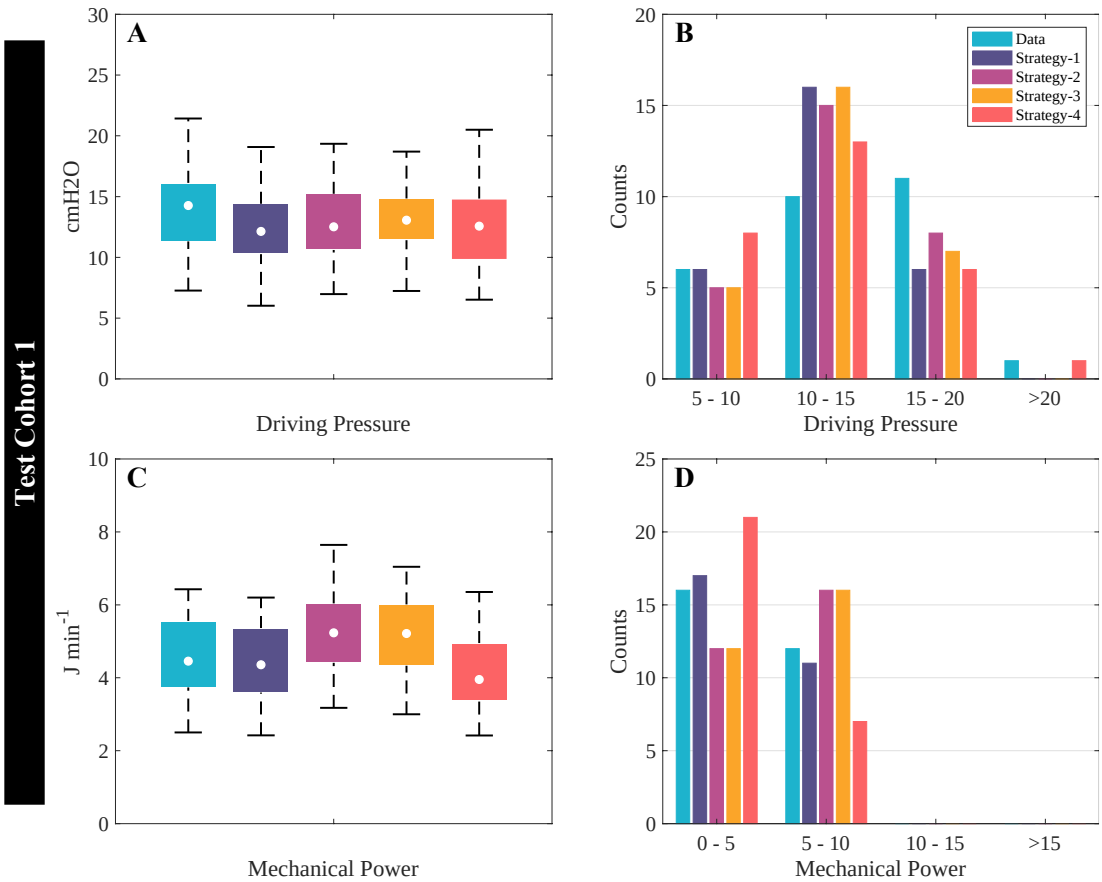

Figure 19. Test Cohort 1, panels illustrate the change in driving pressure (A)-(B) and mechanical power (C)-(D) before and after implementing different strategies.

Box plots on the left (A)-(C) show data as median, interquartile range and actual range while histograms on the right (B)-(D) demonstrate the distribution of all patients' data. Both ΔP and MP were reduced the most in strategies 1 and 4 and raised the most in strategies 2 and 3.

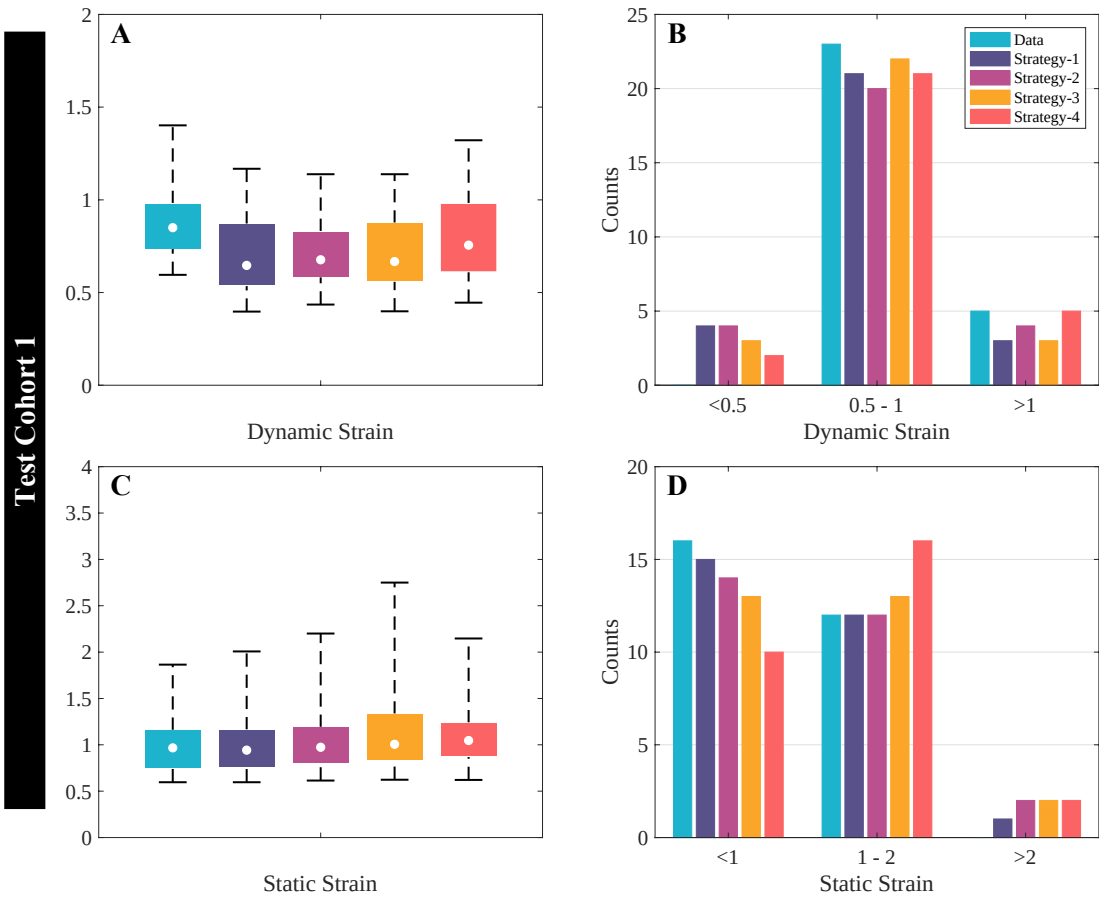

Figure 20. Test Cohort 1, panels compare the dynamic strain (A)-(B) and static strain (C)-(D) before and after implementing different strategies.

Box plots on the left (A)-(C) show data as median, interquartile range and actual range while histograms on the right (B)-(D) demonstrate the distribution of all patients' data.

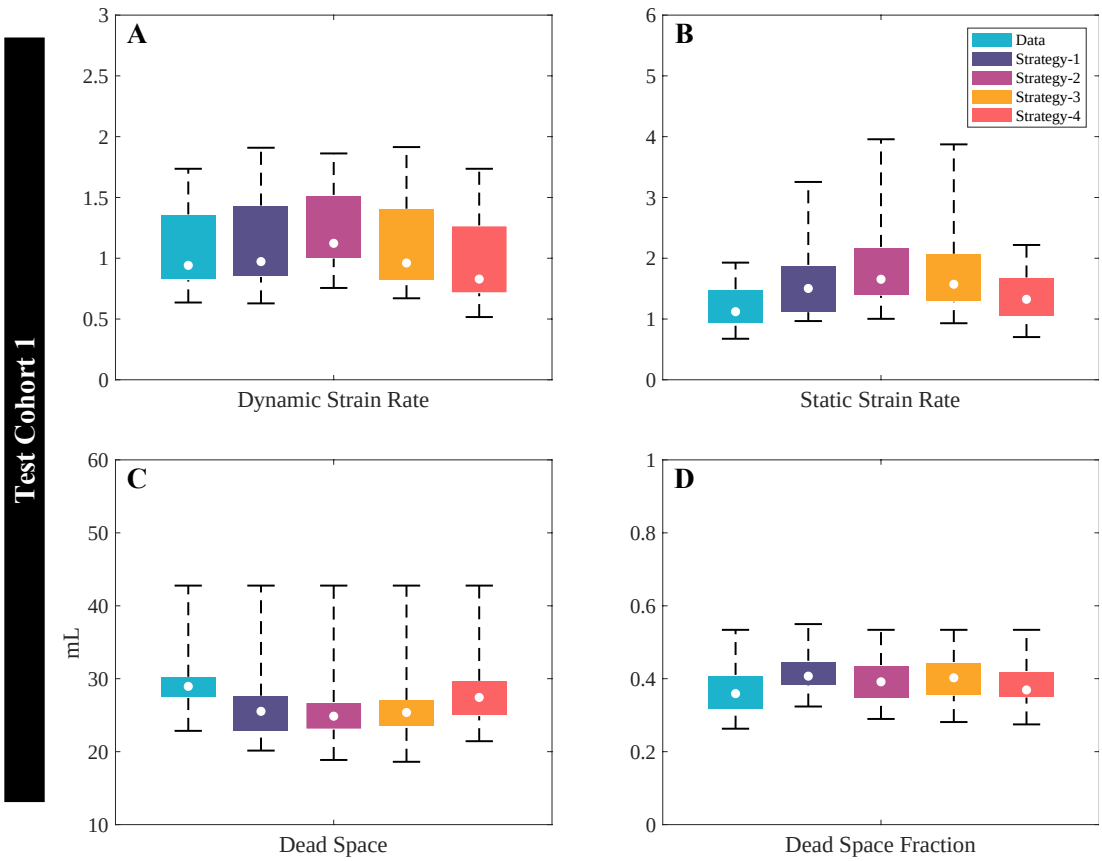

Figure 21. Test Cohort 1, panels compare the dynamic strain rate (A), static strain rate (B), dead space (C) and dead space fraction (D) before and after implementing different strategies.

Box plots show data as median, interquartile range and actual range. All strategies increased dead space fraction as they had little effect on dead space while reducing V_T.

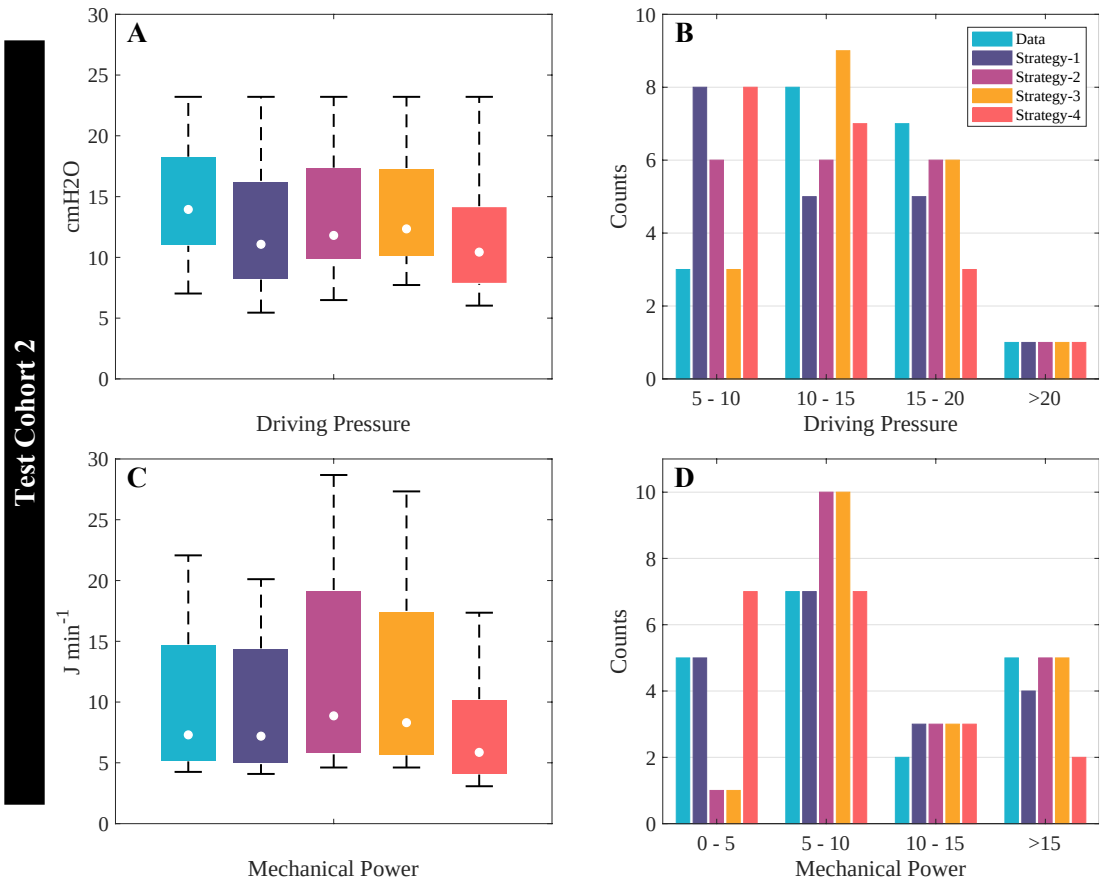

Figure 22. Test Cohort 2, panels illustrate the change in driving pressure (A)-(B) and mechanical power (C)-(D) before and after implementing different strategies.

Box plots on the left (A)-(C) show data as median, interquartile range and actual range while histograms on the right (B)-(D) demonstrate the distribution of all patients' data. Both ΔP and MP were reduced the most in strategies 1 and 4 and raised the most in strategies 2 and 3.

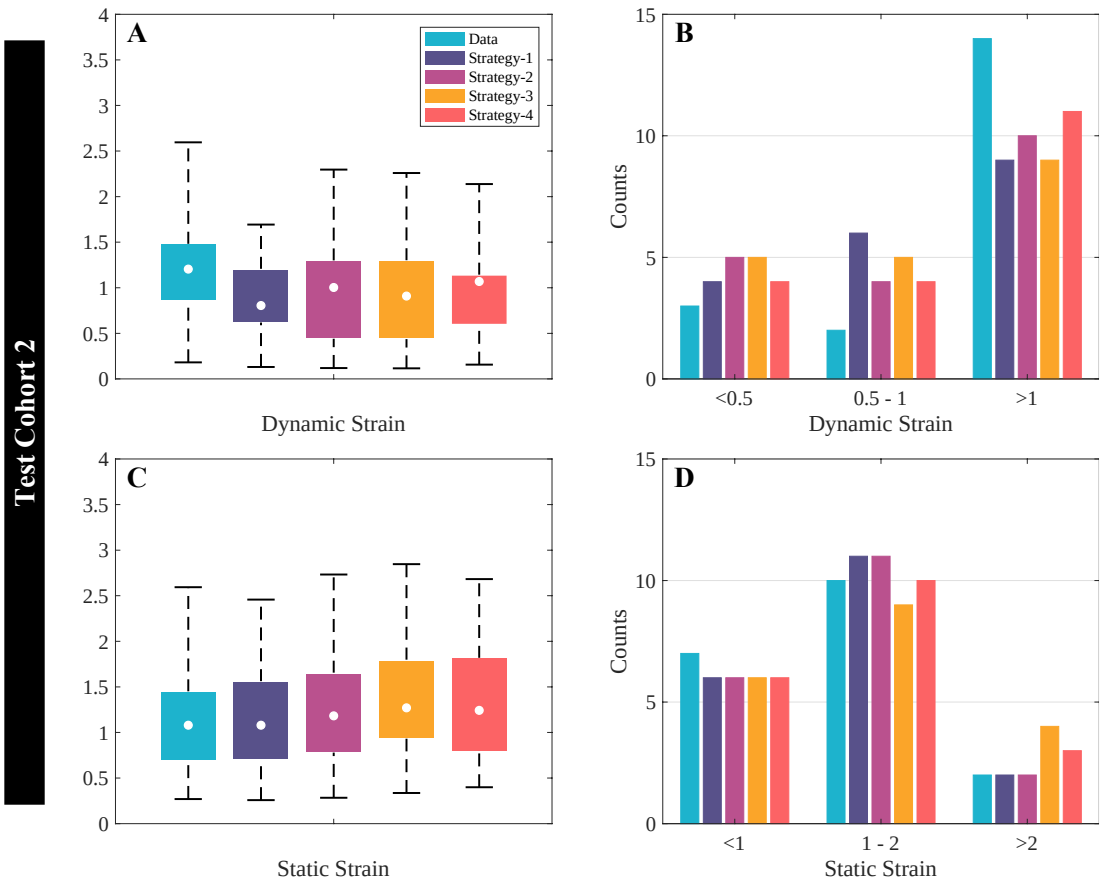

Figure 23. Test Cohort 2, panels compare the dynamic strain (A)-(B) and static strain (C)-(D) before and after implementing different strategies.

Box plots on the left (A)-(C) show data as median, interquartile range and actual range while histograms on the right (B)-(D) demonstrate the distribution of all patients' data. All strategies reduced dynamic strain with a slight increase in static strain.

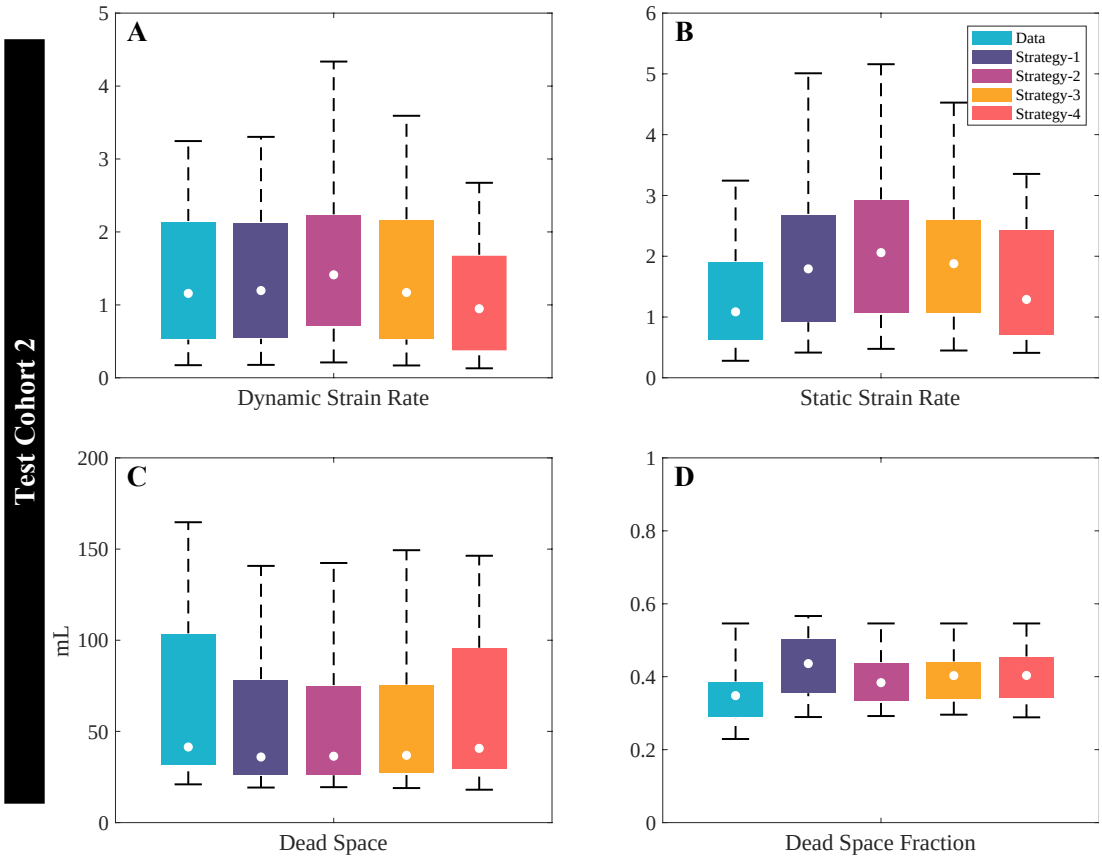

Figure 24. Test Cohort 2, panels compare the dynamic strain rate (A), static strain rate (B), dead space (C) and dead space fraction (D) before and after implementing different strategies.

Box plots show data as median, interquartile range and actual range. All strategies increased dead space fraction as they had little effect on dead space while reducing V_T.

4.5. Discussion

Four separate strategies have been developed and tested for achieving lung protective ventilation in PARDS. A strategy of maintaining MinV allowed for greatest reduction in V_T with small decreases in mechanical power. A strategy of minimizing ΔP resulted in larger reductions in mechanical power, with smaller reductions in V_T. Conversely, strategies aimed at maintaining constant alveolar ventilation, either by manipulating DC or inspiratory flow, are capable of reducing V_T and ΔP, they come at the expense of increasing power. Although some previous studies utilising a uniform low value of V_T showed deleterious effects [140], here V_T was progressively reduced in patients only as long as it did not violate safety constraints on gas exchange or cause any damaging effects. Similarly, while increasing RR in isolation could potentially exacerbate VILI [164, 165], here only RR is increased by modest amounts to compensate for simultaneous reductions in V_T. Our results suggest that there is significant scope for safely adjusting ventilator settings in PARDS to mitigate VILI and demonstrate the utility of simulation to establish testable hypotheses in ventilated children.

Albuali et al. [146] suggested lower V_T was associated with lower mortality in a study of 164 children with PARDS. However, this retrospective study made no allowance for trends showing general improvement in PARDS survival rates over the last decades [149, 166]. Conversely, in a prospective, multicentre observational study, Erickson et al. [148] found higher V_T to be associated with lower mortality. Furthermore, a number of other retrospective and prospective studies failed to identify any significant relationship between V_T and mortality in PARDS [147, 167]. A meta-analysis of observational studies [145] could not establish an association between V_T and mortality in ventilated children, and both PALICC [136] and PEMVECC [139] rely primarily on adult data for their recommendations.

In 2015, PALICC released the first recommendations specifically tailored to PARDS [136], and addressed a number of current issues in patient treatment. Strategies limiting V_T and plateau pressure were marked under "weak agreement." In addition, a survey on stated practice pattern found that although paediatricians theoretically concurred with

adult guidelines to ventilate with lower V_T and pressure constraints, in actual practice, over 25% of PARDS patients are ventilated with V_T > 10 mL kg^{-1} [168], and likely higher in obese children when adjusting for ideal body weight. Likewise, a recent study by Ward et al. [169] revealed poor adherence rates of only 32% (using a V_T cut-off of 6.5 mL kg^{-1}) and 58% (using a cut-off of 8 mL kg^{-1}) for using low V_T.

Despite this, mortality rates in PARDS have improved over the last two decades, part of which may be related to adoption of lung-protective ventilation strategies and extrapolation from adult ARDS literature. Continued resistance to lung-protective ventilation in PARDS, particularly use of V_T > 10 mL kg^{-1}, may reflect concerns regarding whether V_T and ventilator pressures can be safely reduced in this population. Here, the feasibility of adjusting ventilator settings to mitigate VILI within reasonable safety parameters for gas exchange and RR is demonstrated. The reductions achieved are most pronounced in subjects with V_T > 10 mL.kg^{-1} and appear to be generalizable throughout the entire age range and severity encountered in PARDS. While studies of ΔP and mechanical power limits are in their infancy, preliminary data suggest "thresholds" above which these values are associated with worse outcomes [143, 170]. Analysis of our dataset shows that these thresholds are currently being exceeded in many subjects, particularly in children with V_T > 10 mL kg^{-1}.

Static strain represents the initial displacement of the lungs from their original position due to PEEP at the start of ventilation and subsequently stays constant during ventilation unless PEEP is changed. It has been shown that the lung can tolerate increased static strain, provided that the total lung capacity is not exceeded, and that dynamic strain is likely to be more injurious [161, 163]. The change in lung strain is also correlated with the recruited volume of the lung. A recent study showed that lung recruitment causes reduction in dynamic strain while increasing static strain [163]. Hence, both the changes in static and dynamic strain observed in our results suggest general improvement in lung recruitment as a result of the changes to ventilator settings.

Strategy 4 resulted in reduced mechanical power. The original power equation (Eq.44) by Gattinoni et al. can be simplified and re-written as the equation below [142]:

$$MP = RR \times V_T \times \left(PIP - 0.5P_{plat} + 0.5PEEP\right) = RR \times V_T \times (PIP - 0.5\Delta P) \quad (46)$$

Considering the above equation, it can be expected that an increment in inspiratory flow (Eq.39) leads to an increase in power as long as the cause of the change in flow is MinV (i.e. $RR \cdot V_T$). However, when MinV was kept constant and a smaller DC raised the flow, the resultant change in power depends on how PIP and P_{plat} respond to the adjustment – i.e. specifically the change of (PIP-0.5ΔP). As a result, it cannot be concluded that a greater flow would always lead to a rise in the power. Moreover, it should be noted that MinV directly impacts the power, not the flow itself. For instance, patients were ventilated with the same flow in strategy-1 and strategy-3, while the latter has a larger MinV, and so higher power.

The study has a number of limitations. Data were derived from a single institution, and while severity of PARDS and outcomes were similar to other cohorts, generalizability remains to be demonstrated. To minimise possible confounding factors, the model is currently configured to represent patients that are fully sedated under mechanical ventilation, therefore autonomic reflex modules in the model were not utilised. The model also does not include the effect of inflammatory mediators commonly found in PARDS, which are difficult to quantify and isolate in clinical settings. As the model is computational in nature, it does not provide any direct histological or biological evidence of the effects of the proposed ventilation strategies on VILI markers, and therefore further animal and/or human studies should be performed to provide conclusive evidence of their relative effectiveness in achieving more protective ventilation. As adolescents may be diagnosed with either Berlin or PALICC criteria [171], it is unclear whether they would be more appropriately managed with our protocol, or an adult version. The model was developed to focus on VILI, and those chose to use $PaCO_2$, rather than pH. While this may not entirely reflect clinical practice, in which pH is monitored alongside $PaCO_2$, the simulator cannot accommodate something as variable as pH, which is often modified by entire non-ventilator interventions, such as volume resuscitation or exogenous bicarbonate.

Chapter 5:

Evaluating the utility of driving pressure and mechanical power to determine optimally protective ventilator settings in two cohorts of adult and paediatric ARDS patients

5.1. Summary

Mechanical power and driving pressure have recently been proposed as indicators, and possibly drivers, of ventilator-induced lung injury. In this chapter, the utility of these different measures as targets to derive maximally protective ventilator settings is tested. The computational simulator was matched to individual patient data and used to identify strategies that minimize ΔP, MP and a modified version of MP (MMP) that removes the direct linear positive dependence between MP and PEEP. Data from the low tidal volume arm of the ARDSnet trial (N=100) and from an observational study of paediatric ARDS from the Children's Hospital of Philadelphia (N=77 – the same data as used in Chapter 4) was used for the study. Global optimization algorithms evaluated

more than 26.7 million changes to ventilator settings (approximately 150,000 per patient) to identify strategies that minimize ΔP, MP or MMP. Large average reductions in ΔP (23%-Paediatric, 23%-Adult), MP (44%-Paediatric, 66%-Adult) and MMP (61%-Paediatric, 67%-Adult) were achievable in both cohorts when oxygenation and ventilation were allowed to vary within specified safe ranges. Reductions in ΔP (12%-Paediatric, 2%-Adult), MP (24%-Paediatric, 46%-Adult) and MMP (44%-Paediatric, 46%-Adult) were still achievable even when no deterioration in gas-exchange was allowed. Minimum values of MP and MMP in both cohorts were produced by increasing V_T and decreasing respiratory rate. Minimising MMP rather than MP resulted in higher values of PEEP in both cohorts. In the paediatric cohort, minimum ΔP was achieved by reducing V_T and increasing RR and PEEP. The adult dataset had limited scope for further reducing V_T, but ΔP could still be significantly reduced by increasing PEEP. Our analysis identified different ventilatory strategies that minimized ΔP or MP consistently across adult and paediatric datasets. Minimizing standard and alternative formulations of MP led to significant increases in VT. Targeting ΔP for minimisation resulted in ventilator settings that also reduced MP and MMP, but not vice versa.

5.2. Introduction

Mechanical power (Eq.44) [142–144], and driving pressure (Eq.40) [141], have recently been proposed as important measures of VILI in acute respiratory distress syndrome. Arguments for the importance of MP focus on the biophysical role of energy (stress×strain) and dynamics (rates of airway pressure change and cycling frequency) in the injurious potential of mechanical ventilation [144], whereas arguments for the centrality of ΔP are supported by statistical and computational analyses of clinical trial data that show strong correlations between the level of ΔP applied and relative risk of mortality [84, 141]. However, the rationale for both MP and ΔP rely on re-analyses of adult ARDS cohorts, and while initial studies are in progress (NCT03616704 and NCT03939260), an intervention targeting either parameter has yet to be proven efficacious.

To date, there has been no randomized trial to determine the appropriate application of protective ventilation in PARDS, and observational studies are unclear, with conflicting results [145–148]. Ventilator management in children is often extrapolated from adults, with uncertain applicability [172]. PARDS has a distinct epidemiology, with different inciting aetiologies and predictors of outcome [137, 173], relative to adults, necessitating specific investigations in children. Overall, even less evidence is available for children regarding the utility of either MP or ΔP as metrics of VILI or as modifiable ventilator parameters.

To investigate the above issues, the high-fidelity computational simulator is employed and matched to individual patient data from two separate cohorts, paediatric and adult. High-fidelity simulation holds the potential to develop, test, and directly compare ventilation strategies prior to exposing vulnerable patients to potentially damaging interventions. Global optimization algorithms, implemented on high-performance computing clusters, were used to evaluate more than 26.7 million different changes to the baseline ventilator settings to identify those that minimized, in each individual simulated patient, ΔP, MP, and a modified formulation of MP (MMP) based on concerns [174] regarding the direct, positive, linear effect of PEEP on MP in the original MP equation. Changes to ventilator settings were constrained within specified limits, and maximally protective settings optimizing ΔP, MP, and MMP were calculated for two different scenarios (a) allowing, within safe limits, some deterioration in patient gas-exchange from baseline values, and (b) without allowing any deterioration in patient gas exchange. The primary aim of this study was to assess the scope for achieving more protective ventilation by separately minimising ΔP, MP or MMP. A secondary goal of the study was to investigate to what extent protective ventilation strategies identified for the paediatric cohort were consistent with those computed for the adult cohort.

5.3. Materials and Methods

5.3.1. Patient selection

Paediatric cohort

Patients were selected from an ongoing (2011 onwards) observational prospective cohort [149] of intubated children meeting Berlin criteria for ARDS from the Children's Hospital of Philadelphia (CHOP). Seventy-seven subjects between 1 month and 18 years of age (Mean: 3.1, SD: 3.3, 23% severe, 44% moderate and 33% mild ARDS), ventilated via cuffed endotracheal tube during neuromuscular blockade, were selected. For full details see Section 4.3.1.

Adult cohort

Data were extracted from 100 adult ARDS patients randomly selected (14% severe, 66% moderate, 20% mild) from the low tidal volume arm of the ARMA trial [4]. Access to the data was granted by the Biologic Specimen and Data Repository Information Coordinating Centre (BioLINCC) of the National Heart, Lung and Blood Institute (NHLBI). The data were provided in a de-identified state, and informed consent was not required. All patients received mechanical ventilation in assist-control ventilation mode.

5.3.2. Simulator calibration to patient data

Analyses were carried out using the simulator described in Chapter 2 and Chapter 4 (see Section 2.4 and Section 4.3.2). The simulator was matched to individual patient data using advanced global optimisation algorithms (see Section 3.3.1).

5.3.3. Maximally protective ventilation as a constrained optimisation problem

After matching the model to each individual patient, the potential for achieving maximally lung-protective (but acceptably effective) ventilation in these patients was investigated by formulating and numerically solving several different optimisation problems. For each individual patient, advanced global optimisation algorithms implemented on high-performance computing clusters is used to exhaustively search

through more than 26.7 million different changes to the reported ventilator settings – namely V_T, RR, F_IO_2, PEEP and duty cycle DC (inspiratory-to-total time ratio) to identify which settings produced minimum values of the following quantities:

- Driving pressure (Eq.40);
- Mechanical Power (Eq.44);
- A modified version of mechanical power (MMP) [174], given by:

$$\mathrm{MMP} = 0.098 \times \mathrm{RR} \times {V_T}^2 \times \left[0.5 \times \mathrm{EL_{rs}} + \mathrm{RR} \times \frac{(1 + \mathrm{I{:}E})}{60 \times \mathrm{I{:}E}} \times \mathrm{R_{aw}}\right] \qquad (47)$$

which removes the direct linear, positive dependence between MP and PEEP [174].

To ensure the relevance of these optimisation problems to clinical practice, it is necessary to constrain the search for maximally protective settings to include only those that do not compromise the provision of adequate oxygenation and ventilation. This is achieved firstly by defining upper and lower allowable limits for the ventilation settings themselves (Table 6), and secondly by defining allowable limits for the values of patient blood gases PaO_2 and $PaCO_2$ and peak inspiratory pressure (Table 6) produced by the settings. The upper limit of RR in adults is set slightly higher than that in ARDSnet trial (40 vs 35 bpm) as higher RRs were observed at the baseline and were considered a plausible limit by clinicians. Ventilation settings that minimized ΔP, MP and MMP while keeping values of PaO_2, $PaCO_2$ and PIP within their specified limits were then computed for each patient (Approach 1). In the paediatric cohort, these limits were based on those used in the ARDSnet trial, adapted to match paediatric conventions [147, 148, 172, 175]. As the paediatric cohort was developed using decelerating flow, as is most common in paediatrics [176], PIP was used as a constraint rather than P_{plat}. When data indicated that a patient's initial ventilator state did not comply with one or more of the specified safety limits, changes to the settings were only made if they led to an improvement in the relevant parameters (e.g. reducing $PaCO_2$ or PIP).

As an alternative strategy, it is also investigated whether changes to ventilator settings could be found that minimized ΔP, MP and MMP without resulting in any deterioration

in PaO_2 and $PaCO_2$ from their baseline values (Approach 2). An upper limit of 35 cmH_2O was again applied for PIP in the paediatric cohort. Due to relatively higher baseline PIP values in adults, the upper limit of PIP was set to the corresponding baseline values for these patients – Figure 33 and Figure 34.

5.3.4. Statistical analysis

Data are presented as Mean ± SD, or shown graphically using median, interquartile and total ranges. To avoid violation of underlying distribution assumptions, variables were compared using nonparametric statistics when appropriate (i.e. Wilcoxon signed-rank test). A two-sided p-value of < 0.05 was considered significant.

5.4. Results

5.4.1. The simulator accurately represents individual patient data

The ability of the simulator to reproduce patient data was verified by comparing its responses (PaO_2 and $PaCO_2$) against data on the responses of patients from both cohorts. After model calibration, each individual patient in the cohort was simulated for 30 minutes (or until reaching steady state) under volume controlled mechanical ventilation with constant flow in the supine position. The results of matching for the paediatric cohort has been presented in Chapter 4 (see Figure 9 and Figure 10). For adult cohort, Figure 25 (A) and (C) compares the outputs of the simulator with the original data, expressed as median, interquartile range and actual range. Also, Figure 26 (A) and (B) shows the Bland-Altman plots for data points versus simulator output values. These results confirm the capability of the simulator to accurately replicate multiple output values of the patients included in both cohorts across a range of different ventilator settings.

Table 6. Allowable ranges of variation for ventilator parameters (approach 1 and 2) and predefined safety constraints (approach 1).

	Paediatric		Adult	
	Lower Limit	Upper Limit	Lower Limit	Upper Limit
Allowable ranges for ventilator parameters				
PEEP (cmH_2O)	5	18	5	20
RR (bpm)	10	40	10	40
V_T ($mL.kg^{-1}$)	3	12	3	10
DC	0.3	0.6	0.2	0.8
F_IO_2	0.21	1	0.21	1
Predefined safety constraints				
PaO_2 (mmHg)	60	120	55	100
$PaCO_2$ (mmHg)	-	60	-	60
PIP (cmH_2O)	-	35	-	35

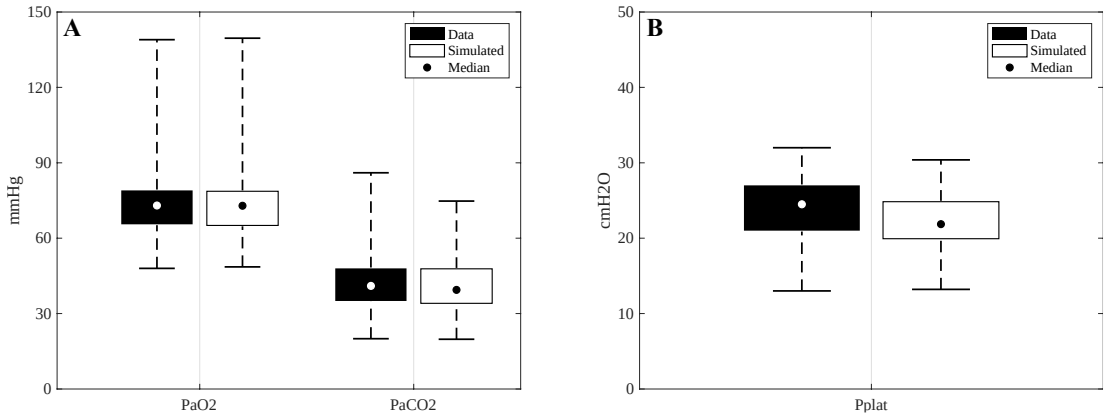

Figure 25. A comparison of the simulator outputs with the original adult patient data in panels (A) and (B), expressed as median, interquartile range and actual range.

The ability of the simulator to reproduce patient data was verified by comparing its responses (PaO_2 and $PaCO_2$) against data on the responses of patients from both cohorts.

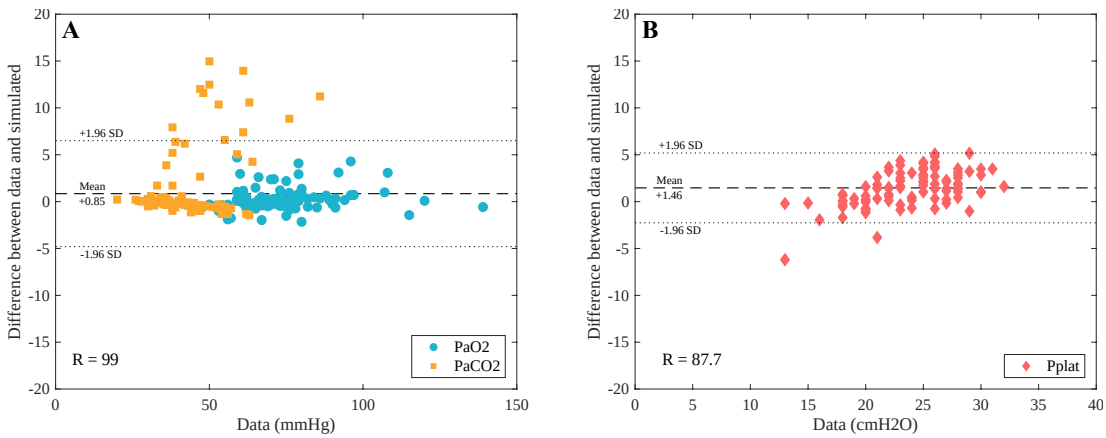

Figure 26. Panels (A) and (B) show the Bland-Altman plots for simulator outputs and original adult patient data. "R" represents the correlation coefficient of the data and the simulated values.

5.4.2. Reductions in ΔP, MP and MMP were achieved in both cohorts

When ABGs were allowed to vary within pre-specified ranges given in Table 6, average maximum reductions in ΔP of 3.0±2.2 cmH_2O (23%) compared to baseline values in the paediatric cohort and 3.2±2.1 cmH_2O (23%) in the adult cohort were achievable – Figure 27. Reductions in ΔP of over 1 cmH_2O were achieved in 95% of paediatric and 82% of adult patients. The corresponding reductions when targeting MP were 3.3±2.6 $J.min^{-1}$ (44%) in the paediatric cohort (87% of whom had MP reduced by more than 20%) and 21.0±5.4 $J.min^{-1}$ (66%) in the adult cohort, with all patients reducing MP by over than 20%. When targeting the modified formulation of mechanical power MMP, the reductions achievable were 3.7±2.3 $J.min^{-1}$ (61%) in the paediatric cohort and 15.2±4.9 $J.min^{-1}$ (67%) in the adult cohort (reductions of more than 20% were achieved in 95% and 99% of the paediatric and adult cohorts respectively). Reductions were statistically significant in all groups (Wilcoxon signed-rank test $p<0.05$). In all the above cases, more protective ventilation was achieved with no significant deterioration in patient oxygenation (PaO_2), although values of patient $PaCO_2$ did consistently tend to increase towards the upper limits – Figure 28. In both cohorts, settings that minimized ΔP also reduced MP and MMP, whereas settings that minimized MP and MMP increased ΔP (largely due to the resulting increases in V_T).

When the optimisations were constrained to allow no deterioration in gas exchange (i.e. only changes to ventilator settings that maintained, or improved, PaO_2 and $PaCO_2$ with respect to their baseline values were allowed), reductions were achievable in ΔP of 1.6±1.4 cmH_2O (12%) compared to baseline values in the paediatric cohort (58% had reductions of more than 1 cmH_2O) and 0.4±1.0 cmH_2O (2%) in the adult cohort (16% had reductions of more than 1 cmH_2O) – Figure 29. The corresponding reductions when targeting MP were 1.7±1.4 $J.min^{-1}$ (24%) in the paediatric cohort and 14.4±4.9 $J.min^{-1}$ (46%) in the adult cohort, with 57% of paediatric and 98% of adult patients having MP reduced by more than 20%. When targeting MMP, the reductions achievable were 2.5±1.5 $J.min^{-1}$ (44%) in the paediatric cohort (90% of whom had reductions of more than 20%) and 10.3±4.4 $J.min^{-1}$ (46%) in the adult cohort, with 97% achieving reductions of more than 20%. Reductions were statistically significant in all cases

(Wilcoxon signed-rank test $p<0.05$). The individual results for both cohorts are shown in Figure 31 and Figure 32.

5.4.3. Minimum values of ΔP and MP are achieved by distinct ventilation strategies

Minimum values of MP in both adult and paediatric cohorts were produced by changes to ventilator settings that *increased* V_T (Paediatric: 1.4±1.8 mL.kg^{-1} (+19%), Adult: 1.9±1.1 mL.kg^{-1} (+34%)), decreased RR (Paediatric: -8.6±5.1 bpm (-34%), Adult: -15.6±5.0 bpm (-56%)), set DC at or close to its specified upper limit of 0.6, and set PEEP at or close to its specified lower limit of 5 cmH_2O – Figure 35 to Figure 38. F_IO_2 increased in both paediatric and adult cohorts (Paediatric: +39%, Adult: +26%).

Similar changes in V_T, RR and DC were observed in both cohorts when targeting the MMP. As expected, minimising MMP rather than MP resulted in higher values of PEEP in both paediatric and adult cohorts (Paediatric: 2.9±4.6 cmH_2O (+39%), Adult: 3.5±5.0 cmH_2O (+52%)) along with lower values of F_IO_2 in paediatric patients (-21%).

In the paediatric cohort, minimum ΔP was achieved by reducing V_T (1.3±1.6 mL.kg^{-1} (-15%)) while increasing RR and PEEP (2.3±8.2 bpm (+11%) and 2.4±4.5 cmH_2O (+34%) respectively). In the adult cohort, no significant reductions in V_T were possible (unsurprisingly, since the selected patients were from the low V_T arm of the ARDSnet trial), but ΔP could still be reduced, principally by increasing PEEP (2.2±3.5 cmH_2O (+32%)). No substantial changes in DC were observed in either cohort when targeting ΔP. Patterns of changes in ventilator settings were strongly consistent in most cases between Approach 1 (allowing some deterioration in blood gas values) and Approach 2 (allowing no deterioration in blood gas values), although when minimising ΔP in paediatric patients, Approach 2 produced higher values of F_IO_2 than Approach 1, in order to satisfy the requirement for no deterioration in oxygenation.

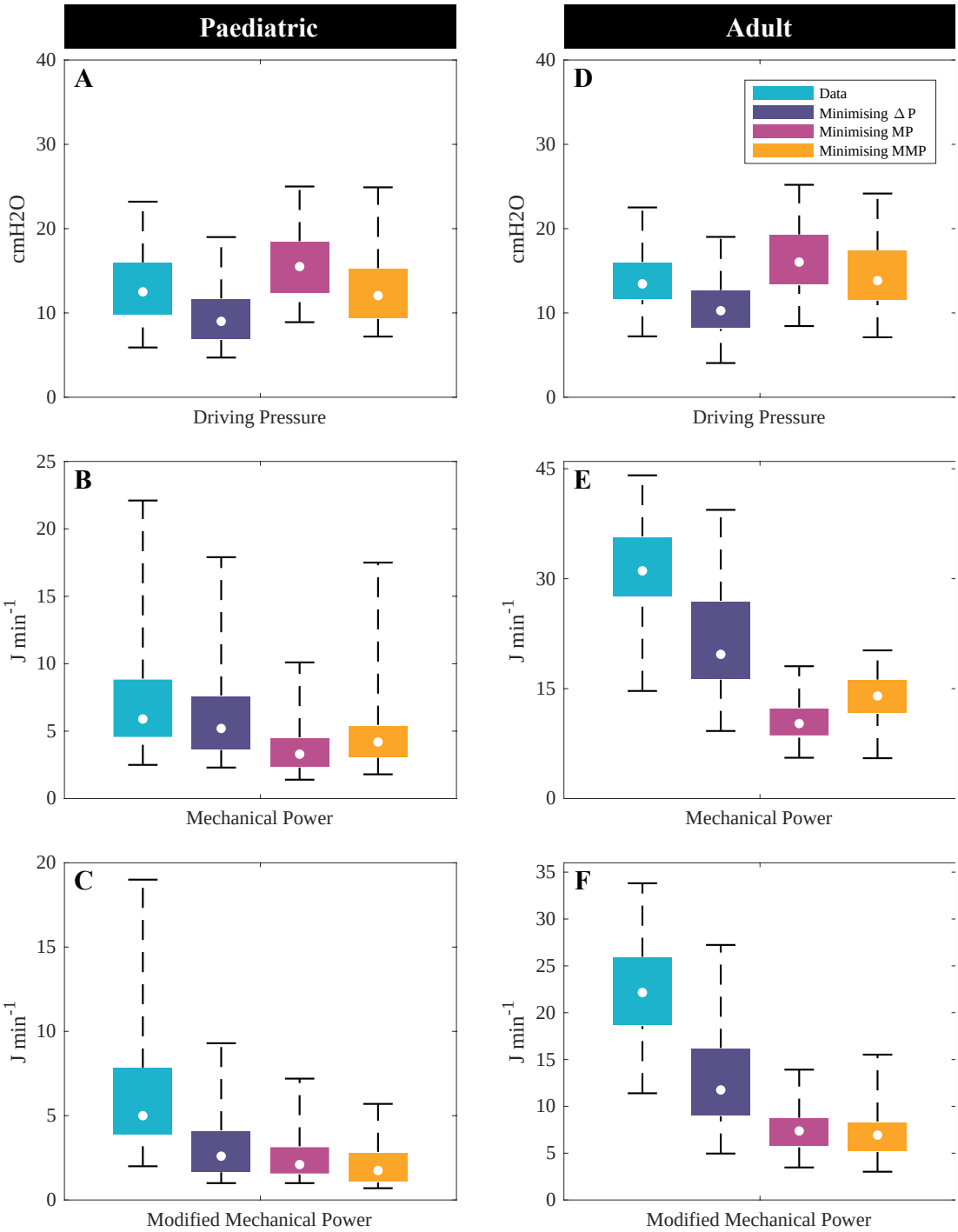

Figure 27. Approach 1 – Change in driving pressure, mechanical power and modified mechanical power when minimising different targets (i.e. ΔP, MP and MMP) and allowing some deterioration in patient gas-exchange. Box plots demonstrate data as median, interquartile range and actual. Minimising ΔP also reduced MP and MMP while minimising MP or MMP increased ΔP.

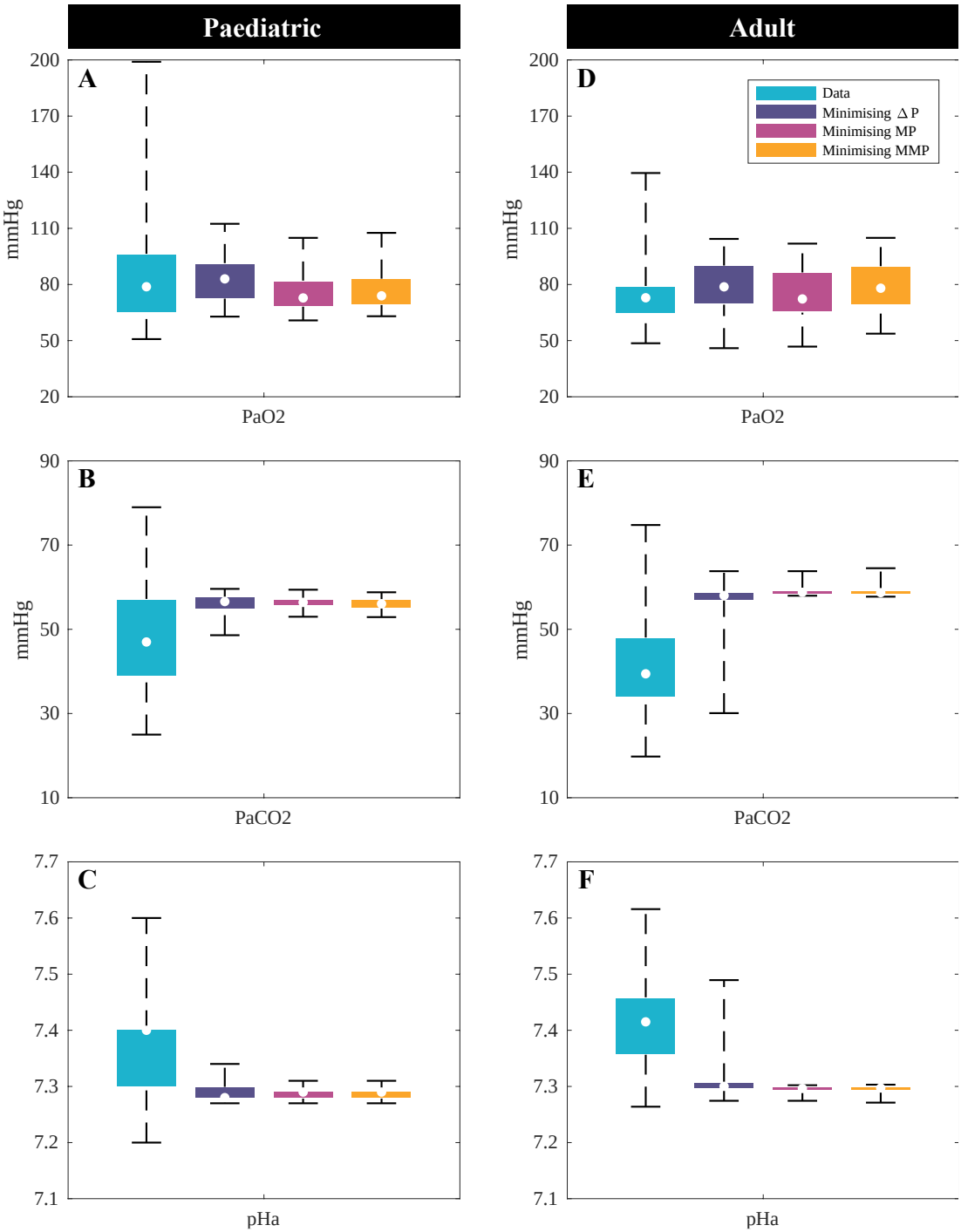

Figure 28. Approach 1 – Change in PaO_2, $PaCO_2$ and pH when minimising different targets and allowing some deterioration in patient gas-exchange. Panels (A) to (C) show results for the paediatric cohort and (D) to (F) for the adult cohort. Box plots demonstrate data as median, interquartile range and actual.

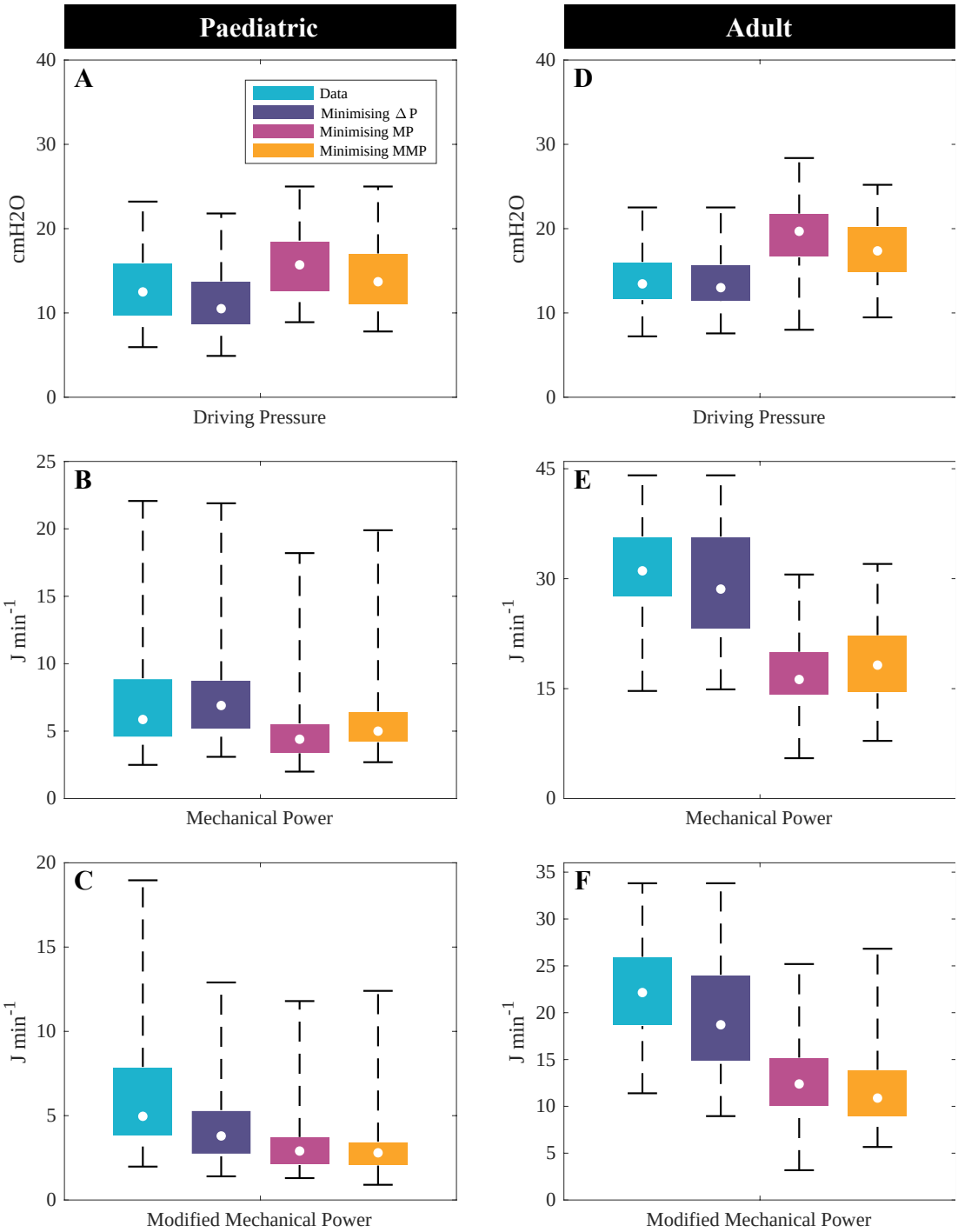

Figure 29. Approach 2 – Change in driving pressure, mechanical power and modified mechanical power when minimising different targets (i.e. ΔP, MP and MMP) and allowing no deterioration in gas-exchange. Panels (A) to (C) show results for the paediatric cohort and (D) to (F) for the adult cohort. Box plots demonstrate data as median, interquartile range and actual.

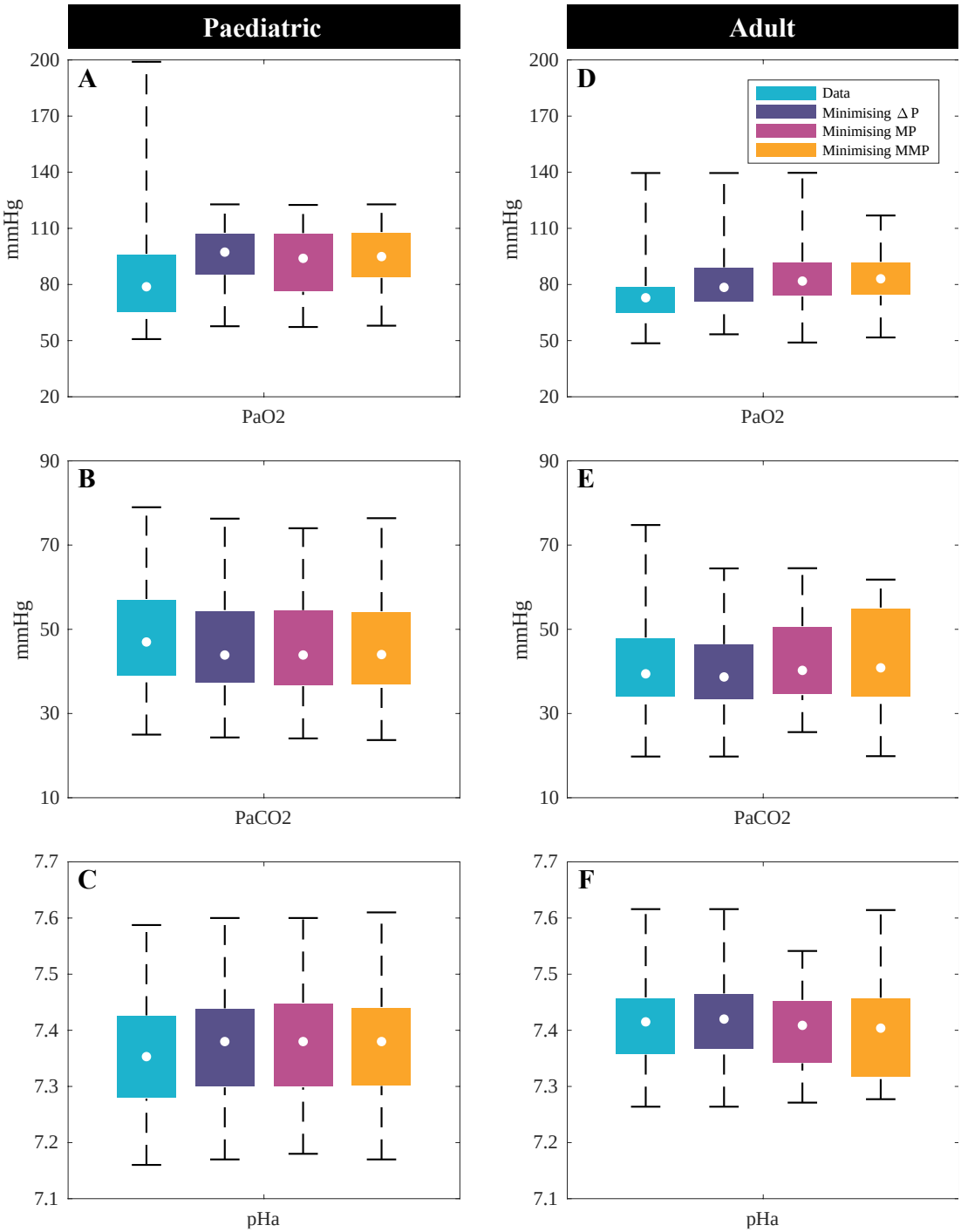

Figure 30. Approach 2 – Change in PaO_2, $PaCO_2$ and pH when minimising different targets and allowing no deterioration in gas-exchange. Panels (A) to (C) show results for the paediatric cohort and (D) to (F) for the adult cohort. Box plots demonstrate data as median, interquartile range and actual.

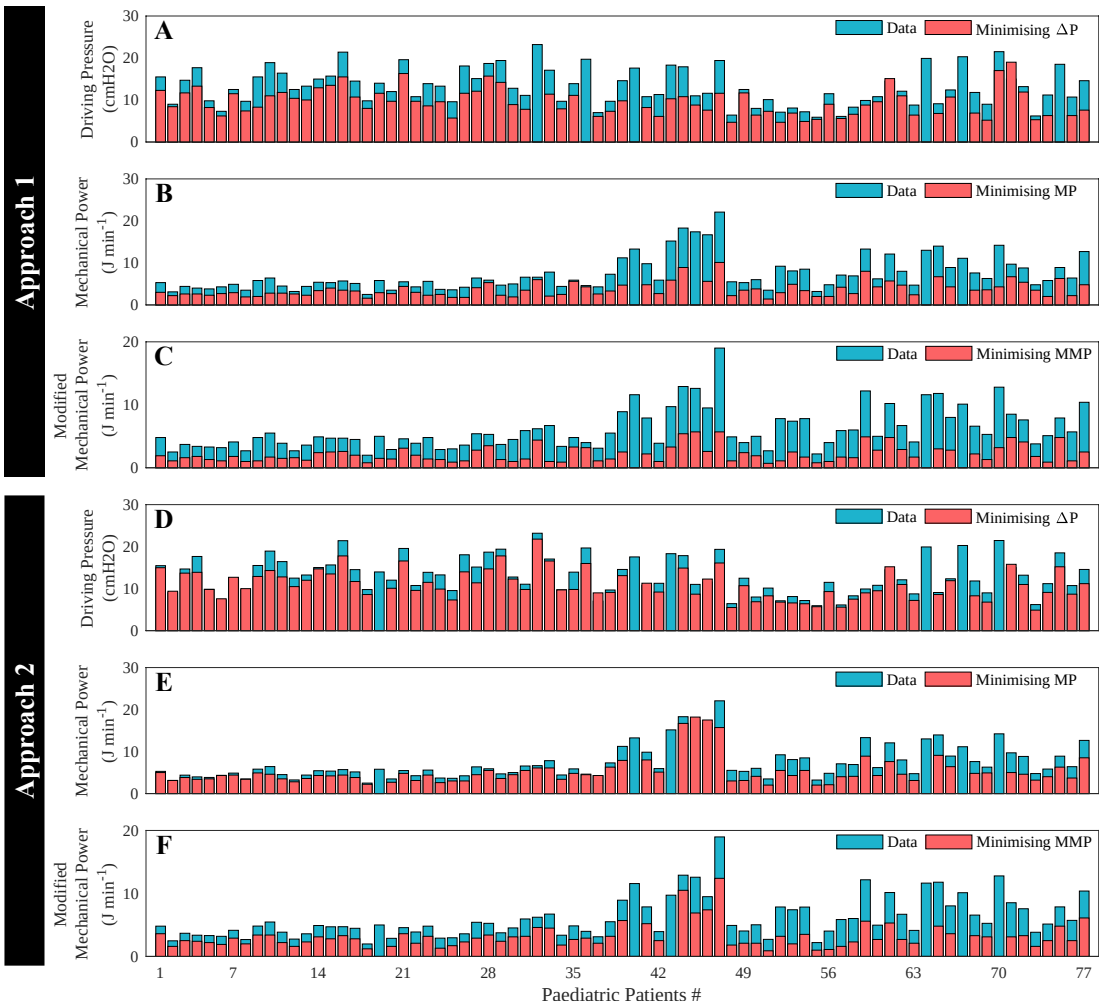

Figure 31. Paediatric Patients – Initial and minimised values of ΔP, MP and MMP in individual patients.

Panels (A) to (C) show results for Approach1 (i.e. allowing some deterioration in patient gas-exchange). Panels (D) to (F) show results for Approach 2 (i.e. allowing some deterioration in patient gas-exchange.)

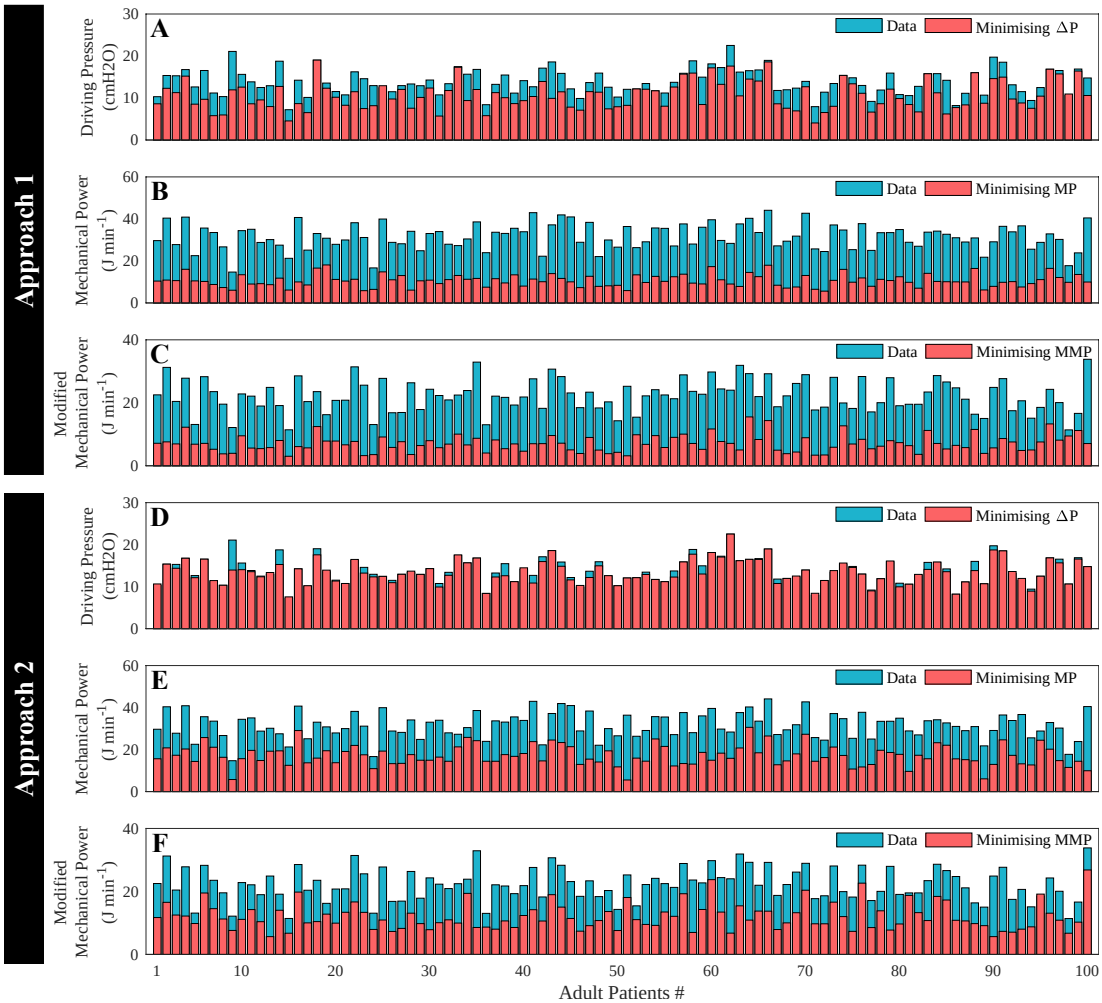

Figure 32. Adult Patients – Initial and minimised values of ΔP, MP and MMP in individual patients.

Panels (A) to (C) show results for Approach1 (i.e. allowing some deterioration in patient gas-exchange). Panels (D) to (F) show results for Approach 2 (i.e. allowing some deterioration in patient gas-exchange.)

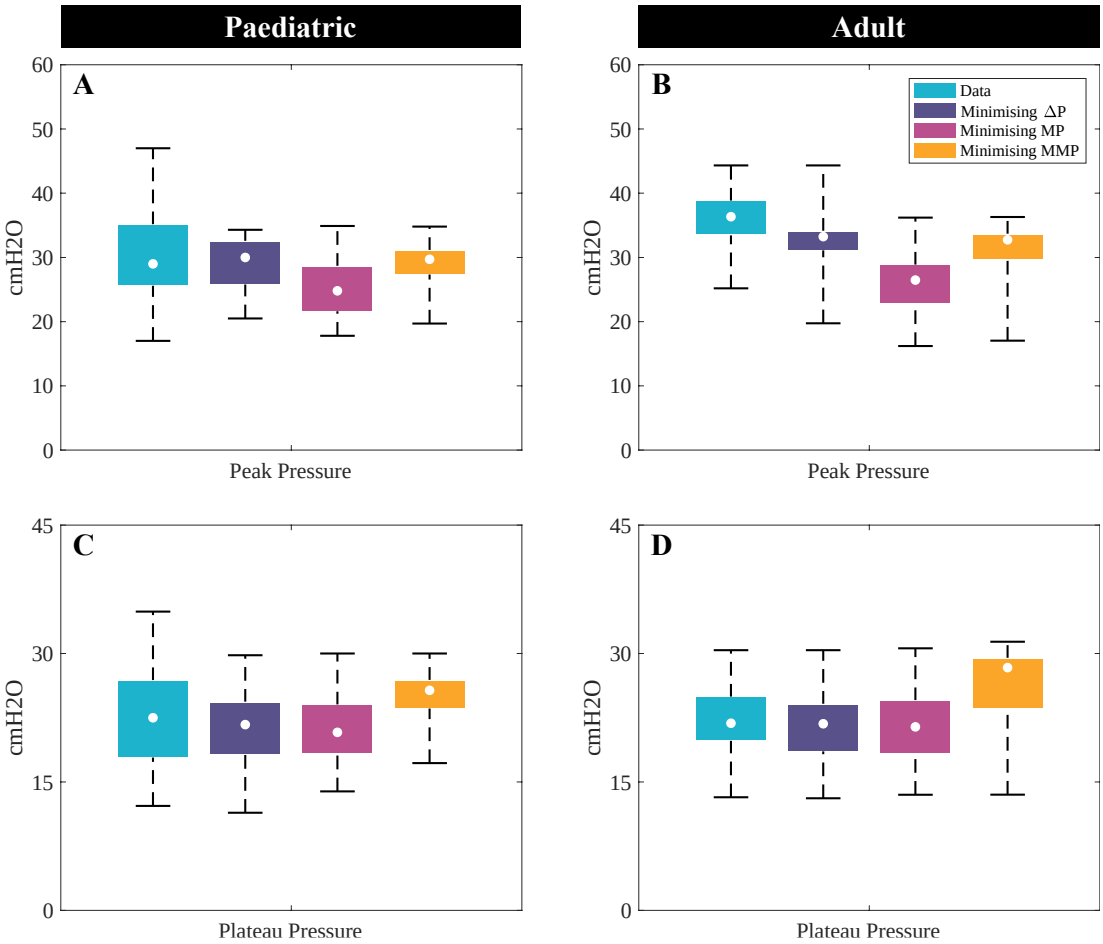

Figure 33. Approach 1 – Change in peak pressure and plateau pressure when minimising different targets (i.e. ΔP, MP and MMP) and allowing some deterioration in patient gas-exchange.

Panels (A) to (B) show results for the paediatric cohort and (C) to (D) for the adult cohort. Box plots demonstrate data as median, interquartile range and actual. Minimising MP was associated to lower levels of peak pressure. Minimising MMP increased plateau pressure the most.

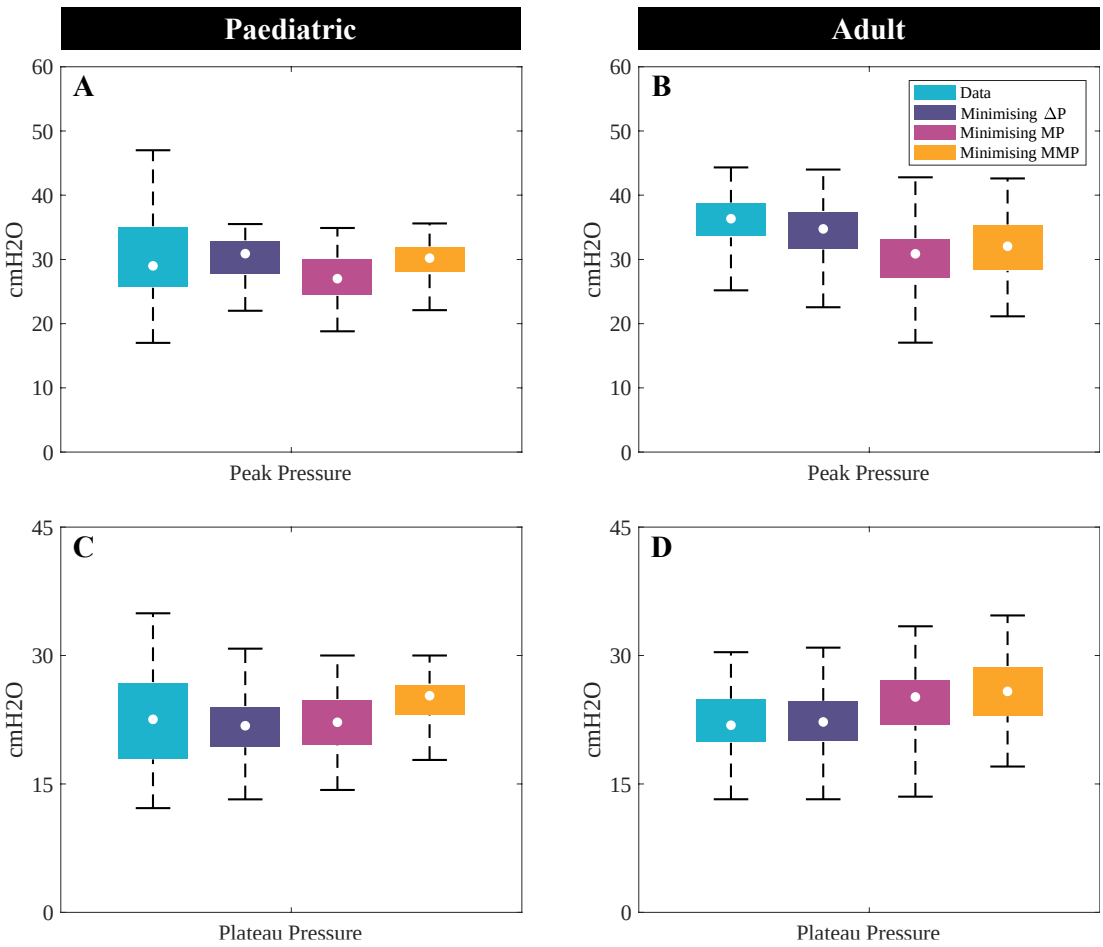

Figure 34. Approach 2 – Change in peak pressure and plateau pressure when minimising different targets (i.e. ΔP, MP and MMP) and allowing no deterioration in gas-exchange.

Panels (A) to (B) show results for the paediatric cohort and (C) to (D) for the adult cohort. Box plots demonstrate data as median, interquartile range and actual. Minimising MP was associated to lower levels of peak pressure. Minimising MMP increased plateau pressure the most.

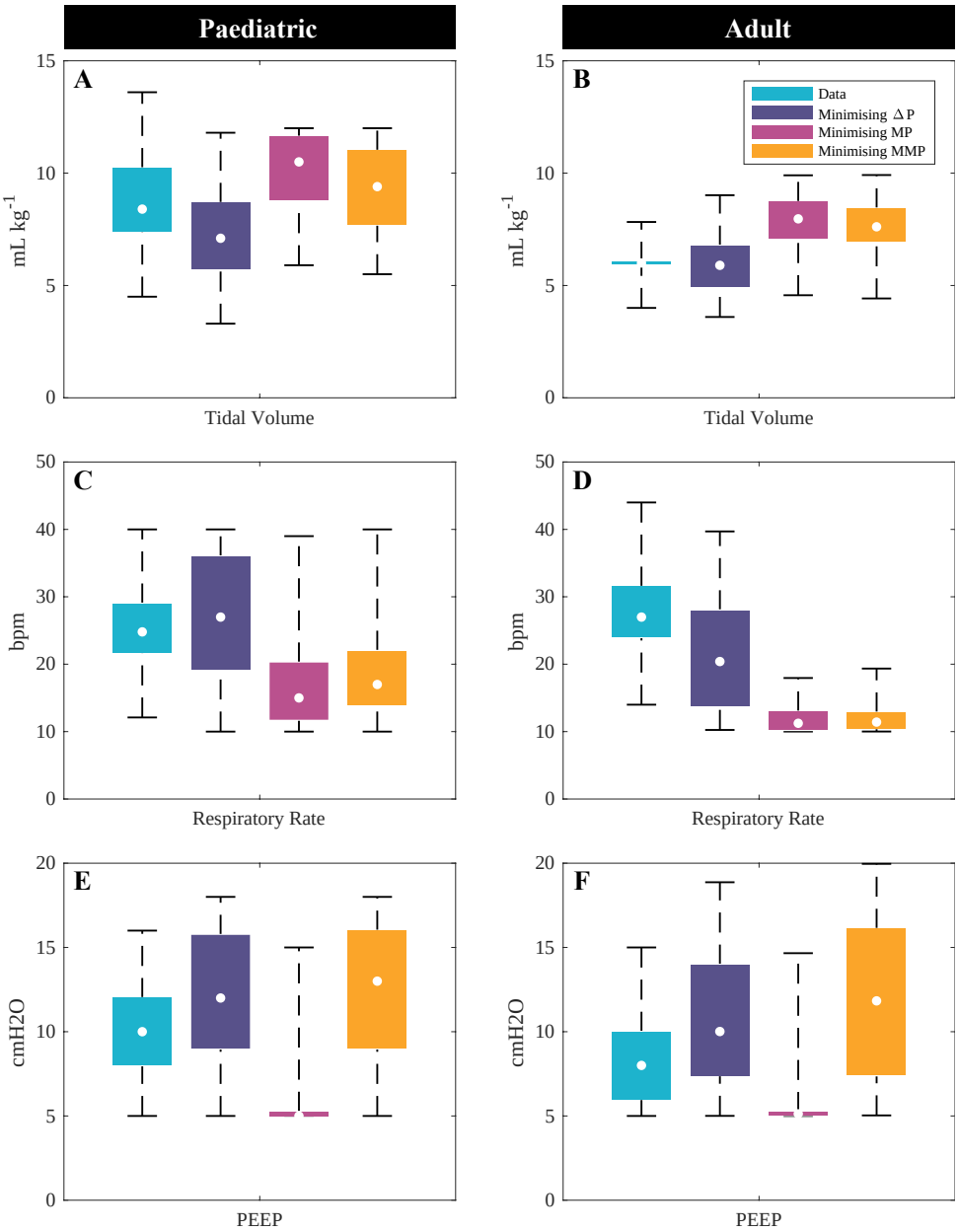

Figure 35. Approach 1 – Figure shows the changes in tidal volume, respiratory rate and PEEP that minimize different targets (i.e. ΔP, MP and MMP).

Panels (A), (C) and (E) show results for the paediatric cohort while (B), (D) and (F) are for the adult cohort. Box plots demonstrate data as median, interquartile range and actual. Minimising ΔP was achieved by lowering V_T and increasing RR and PEEP. Minimising MP led to higher levels of V_T and lower levels of RR and PEEP.

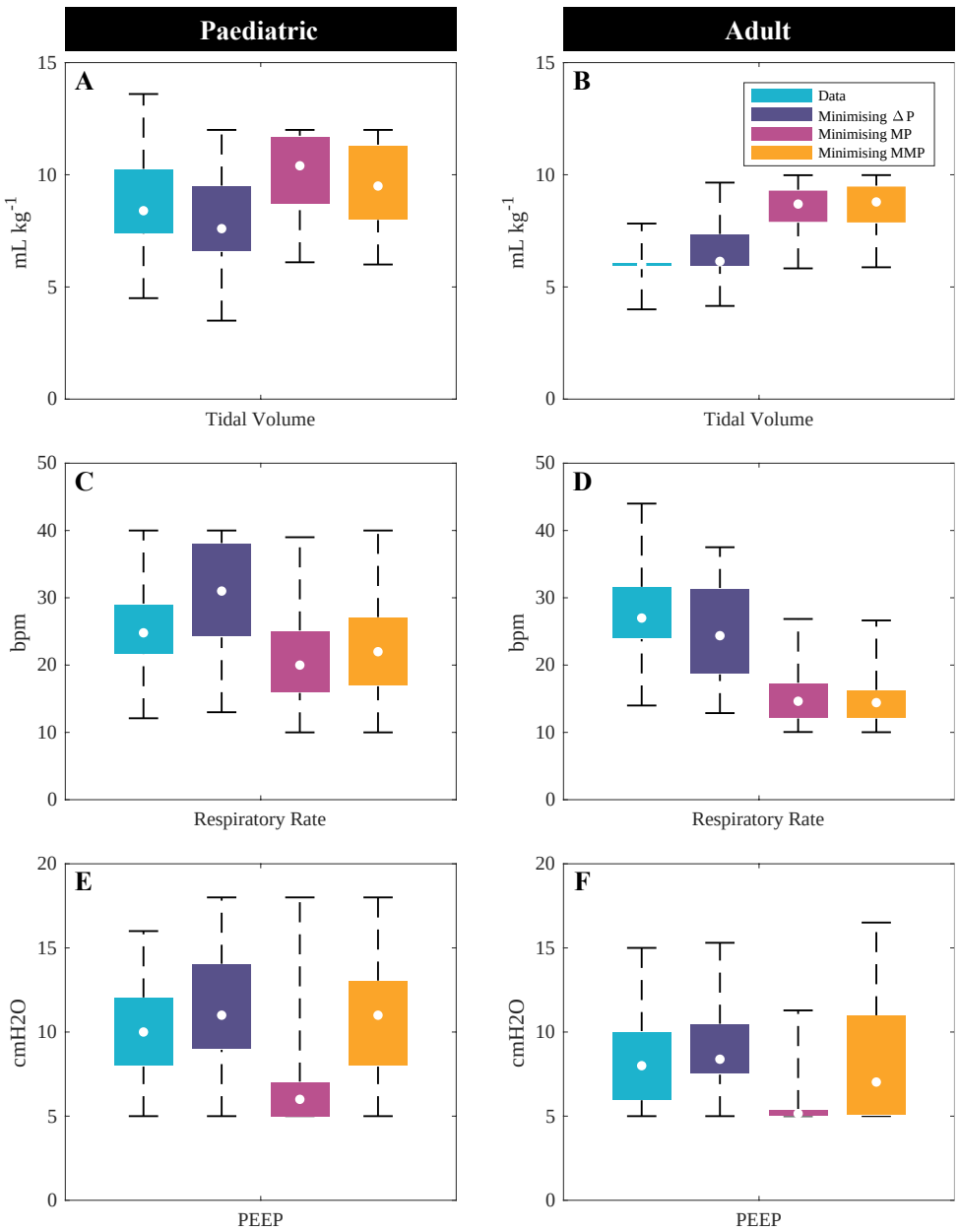

Figure 36. Approach 2 – Figure shows the changes in tidal volume, respiratory rate and PEEP that minimize different targets (i.e. ΔP, MP and MMP).

Panels (A), (C) and (E) show results for the paediatric cohort while (B), (D) and (F) are for the adult cohort. Box plots demonstrate data as median, interquartile range and actual. Minimising ΔP was achieved by lowering V_T and increasing RR and PEEP. Minimising MP led to higher levels of V_T and lower levels of RR and PEEP.

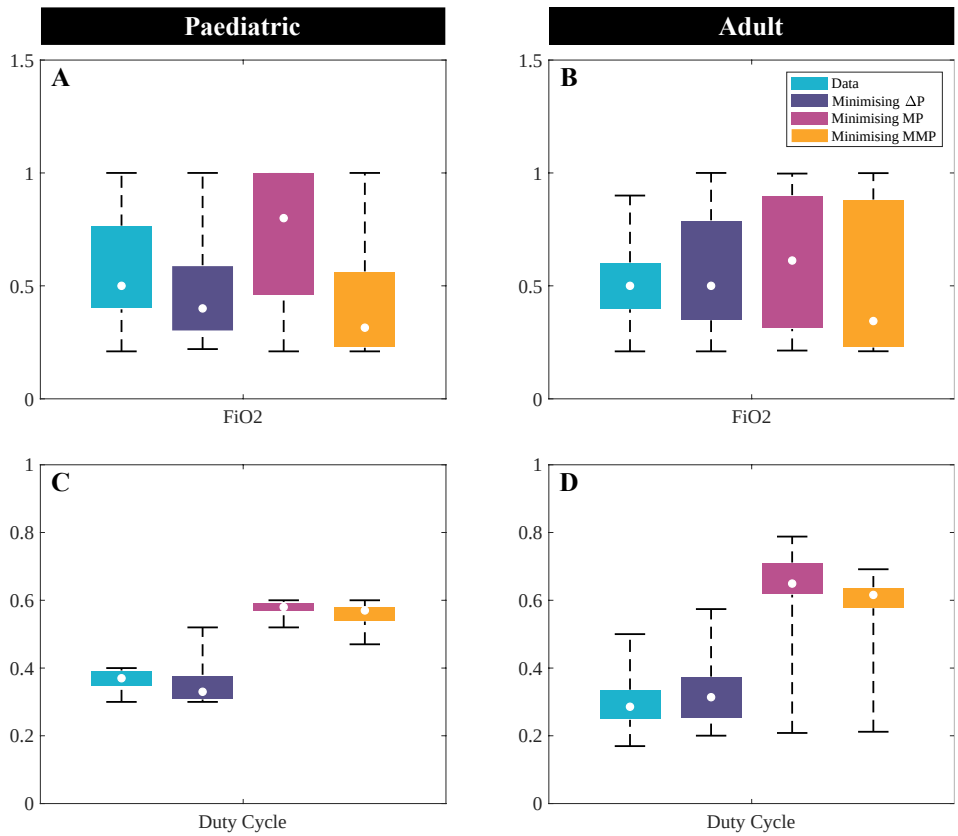

Figure 37. Approach 1 – Figure shows the changes in F_IO_2 and duty cycle that minimize different targets (i.e. ΔP, MP and MMP).

Panels (A) and (C) show results for the paediatric cohort while (B) and (D) are for the adult cohort. Box plots demonstrate data as median, interquartile range and actual. Minimising MP was associated with higher levels of F_IO_2. Also, the values of duty cycle were close to its upper limit when minimising MP and MMP.

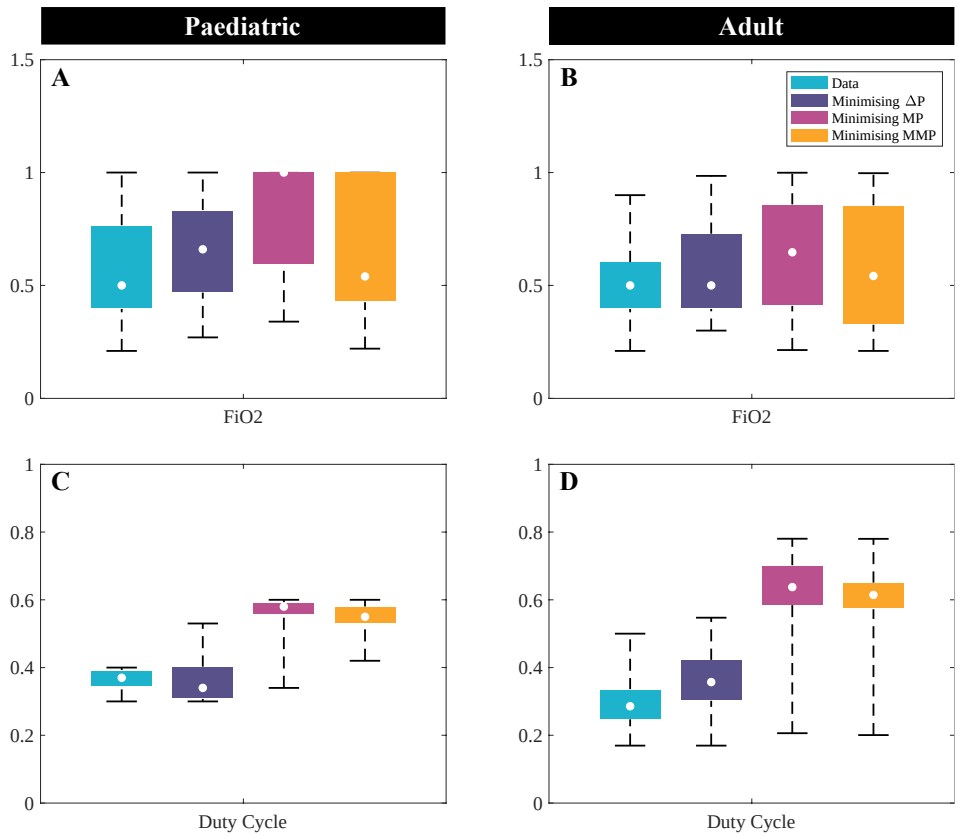

Figure 38. Approach 2 – Figure shows the changes in F_IO_2 and duty cycle that minimize different targets (i.e. ΔP, MP and MMP).

Panels (A) and (C) show results for the paediatric cohort while (B) and (D) are for the adult cohort. Box plots demonstrate data as median, interquartile range and actual. Minimising MP was associated with higher levels of F_iO_2. Also, the values of duty cycle were close to its upper limit when minimising MP and MMP.

5.5. Discussion

Our results provide several new insights into the types of ventilation strategies that are likely to minimize different indicators of VILI in ARDS patients. A high degree of consistency was observed in settings that minimized ΔP, MP and MMP across the diverse patient cohorts in both datasets, providing grounds for optimism that strategies for maximally protective ventilation could be developed that would be widely applicable in ARDS.

Perhaps the most counterintuitive result is that maximum reductions in MP and MMP are consistently achieved by changes to ventilator settings that involve increasing V_T (Figure 27) since from both the standard (Eq.44) and modified (Eq.47) formula for MP it seems obvious that lowering V_T should lower MP. Crucially, however, this ignores the impact of incorporating constraints on allowable deterioration in patient gas-exchange, which would always exist in treatment strategies implemented at the bedside. These constraints, combined with the complexity of making simultaneous adjustments to multiple ventilator settings, add a host of other trade-offs, that render the optimal combination of ventilator settings almost impossible to predict based on clinical intuition alone. The presented results point to a complex interplay between ventilator parameters which would support the development of a closed-loop system that can incorporate direct patient inputs, thereby providing individualised safe and effective mechanical ventilation based on the proposed safety limits and target parameter to minimise, input by clinicians at the bedside. However, when designing closed-loop system the model needs to consider the dynamic state of a patient so tuning itself as the patient physiology changes over time (i.e. the patient gets worse/better). Furthermore, the findings can be used to design bespoke guidelines on appropriate ventilator settings for clinical trials on low vs high ΔP, MP or MMP. These guidelines would be based on a variety of individual patient data such as disease severity, age, etc. rather than a one-size-fits-all instruction.

In the paediatric cohort, minimum values of ΔP were consistently achieved by reducing V_T and increasing RR and PEEP. Interestingly, this strategy has much in common with

the ARDSnet trial protocol, which lowered V_T while increasing RR. Some have postulated that this combination led to increased intrinsic (and hence total) PEEP [177], which may have contributed to the mortality benefit in this trial. However, it should be noted that subsequent trials of higher versus lower PEEP have not demonstrated a mortality benefit in heterogeneous ARDS populations [156, 178–180]. Since the selected patients in the adult cohort were from the low V_T arm of the trial, no further reductions in V_T were possible without violating imposed constraints on gas exchange. However, ΔP could still be significantly reduced in this cohort by moderately increasing PEEP.

Our findings provide novel and important insights into the challenges of using either ΔP or MP to develop protective lung ventilatory strategies. In our models, targeting reductions in ΔP led to increased RR and increased PEEP. While a strong association between higher ΔP and mortality has been demonstrated in multiple datasets, including by Amato et al [141], and in the LUNG SAFE global patient cohort [181], ΔP was not a therapeutic target in these patients, and causality remains elusive. There is data suggesting that increasing RR [165] and PEEP [182] beyond safe thresholds can be deleterious in injured lungs. Furthermore, in the Alveolar Recruitment for ARDS Trial (ART) clinical trial [183], a ventilatory strategy that decreased ΔP resulted in increased mortality. The usefulness of targeting ΔP directly thus remains to be demonstrated.

These concerns also apply to strategies that target reductions in MP. While MP represents a more complete attempt to describe the contributions of multiple parameters to VILI by invoking their "energy cost," the relative contributions of the different parameters (i.e., their relatively equal "weightings" in the formula) remains the subject of debate. An example is the controversy around how PEEP contributes to MP [174]. Our results show that different formulations of the MP equation lead to different optimal strategies; specifically, higher PEEP when optimizing MMP. Our finding that strategies that minimize MP and MMP increase V_T highlights the challenges of targeting one specific parameter in designing protective ventilatory strategies. This is particularly important given the findings from recent pre-clinical animal studies that, for the same MP, strategies employing higher rather than lower V_T had increased injury [184, 185]. All these findings highlight the need for prospective validation of ventilator strategies

that target reduced MP. Of importance, computational modelling of the impact of targeting these parameters (or combinations of different VILI indices) may identify promising non-intuitive combinations of ventilator settings for clinical testing, and also allow more effective stratification of patient populations by revealing differences in the effects of ventilation strategies across heterogeneous patient populations.

The study has a number of limitations. The paediatric dataset was derived from a single institution, and while the severity of ARDS and outcomes were similar to other cohorts, generalizability cannot be assumed. To minimise confounding, the model was configured to represent patients who are fully sedated and/or paralyzed; therefore, autonomic reflex modules were not utilised. The model also does not include the effect of inflammatory mediators, which are difficult to quantify and to isolate in clinical settings. As the model is computational in nature, it does not provide any direct physiologic, histological or biological evidence of the effects of the proposed ventilation strategies on VILI, and further animal and human studies should be performed to provide conclusive evidence of their effectiveness in achieving more protective ventilation. The model was developed to focus on ventilator settings affecting VILI; thus, constraints are set on $PaCO_2$ rather than pH, which is often modified by entirely non-ventilator interventions, such as volume resuscitation or exogenous bicarbonate.

However, the study also has several unique strengths. Over 26.7 million distinct combinations of ventilator settings were implemented and evaluated on two separate cohorts of patients with ARDS. It is difficult to imagine such a comprehensive exploration of different ventilation strategies ever being possible via animal or clinical trials. The study also allows a direct comparison of the effects of protective ventilation strategies in adult and paediatric ARDS patients. Our results clearly demonstrate the utility of pilot studies using high-fidelity simulation to assess novel interventions targeting MP or ΔP (or any other VILI indicator), and hence to inform the design of more targeted and effective clinical trials on actual patients.

Chapter 6:

Computational simulation of mechanically ventilated neonates

6.1. Summary

This chapter presents preliminary results on the adaptation of the computational simulator described in Chapter 2, Section 2.4, to the case of neonatal pathophysiology. Model equations and parameters were revised to represent the particular physiological characteristics of neonatal patients. The adapted model was matched to new data obtained from mechanically ventilated patients in the Neonatal Intensive Care Unit of Nottingham University Hospitals and is shown to accurately reproduce the values of key physiological parameters. This new model constitutes the first detailed computational simulator specifically tailored to neonatal ICU patients, and can be used as an investigational tool for developing and evaluating novel therapeutic strategies, as well as for developing future closed-loop ventilation modes for this patient group.

6.2. Introduction

Along with the administration of antepartum corticosteroids and replacement surfactant therapy, mechanical ventilation to provide lifesaving support for infants with respiratory

failure has been a key factor in improving neonatal survival, especially for preterm infants born before 30 weeks' gestation with immature lung function. Mechanical ventilation of neonatal intensive care unit (NICU) patients is common - according to the SUPPORT trial (Study to Understand Prognoses and Preferences for Outcomes and Risks of Treatment), more than 80% of premature neonates (<28 weeks gestation) require invasive ventilation at some point, due to a number of reasons (e.g. poor gas exchange, increased work of breathing, apnoea of prematurity and/or the need for surfactant-replacement therapy) [186]. Although mechanical ventilation can be lifesaving, it may also cause lung injury resulting in bronchopulmonary dysplasia (BPD), a major complication of prematurity with an incident rate of 31% for babies born at <32 weeks gestation [187] (when babies still need mechanical ventilation at their original due dates, RDS is also considered as BPD). As a result, significant efforts have been made to develop new treatment strategies, including the use of early continuous positive airway pressure (CPAP) in preterm infants at risk of neonatal respiratory distress syndrome (RDS), and strategies for neonatal ventilator care to maintain adequate gas exchange but minimize lung damage.

These efforts have been hampered by a number of factors. Ventilated, critically ill newborn babies are prone to sudden and large changes in their respiratory state, requiring frequent and rapid interventions by skilled but busy ICU staff. If not acted on promptly, these can increase the risk of brain injury or eye disorders resulting in long-term disabilities and blindness. Tight physiological control of parameters such as arterial oxygen partial pressure (too low increases mortality, too high risks sight loss) and arterial carbon dioxide partial pressure (too low risks brain injury, too high risks inducing intracranial hemorrhage, consciousness alterations, cataphora, and hyperspasmia) is essential to reduce these risks. For example, the recently completed Boost II trial [188] demonstrated that failure to keep premature infants in a tight oxygen saturation window (91-95%) increased mortality (greater time spent <91%) or blindness and chronic lung disease (greater time spent >95%). However, maintaining these strict targets is labour-intensive and, in that study, was achieved only 40% of the time [189]. Closed-loop ventilation control modes might offer a solution to these problems. Such

technologies are now available for adult patients on some ventilators, e.g. INTELLiVENT-ASV™ (Hamilton Medical), which automatically control ventilator settings such as inspired oxygen and PEEP based on clinician-guided targets and physiological inputs from the patient. Clinical trials on adult patients [190–192] have, so far, found these systems to be feasible and safe. However, there has only been a single study investigating the application of such technologies to paediatric patients [193], and the particular challenges associated with neonatal pathophysiology have so far precluded the application of these approaches to newborn babies.

An additional complication is that current guidelines for the mechanical ventilation of neonatal patients have largely been adapted from developments in the treatment of adult patients, despite widespread acceptance that paediatric patients are not just "little adults" [194]. For example, despite its long-standing existence, neonatal respiratory distress syndrome remained undefined until the Montreux definition of NARDS was introduced in 2017 [195]. However, despite the recommendations for mechanical ventilation for children and neonates from PALICC, the Paediatric Mechanical Ventilation Consensus Conference (PEMVECC) and European Consensus Guidelines on management of NARDS [136, 139, 196], reducing newborn morbidity and mortality still remains a significant global challenge.

In developing countries the mortality rate in ventilated neonates due to respiratory distress syndrome remains high (40-60%) [197]. Furthermore, despite advances in intensive care, many newborn premature babies who survive RDS, go on to develop chronic lung disease, BPD or barotrauma as a consequence of ventilator induced lung injury as well as other side effects such as long-term brain injury and blindness.

Clinician workload has been shown to be directly linked to patient outcomes [198], and a significant number of life-threatening human errors regularly occur (1.7 human errors per ICU patient per day) [199]. The number of patients undergoing mechanical ventilation in ICUs is expected to continue to increase (e.g. a study [200] showed that, overall, admission rates during the 6-year study period increased from 64.0 to 77.9 per

1000 live births), with significant associated costs to healthcare services due to prolonged periods of mechanical ventilation.

A high-fidelity computational simulator that could be shown to reproduce individual patient responses to changes in ventilation settings would be a valuable tool for evaluating novel treatment strategies, and for developing and validating closed-loop ventilation modes for neonatal patients. Several respiratory physiology simulators have been developed for adult and paediatric patients, [27, 64, 72, 73, 151], each of varying complexity and demonstrated validity. However, there is currently no such model available for neonatal subjects. This chapter introduces such a model, which has been adapted from the highly detailed representation of cardiorespiratory pathophysiology described in Chapter 2. The model has been modified to simulate neonatal patients by performing a detailed revision of both the model structure and parameters, as detailed below.

6.3. Materials and Methods

6.3.1. Patient selection

To date, data have been collected from 8 neonatal patients from the neonatal intensive care unit of the Queen's Medical Centre, Nottingham University Hospital, for the purposes of model calibration and validation as part of the NeoPredict Study (East Midlands NHS Ethics Committee 18/EM/0033). Patients' gestational age ranged from 26 to 36 weeks. An endotracheal tube (3 mm internal diameter) was used for all patients. The relevant patient and mechanical ventilation data are listed in Table 7. In the table, blood sample type C denotes capillary blood, V denotes venous blood and A denotes arterial blood. All patients were preterm.

6.3.2. Simulator development and calibration to patient data

The neonatal simulator was developed by performing a detailed revision of both the model structure and parameters in light of the key differences between neonatal and adult physiology. The extremely small volumes of neonates' lungs, as well as their large respiratory and vascular resistances make simulating the neonatal respiratory system

challenging. Physiological features such as lung volume, cardiac output, oxygen consumption and airway resistance are weight-dependent in neonates, and some parameters such as pulmonary vascular resistance are highly variable during the first hours of life. The cardiac output and the volume of functional residual capacity are estimated in the model using the following equations [201, 202]:

$$\begin{cases} \mathrm{CO} = 265 \times \mathrm{weight} & \mathrm{weight} < 1.5\ (\mathrm{kg}) \\ \mathrm{CO} = 253 \times \mathrm{weight} & 1.5 < \mathrm{weight} < 2.5\ (\mathrm{kg}) \\ \mathrm{CO} = 241 \times \mathrm{weight} & \mathrm{weight} > 2.5\ (\mathrm{kg}) \end{cases} \quad (\mathrm{mL\ min^{-1}}) \tag{48}$$

$$\mathrm{V_{frc}} = (20.7 \times \mathrm{weight}) - 6.3 \quad (\mathrm{ml}) \tag{49}$$

In the above, the units for CO and V_{frc} are mL min^{-1} and mL respectively. The total airway resistance is notably higher in neonatal patients than in adults and decreases as babies grow older. This resistance is distributed between the main airway and 100 parallel alveolar compartments in the model. Every alveolar compartment also has two resistances placed in series, namely the alveolar inlet resistance and the upper bronchial resistance. The pulmonary vascular resistance is very large during foetal life, and drops sharply to about 3-4 mmHg min L^{-1} during the first 24 hours of life as gas exchange is the primary function of the postnatal lung [203].

Both anatomical and alveolar dead spaces have been shown to increase with decreasing weight and gestation. Moreover, newborn babies have larger total anatomical dead space per kg of body weight in comparison with adults, due to the larger head to body mass ratio. The value of V_D is 3 to 6 mL kg^{-1} in preterm infants weighing around 1 kg [204, 205]. Newborn babies have a higher haemoglobin concentration compared to adults, with a minimum acceptable value of about 110 g L^{-1}. This value begins to fall within the first week after delivery [206, 207]. Oxygen consumption in neonates is also more than twice that of adults on a per kg basis. There is a large rise in metabolic rate in the first 24 hours for normal term babies; however, the rate of increase is slower in those born prematurely. Preterm babies also have a lower oxygen consumption rate compared with

term babies. The optimized value for oxygen consumption in the model is selected from a range of 4 to 10 mL kg^{-1} min^{-1} [208, 209].

Furthermore, to characterize the stiffer nature of paediatric lungs at baseline (i.e. lower alveolar compliance) the denominator of Eq.16 is reduced to 2000, 5000, 12000 and 50000 cmH_2O mL^{-2} for patients younger than 1, 1 to 2, 3 to 5 and 8 to 10 years old respectively. These values are obtained experimentally so that the pressure-volume equation of each alveolar compartment produces the appropriate level of pressures at the baseline, given the small tidal volumes in neonatal subjects.

The simulator was matched to individual patient data using advanced global optimisation algorithms described in Chapter 3 (see Section 3.3.1). The variable model parameters (x) that were allowed to vary in the optimization include the three key alveolar features mentioned previously (P_{ext}, k and TOP) independently for each of the 100 alveolar compartments, as well as values for the respiratory quotient (RQ), total oxygen consumption, haemoglobin, volume of anatomical dead space and anatomical shunt. The optimization problem is formulated to find the configuration of model parameters (x) that minimize the cost function J given below:

$$\min_{x} \mathrm{J} = \sqrt{\sum_{i=1}^{6} \frac{\widehat{\mathrm{Y}}_i - \mathrm{Y}_i}{\mathrm{Y}_i}} \tag{50}$$

with

$$\mathrm{Y} = [\mathrm{PO_2}, \mathrm{PCO_2}, \mathrm{PIP}, \mathrm{mPaw}, \mathrm{P_{min}}, \mathrm{TOP_{mean}}] \tag{51}$$

where Y is the vector of data values and $\widehat{\mathrm{Y}}$ denotes the vector of model estimated values. Table 8 presents a summary of the parameters included in (x), with their dimensions and allowable range of variation (chosen to reflect physiologically reasonable limits).

Table 7. The neonatal patient data and ventilator settings

ID	RR	F_IO_2	DC	PEEP	V_T	Sample Type	PO_2	PCO_2	P_{min}	PIP	mPaw
	(bpm)			(cmH_2O)	(mL)		(kPa)		(cmH_2O)		
#1	47	0.21	0.24	5	4.3	C	5.2	7.0	4.7	11	6.3
#2	45	0.21	0.29	5	4.7	V	4.4	7.5	4.6	21	9.3
#3	40	0.21	0.26	5	6.1	C	4.9	5.4	4	29	10
#4	50	0.21	0.25	5	5.5	C	4.1	6.8	4.9	15	7
#5	55	0.25	0.30	7	5.5	V	4.8	7.2	6.8	20	11
#6	61	0.27	0.31	6	5	A	8.4	5.3	5.7	20	10
#7	50	0.21	0.23	5	6.3	A	7.8	3.9	4.7	21	11
#8	66	0.21	0.36	5.5	11.5	A	6.4	4.3	4.6	18	7.9

Table 8. Model parameters (x) used for matching patient data, dimensions and ranges

Parameter (x)	Size	Range
P_{ext}	100	[-70,10]
k	100	[-2,1]
TOP (cmH_2O)	100	[5,100]
RQ	1	[0.7,0.9]
VO_2 (mL kg^{-1} min^{-1})	1	[4,10]
Hb (g L^{-1})	1	[110,200]
Anatomical shunt (%)	1	[1,2]
V_D (mL kg^{-1})	1	[3,6]

6.4. Results

Currently, the simulator can be only matched to either venous or arterial blood gasses, since the blood from arterial or venous samples is fully oxygenated or deoxygenated, and consequently it is known at what stage to feed the data into the model. For safety reasons, clinicians try to avoid taking arterial or venous samples in neonatal subjects, preferring to use capillary blood gas values instead. However, with capillary samples, tissue gas exchange may not have been completed, and thus these data are more difficult to use for model calibration.

Hence, only the five patients with arterial or venous blood samples have been used in the study at this point; all patients were diagnosed with neonatal respiratory distress syndrome. Patients were simulated for 30 minutes under mechanical ventilation with constant flow inflation and with no recruitment manoeuvre intervention. Reduced alveolarization was not modelled in the patients as there was no data on it, although it could be incorporated into the simulator by combining multiple alveolar compartments into one compartment. Table 9 compares the outputs of the simulations with the original patient data. All presented model outputs have been averaged over 1 minute. As shown, the simulator accurately reproduced the measured values of several key ventilation parameters for all patients.

Table 9. Results for neonatal dataset – data vs. values computed by the simulator

ID	Sample Type	PO_2 (kPa)		PCO_2 (kPa)		P_{min} (cmH_2O)		PIP (cmH_2O)		mPaw (cmH_2O)	
		Data	Model	Data	Model	Data	Model	Data	Model	Data	Model
#2	V	4.4	4.8	7.5	7.2	4.6	5.1	21	21.0	9.3	9.1
#5	V	4.8	4.8	7.2	7.0	6.8	6.9	20	20.1	11	10.9
#6	A	8.4	8.4	5.3	5.2	5.7	6.0	20	20.1	10	9.9
#7	A	7.8	7.7	3.9	3.9	4.7	5.0	21	21.2	11	10.9
#8	A	6.4	6.4	4.3	4.3	4.6	5.5	18	18.1	7.9	7.7

The model was demonstrated to accurately reproduce the available clinical data for five preterm neonatal patients with measurements of arterial or venous blood gas values.

6.5. Discussion

The first results from the development of a detailed, highly-fidelity computational simulator of neonatal cardiorespiratory physiology have been presented. The model was demonstrated to accurately reproduce the available clinical data for five preterm neonatal patients with measurements of arterial or venous blood gas values – data from several more patients is currently being collected and will be incorporated in any future studies. As it is refined and developed, this model will provide a novel and useful tool for investigating novel treatment strategies, improving recommendations and guidelines for choosing ventilator settings, and developing closed-loop ventilation control modes that are specifically tailored to neonates.

Capillary gas tensions (and pH) always lie somewhere between the arterial values and the local venous values. The problem is that how close the CBG is to the ABG is unpredictable. High local flow, or low local metabolism can 'arterialise' the values, while poor flow or high local oxygen consumption can make the values more like central venous values. Some of that concern is theoretical, since CBG tend to be taken from tissues of low metabolic activity (i.e. skin). The other issue is that some values change a lot between arterial and venous blood (e.g. PO_2, particularly when supplemental oxygen is given, such that PaO_2 is high), while some values only change a little (e.g. PCO_2). Future work will focus on incorporating physiologically realistic representations of capillary blood characteristics into the model, which will significantly increase the numbers of patients from whom data for model calibration and validation can be obtained.

Chapter 7:

Conclusions and future work

It is widely accepted that modification of existing approaches to mechanical ventilation to incorporate novel treatment strategies could reduce pulmonary injury, cardiovascular impairment, and mortality rates, particularly if combined with novel pharmaceuticals. To date, however, the complex and often opaque dynamical interactions of the alveoli, airways, chest wall, heart and blood vessels has severely limited progress towards the development of therapeutic strategies optimised to specific diseases and individual.

Critically ill patients are routinely monitored in great detail, providing extensive, high quality data-streams for model design & configuration and patient-matching. Models based on these datasets can incorporate very complex system dynamics that may be validated against responses of individual patients, for use as investigational surrogates. In contrast to trials on animal models and humans, in silico models of individualised patient and disease pathology are completely configurable, reproducible and reusable – different treatments, or combinations of treatments, can be applied to the same patient or subset of virtual patients, in order to understand mode of action, quantitatively compare effectiveness in various scenarios, and optimise interventions for particular clinical objectives and particular patient groups (or individuals).

This thesis has presented work advancing research in this area on several fronts.

Chapter 3 investigated the efficacy of a modulator of soluble guanylate cyclase in COPD patients with PH by using computer simulation. In this study, close matching of the simulator to data on three patients was demonstrated. Calculations of blood gas concentrations for these virtual patients, considering the observed temporal profile of average PVR changes after oral administration of Riociguat (Bayer), resulted in predictions of changes in PaO_2 and $PaCO_2$ that were consistent with those observed in the previous clinical study. These results can be considered as a validation of the capability of the pulmonary simulator to reliably describe the effects on gas exchange of compounds acting on the vascular resistance, in particular those stimulating sGC activity. Additional validations can be achieved by confirmation of the outcomes in a clinical trial. Furthermore, this study showed that administering an sGC via dry powder inhalation can reduce pulmonary hypertension without deteriorating oxygenation, particularly when administration is combined with exercise. These results highlight the potential advantages of administering sGC's to patients via dry powder inhalation, rather than systemically.

Analysis of an extensive database on PARDS patients in Chapter 4 suggested patients may be being routinely over-ventilated, and that there is scope for achieving more protective ventilation without compromising gas exchange. The results suggest that interventions based on (i) progressively lowering V_T while maintaining constant MinV, and (ii) adjusting PEEP and V_T to reduce ΔP, can produce significant reductions in multiple key parameters associated with VILI without compromising safety. Such interventions could be readily implemented at the bedside by clinicians directly (similar to recruitment manoeuvres), or automatically via closed-loop control algorithms in next-generation ventilators, although actual implementation will require a prospective trial. Although previous studies of the effects of lowering V_T in PARDS have yielded inconclusive results, our results indicate that such strategies can be implemented safely, supporting the design of true randomized trials to better delineate the role of low tidal volume ventilation in PARDS. Finally, the results suggest a number of other potentially beneficial interventions which could also be evaluated in future simulation and in vivo

studies, including minimizing RR by using a long inspiratory time, and minimizing strain rate either by reducing inspiratory flow or by increasing FRC through adding PEEP.

In Chapter 5, novel ventilatory strategies were identified that minimized ΔP, MP, and MMP in datasets from adults and children with ARDS. The identified strategies were consistent within each patient group, and were similar in both adults and children, suggesting that protective ventilatory strategies derived from studies in adults may have utility in children with ARDS. Minimising MP resulted in the use of higher V_T; since this contradicts the current consensus on using lower V_T it raises questions regarding the use of MP as a direct target to minimize VILI, at least as currently formulated. Although, it should be noted that lowering MP could generally be possible by lowering V_T, but the lowest value of MP is associated with use of higher V_T which suggests ΔP is a better target to be minimised rather than MP. Overall, these findings demonstrate the limitations of ventilatory strategies that target either ΔP or MP, highlighting the need to continue to refine these targets, and for ultimate validation of these strategies in clinical trials.

Chapter 6 presented the development of the first detailed computational simulator capable of modelling neonatal respiratory physiology in the RDS disease state. The preliminary results of matching the model to the data collected from the Queen's Medical Centre indicate that all the available clinical data on the responses of individual patients to a range of different ventilator settings are accurately reproduced by the model. The application of this model to investigate novel treatment strategies could make an important contribution to the field, in terms of obtaining better understanding of the disease, evaluating different treatment strategies such as recruitment manoeuvres and improving recommendations and guidelines for choosing ventilator settings. Using the simulator, multi-intervention treatment strategies for specific clinical objectives can be simulated and evaluated in a safe, and cost-efficient manner. The simulation model can be used for investigating alternative ventilator settings that could lower that risk of VILI. Drug intervention effects can also be integrated into the model. These questions are the subject of current research by the author.

Bibliography

1. Meyer JA. A Practical mechanical respirator, 1929: The "iron lung." Ann Thorac Surg. 1990;50:490–3. doi:10.1016/0003-4975(90)90508-4.

2. Fenstermacher D, Hong D. Mechanical ventilation: what have we learned? Crit Care Nurs Q. 2004;27:258–94. doi:10.1097/00002727-200407000-00006.

3. Villar J, Kacmarek RM, Hedenstierna G. From ventilator-induced lung injury to physician-induced lung injury: why the reclutance to use small tidal volume? Acta Anaesthesiol Scand. 2004;48:267–71.

4. ARDS Network. Ventilation With Lower Tidal Volumes As Compared With Traditional Tidal Volumes for Acute Lung Injury and the Acute Respiratory Distress Syndrome. N Engl J Med. 2000;342:1301–8. doi:10.1056/NEJM200005043421801.

5. Hickling KG, Walsh J, Henderson S, Jackson R. Low mortality rate in adult respiratory distress syndrome using low-volume, pressure-limited ventilation with permissive hypercapnia: a prospective study. Critical care medicine. 1994;22:1568–78. doi:10.1097/00003246-199422100-00011.

6. Amato MBP, Barbas CSV, Medeiros DM, Magaldi RB, Schettino GP, Lorenzi-Filho G, et al. Effect of a protective-ventilation strategy on mortality in the acute respiratory distress syndrome. N Engl J Med. 1998;338:347–54. doi:10.1056/NEJM199802053380602.

7. Villar J, Kacmarek RM, Perez-Mendez L, Aguirre-Jaime A. A high positive end-expiratory pressure, low tidal volume ventilatory strategy improves outcome in persistent acute respiratory distress syndrome: a randomized, controlled trial. Crit Care Med. 2006;34:1311–8.

8. Goligher EC, Ferguson ND, Brochard LJ. Clinical challenges in mechanical ventilation. Lancet. 2016;387:1856–66. doi:10.1016/S0140-6736(16)30176-3.

9. Tehrani FT. Automatic control of mechanical ventilation. Part 1: theory and history of the technology. J Clin Monit Comput. 2008;22:409–15. doi:10.1007/s10877-008-9150-z.

10. Tehrani FT. Automatic control of mechanical ventilation. Part 2: the existing techniques and future trends. J Clin Monit Comput. 2008;22:417–24. doi:10.1007/s10877-008-9151-y.

11. Bouadma L, Lellouche F, Cabello B, Taillé S, Mancebo J, Dojat M, et al. Computer-driven management of prolonged mechanical ventilation and weaning: a pilot study.

Intensive Care Med. 2005;31:1446–50. doi:10.1007/s00134-005-2766-2.

12. Dojat M, Brochard L, Lemaire F, Harf A. A knowledge-based system for assisted ventilation of patients in intensive care units. Int J Clin Monit Comput. 1992;9:239–50. doi:10.1007/BF01133619.

13. Curley GF, Laffey JG, Zhang H, Slutsky AS. Biotrauma and Ventilator Induced Lung Injury: Clinical implications. Chest. 2016. doi:10.1016/j.chest.2016.07.019.

14. de Prost N, Ricard J-D, Saumon G, Dreyfuss D. Ventilator-induced lung injury: historical perspectives and clinical implications. Ann Intensive Care. 2011;1:28. doi:10.1186/2110-5820-1-28.

15. Dreyfuss D, Saumon G. Barotrauma is volutrauma, but which volume is the one responsible? Intensive Care Med. 1992;18:139–41.

16. Ioannidis G, Lazaridis G, Baka S, Mpoukovinas I, Karavasilis V, Lampaki S, et al. Barotrauma and pneumothorax. J Thorac Dis. 2015;7:S38–43. doi:10.3978/j.issn.2072-1439.2015.01.31.

17. Anzueto A, Frutos-Vivar F, Esteban A, Alía I, Brochard L, Stewart T, et al. Incidence, risk factors and outcome of barotrauma in mechanically ventilated patients. Intensive Care Med. 2004;30:612–9. doi:10.1007/s00134-004-2187-7.

18. Tejerina E, Frutos-Vivar F, Restrepo MI, Anzueto A, Abroug F, Palizas F, et al. Incidence, risk factors, and outcome of ventilator-associated pneumonia. J Crit Care. 2006;21:56–65. doi:10.1016/j.jcrc.2005.08.005.

19. Slutsky AS. ACCP Consensus Conference - Mechanical Ventilation. Chest. 1993;104:1833–59.

20. Slutsky AS, Ranieri VM. Ventilator-induced lung injury. N Engl J Med. 2013;369:2126–36. doi:10.1056/NEJMra1208707.

21. Briel M, Meade M, Mercat A, Brower RG, Talmor D, Walter SD, et al. Higher vs lower positive end-expiratory pressure in patients with acute lung injury and acute respiratory distress syndrome: systematic review and meta-analysis. JAMA. 2010;303:865–73. doi:10.1001/jama.2010.218.

22. Talmor D. Mechanical Ventilation Guided by Esophageal Pressure in Acute Lung Injury Daniel. N Engl J Med. 2008;108:12042–7. doi:10.1056/NEJMp1415160.

23. Gattinoni L, Caironi P, Cressoni M, Chiumello D, Ranieri VM, Quintel M, et al. Lung Recruitment in Patients with the Acute Respiratory Distress Syndrome. N Engl J Med. 2006;354:1775–86. doi:10.1056/NEJMoa052052.

24. Biehl M, Kashiouris MG, Gajic O. Ventilator-induced lung injury: minimizing its impact in patients with or at risk for ARDS. Respir Care. 2013;58:927–37.

25. Ochiai R. Mechanical ventilation of acute respiratory distress syndrome. J intensive care. 2015;3:25. doi:10.1186/s40560-015-0091-6.

26. Rittayamai N, Brochard L. Recent advances in mechanical ventilation in patients

with acute respiratory distress syndrome. Eur Respir Rev. 2015;24:132–40. doi:10.1183/09059180.00012414.

27. Rees SE, Allerød C, Murley D, Zhao Y, Smith BW, Kjaergaard S, et al. Using physiological models and decision theory for selecting appropriate ventilator settings. J Clin Monit Comput. 2006;20:421–9.

28. Morris a H. Decision support and safety of clinical environments. Qual Saf Health Care. 2002;11:69–75.

29. Allerød C, Rees SE, Rasmussen BS, Karbing DS, Kjærgaard S, Thorgaard P, et al. A decision support system for suggesting ventilator settings: Retrospective evaluation in cardiac surgery patients ventilated in the ICU. Comput Methods Programs Biomed. 2008;92:205–12.

30. Hardman JG, Ross JJ. Modelling: A core technique in anaesthesia and critical care research. Br J Anaesth. 2006;97:589–92.

31. Hardman JG, Moppett IK, Mahajan RP. Validity, credibility, and applicability: The rise and rise of the surrogate. Br J Anaesth. 2008;101:595–6.

32. Chase JG, Compte AJ Le, Preiser J-C, Shaw GM, Penning S, Desaive T, et al. Physiological modeling, tight glycemic control, and the ICU clinician: what are models and how can they affect practice? Ann Intensive Care. 2011;1:11. doi:10.1186/2110-5820-1-11.

33. Kitano H. Biological robustness. Nat Rev Genet. 2004;5:826–37. doi:10.1038/nrg1471.

34. Slyke DD Van, Cullen GE. Studies of Acidosis: I. The bicarbonate concentration of the blood plasma; its significance, and its determination as a measure of acidosis. J Biol Chem. 1917;30:289–346.

35. Slyke DD Van. Studies of Acidosis: XVII. The normal and abnormal variations in the acid-base balance of the blood. J Biol Chem. 1921;48:153–76.

36. Henderson LJ. The Equilibrium Between Oxygen And Carbonic Acid In Blood. J Biol Chem. 1920;41:401–30.

37. Kelman GR. Digital computer subroutine for the conversion of oxygen tension into saturation. J Appl Physiol. 1966;21:1375–6.

38. Rahn H. A concept of mean alveolar air and the ventilation-bloodflow relationships during pulmonary gas exchange. J Appl Physiol. 1949;21:21–30.

39. ROSENTHAL TB. The effect of temperature on the pH of blood and plasma in vitro. J Biol Chem. 1948;173:25–30.

40. Siggaard-Andersen O. Blood acid-base alignment normogram. Scandinav J Clin Lab Investig. 1963;15:211–7.

41. Douglas A, Jones N, Reed J. Calculation of whole blood CO2 content. J Appl Physiol. 1988;65:473–7.

42. Austin WH, Lacombe E, Rand PW, Chatterjee M. Solubility of carbon dioxide in serum from 15 to 38 C. J Appl Physiol. 1963;18:301–4.

43. Visser BF. Pulmonary diffusion of carbon dioxide. Phys Med Biol. 1960;5:155–66. doi:10.1088/0031-9155/5/2/305.

44. Severinghaus JW. Blood gas calculator. J Appl Physiol. 1966;21:1108–16. doi:10.1152/jappl.1966.21.3.1108.

45. Severinghaus JW. Simple, accurate equations for human blood {O}$_2$ dissociation computations. J Appl Physiol. 1979;46:599–602.

46. Comerford A, Rausch S, Al E. Computational Modelling of the Respiratory System for Improvement of Mechanical Ventilation Strategies. In: High Performance Computing in Science and Engineering, Garching/Munich 2009. 2010. p. 267–77. doi:10.1007/978-3-642-33374-3.

47. Das A, Cole O, Chikhani M, Wang W, Ali T, Haque M, et al. Evaluation of lung recruitment maneuvers in acute respiratory distress syndrome using computer simulation. Crit Care. 2015;19:8. doi:10.1186/s13054-014-0723-6.

48. Roth CJ, Yoshihara L, Ismail M, Wall WA. Computational modelling of the respiratory system: Discussion of coupled modelling approaches and two recent extensions. Comput Methods Appl Mech Eng. 2016. doi:10.1016/j.cma.2016.08.010.

49. Wang W, Das A, Cole O, Chikhani M, Hardman JJGJ, Bates DDGD, et al. Computational simulation indicates that moderately high-frequency ventilation can allow safe reduction of tidal volumes and airway pressures in ARDS patients. Intensive Care Med Exp. 2015;3:33. doi:10.1186/s40635-015-0068-8.

50. Yem JS, Turner MJ, Baker AB, Young IH, Crawford ABH. A tidally breathing model of ventilation, perfusion and volume in normal and diseased lungs. Br J Anaesth. 2006;97:718–31.

51. Chikhani M, Das A, Haque M, Wang W, Bates D, Hardman JG. High PEEP in ARDS : quantitative evaluation between improved oxygenation and decreased oxygen delivery. 2016.

52. Hahn CEW, Farmery AD. Gas exchange modelling: no more gills, please. Br J Anaesth. 2003;91:2–15. doi:10.1093/bja/aeg142.

53. Grodins FS, Buell J, Bart AJ. Mathematical analysis and digital simulation of the respiratory control system. J Appl Physiol. 1967;22:260–76. doi:10.1152/jappl.1967.22.2.260.

54. GRODINS FS, GRAY JS, SCHROEDER KR, NORINS AL, JONES RW. Respiratory responses to CO2 inhalation; a theoretical study of a nonlinear biological regulator. J Appl Physiol. 1954;7:283–308. doi:10.1152/jappl.1954.7.3.283.

55. Stuhmiller JH, Stuhmiller LM. A mathematical model of ventilation response to inhaled carbon monoxide. J Appl Physiol. 2005;98:2033–44. doi:10.1152/japplphysiol.00034.2005.

56. Ursino M, Magosso E, Avanzolini G. An integrated model of the human ventilatory control system: the response to hypoxia. Clin Physiol. 2001;21:465–77. doi:10.1046/j.1365-2281.2001.00350.x.

57. Saunders KB, Bali HN, Carson ER. A breathing model of the respiratory system: The controlled system. J Theor Biol. 1980;84:135–61. doi:http://dx.doi.org/10.1016/S0022-5193(80)81041-1.

58. Chiari L, Avanzolini G, Ursino M. A Comprehensive Simulator of the Human Respiratory System: Validation with Experimental and Simulated Data. Ann Biomed Eng. 1997;25:985–99.

59. Hinds CJ, Roberts MJ, Ingram D, Dickinson CJ. Computer simulation to predict patient responses to alterations in the ventilation regime. Intensive Care Med. 1984;10:13–22. doi:10.1007/bf00258063.

60. Hinds CJ, Ingram D, Adams L, Cole PV, Dickinson CJ, Kay J, et al. An evaluation of the clinical potential of a comprehensive model of human respiration in artificially ventilated patients. Clin Sci. 1980;58:83–9.

61. Petrini MF, Robertson HT, Hlastala MP. Interaction of series and parallel dead space in the lung. Respir Physiol. 1983;54:121–36. doi:10.1016/0034-5687(83)90118-4.

62. Hickling KG. The pressure-volume curve is greatly modified by recruitment: A mathematical model of ards lungs. Am J Respir Crit Care Med. 1998;158:194–202.

63. West JB. Ventilation-perfusion inequality and overall gas exchange in computer models of the lung. Respir Physiol. 1969;7:88–110. doi:10.1016/0034-5687(69)90071-1.

64. Dickinson C. A Computer Model of Human RespiratIon: VentilatIon-Blood Gas Transport and Exchange Hydrogen Ion regulatIon. 1977.

65. Swanson GD, Sherrill DL. A model evaluation of estimates of breath-to-breath alveolar gas exchange. J Appl Physiol. 1983;55:1936–41. doi:10.1152/jappl.1983.55.6.1936.

66. Hotchkiss JR, Crooke PS, Adams AB, Marini JJ. Implications of a biphasic two-compartment model of constant flow ventilation for the clinical setting. J Crit Care. 1994;9:114–23. doi:10.1016/0883-9441(94)90022-1.

67. Vidal Melo MF, Loeppky JA, Caprihan A, Luft UC. Alveolar ventilation to perfusion heterogeneity and diffusion impairment in a mathematical model of gas exchange. Comput Biomed Res. 1993;26:103–20. doi:10.1006/cbmr.1993.1007.

68. Vidal Melo MF. Effect of cardiac output on pulmonary gas exchange: role of diffusion limitation with V : A/Q : mismatch. Respir Physiol. 1998;113:23–32.

69. Joyce CJ, Hickling KG. Permissive hypercapnia and gas exchange in lungs with high Qs/Qt: A mathematical model. Br J Anaesth. 1996;77:678–83.

70. Farmery AD, Roe PG. A model to describe the rate of oxyhaemoglobin desaturation during apnoea. Br J Anaesth. 1996;76:284–91. doi:10.1093/bja/76.2.284.

71. Liu CH, Niranjan SC, Clark JW, San KY, Zwischenberger JB, Bidani A. Airway mechanics, gas exchange, and blood flow in a nonlinear model of the normal human lung. J Appl Physiol. 1998;84:1447–69. doi:10.1152/jappl.1998.84.4.1447.

72. Rutledge GW. VentSim: a simulation model of cardiopulmonary physiology. Proceedings Symp Comput Appl Med Care. 1994;:878–83. http://www.ncbi.nlm.nih.gov/pubmed/7950050.

73. Kapitan KS. Teaching pulmonary gas exchange physiology using computer modeling. AJP Adv Physiol Educ. 2008;32:61–4. doi:10.1152/advan.00099.2007.

74. Flechelles O, Ho A, Hernert P, Emeriaud G, Zaglam N, Cheriet F, et al. Simulations for mechanical ventilation in children: Review and future prospects. Critical Care Research and Practice. 2013;2013. doi:10.1155/2013/943281.

75. Cherniack NS, Longobardo GS. Mathematical models of periodic breathing and their usefulness in understanding cardiovascular and respiratory disorders. Exp Physiol. 2006;91:295–305.

76. Hardman JG, Al-Otaibi HM. Prediction of Arterial Oxygen Tension: Validation of a Novel Formula. Am J Respir Crit Care Med. 2010;182:435–6. doi:10.1164/ajrccm.182.3.435.

77. McCahon RA, Columb MO, Mahajan RP, Hardman JG. Validation and application of a high-fidelity, computational model of acute respiratory distress syndrome to the examination of the indices of oxygenation at constant lung-state. Br J Anaesth. 2008;101:358–65. doi:10.1093/bja/aen181.

78. Das A, Gao Z, Menon PP, Hardman JG, Bates DG. A systems engineering approach to validation of a pulmonary physiology simulator for clinical applications. J R Soc Interface. 2011;8:44–55. doi:10.1098/rsif.2010.0224.

79. Hardman JG, Wills JS. The development of hypoxaemia during apnoea in children: a computational modelling investigation. Br J Anaesth. 2006;97:564–70. doi:10.1093/bja/ael178.

80. Hardman JG, Aitkenhead AR. Validation of an Original Mathematical Model of CO2 Elimination and Dead Space Ventilation. Anesth Analg. 2003;97:1840–5. doi:10.1213/01.ANE.0000090315.45491.72.

81. Hardman JG, Bedforth NM. Estimating venous admixture using a physiological simulator. Br J Anaesth. 1999;82:346–9. doi:10.1093/bja/82.3.346.

82. Hardman JG, Aitkenhead AR. Estimation of Alveolar Deadspace Fraction Using Arterial and End-Tidal CO 2 : A Factor Analysis Using a Physiological Simulation. Anaesth Intensive Care. 1999;27:452–8. doi:10.1177/0310057X9902700503.

83. Wang W, Das A, Ali T, Cole O, Chikhani M, Haque M, et al. Can computer simulators accurately represent the pathophysiology of individual COPD patients? Intensive Care Med Exp. 2014;2:23. doi:10.1186/s40635-014-0023-0.

84. Das A, Camporota L, Hardman JG, Bates DG. What links ventilator driving

pressure with survival in the acute respiratory distress syndrome? A computational study. Respir Res. 2019;20. doi:10.1186/s12931-019-0990-5.

85. Marshall BE, Clarke WR, Costarino AT, Chen L, Miller F, Marshall C. The dose-response relationship for hypoxic pulmonary vasoconstriction. Respir Physiol. 1994;96:231–47. doi:10.1016/0034-5687(94)90129-5.

86. Kelman GR, Nunn JF. Nomograms for correction of blood Po2, Pco2, pH, and base excess for time and temperature. J Appl Physiol. 1966;21:1484–90. doi:10.1152/jappl.1966.21.5.1484.

87. Siggaard-Andersen O. The Van Slyke Equation. Scand J Clin Lab Invest. 1977;37:15–20. doi:10.3109/00365517709098927.

88. Crotti S, Mascheroni D, Caironi P, Pelosi P, Ronzoni G, Mondino M, et al. Recruitment and derecruitment during acute respiratory failure: a clinical study. Am J Respir Crit Care Med. 2001;164:131–40. doi:10.1164/ajrccm.164.1.2007011.

89. Kent BD, Mitchell PD, Mcnicholas WT. Hypoxemia in patients with COPD: Cause, effects, and disease progression. Int J COPD. 2011;6:199–208. doi:10.2147/COPD.S10611.

90. Murray CJ, Lopez AD. Alternative projections of mortality and disability by cause 1990–2020: Global Burden of Disease Study. Lancet. 1997;349:1498–504. doi:10.1016/S0140-6736(96)07492-2.

91. World Health Organization. The global burden of disease : 2004 update. 2008.

92. World Health Organization. World health statistics 2008. 2008.

93. Halbert RJ, Natoli JL, Gano A, Badamgarav E, Buist AS, Mannino DM. Global burden of COPD: systematic review and meta-analysis. Eur Respir J. 2006;28:523–32. doi:10.1183/09031936.06.00124605.

94. Mannino DM, Buist AS. Global burden of COPD: risk factors, prevalence, and future trends. Lancet. 2007;370:765–73. doi:10.1016/S0140-6736(07)61380-4.

95. Shujaat A, Bajwa AA, Cury JD. Pulmonary Hypertension Secondary to COPD. Pulm Med. 2012;2012:1–16. doi:10.1155/2012/203952.

96. Chaouat A, Naeije R, Weitzenblum E. Pulmonary hypertension in COPD. Eur Respir J. 2008;32:1371–85. doi:10.1183/09031936.00015608.

97. Barberà JA, Peinado VI, Santos S. Pulmonary hypertension in chronic obstructive pulmonary disease. Eur Respir J. 2003;21:892–905. doi:10.1183/09031936.03.00115402.

98. Boerrigter BG, Bogaard HJ, Trip P, Groepenhoff H, Rietema H, Holverda S, et al. Ventilatory and Cardiocirculatory Exercise Profiles in COPD. Chest. 2012;142:1166–74. doi:10.1378/chest.11-2798.

99. Blanco I, Santos S, Gea J, Güell R, Torres F, Gimeno-Santos E, et al. Sildenafil to improve respiratory rehabilitation outcomes in COPD: a controlled trial. Eur Respir J. 2013;42:982–92. doi:10.1183/09031936.00176312.

100. Rao RS, Singh S, Sharma BB, Agarwal V V, Singh V. Sildenafil improves six-minute walk distance in chronic obstructive pulmonary disease: a randomised, double-blind, placebo-controlled trial. Indian J Chest Dis Allied Sci. 53:81–5.

101. Blanco I, Gimeno E, Munoz PA, Pizarro S, Gistau C, Rodriguez-Roisin R, et al. Hemodynamic and Gas Exchange Effects of Sildenafil in Patients with Chronic Obstructive Pulmonary Disease and Pulmonary Hypertension. Am J Respir Crit Care Med. 2010;181:270–8. doi:10.1164/rccm.200907-0988OC.

102. Holverda S, Rietema H, Bogaard HJ, Westerhof N, Postmus PE, Boonstra A, et al. Acute effects of sildenafil on exercise pulmonary hemodynamics and capacity in patients with COPD. Pulm Pharmacol Ther. 2008;21:558–64. doi:10.1016/j.pupt.2008.01.012.

103. Rietema H, Holverda S, Bogaard HJ, Marcus JT, Smit HJ, Westerhof N, et al. Sildenafil treatment in COPD does not affect stroke volume or exercise capacity. Eur Respir J. 2008;31:759–64. doi:10.1183/09031936.00114207.

104. Alp S, Skrygan M, Schmidt WE, Bastian A. Sildenafil improves hemodynamic parameters in COPD—an investigation of six patients. Pulm Pharmacol Ther. 2006;19:386–90. doi:10.1016/j.pupt.2005.09.006.

105. Stolz D, Rasch H, Linka A, Di Valentino M, Meyer A, Brutsche M, et al. A randomised, controlled trial of bosentan in severe COPD. Eur Respir J. 2008;32:619–28. doi:10.1183/09031936.00011308.

106. Valerio G, Bracciale P, Grazia D'Agostino A. Effect of bosentan upon pulmonary hypertension in chronic obstructive pulmonary disease. Ther Adv Respir Dis. 2009;3:15–21. doi:10.1177/1753465808103499.

107. Vonbank K. Controlled prospective randomised trial on the effects on pulmonary haemodynamics of the ambulatory long term use of nitric oxide and oxygen in patients with severe COPD. Thorax. 2003;58:289–93. doi:10.1136/thorax.58.4.289.

108. Kanniess F, Jörres RA, Magnussen H. Combined inhalation of nitric oxide and oxygen in patients with moderate to severe COPD: Effect on blood gases. Respir Med. 2001;95:927–34. doi:10.1053/rmed.2001.1186.

109. Ashutosh K. Use of nitric oxide inhalation in chronic obstructive pulmonary disease. Thorax. 2000;55:109–13. doi:10.1136/thorax.55.2.109.

110. Germann P, Ziesche R, Leitner C, Roeder G, Urak G, Zimpfer M, et al. Addition of Nitric Oxide to Oxygen Improves Cardiopulmonary Function in Patients With Severe COPD. Chest. 1998;114:29–35. doi:10.1378/chest.114.1.29.

111. Yoshida M, Taguchi O, Gabazza EC, Kobayashi T, Yamakami T, Kobayashi H, et al. Combined inhalation of nitric oxide and oxygen in chronic obstructive pulmonary disease. Am J Respir Crit Care Med. 1997;155:526–9. doi:10.1164/ajrccm.155.2.9032189.

112. Roger N, Barberà JA, Roca J, Rovira I, Gómez FP, Rodriguez-Roisin R. Nitric oxide inhalation during exercise in chronic obstructive pulmonary disease. Am J Respir Crit Care Med. 1997;156 3 I:800–6. doi:10.1164/ajrccm.156.3.9611051.

113. Barberà J., Roger N, Roca J, Rodriguez-Roisin R, Rovira I, Higenbottam T. Worsening of pulmonary gas exchange with nitric oxide inhalation in chronic obstructive pulmonary disease. Lancet. 1996;347:436–40. doi:10.1016/S0140-6736(96)90011-2.

114. Adnot S, Kouyoumdjian C, Defouilloy C, Andrivet P, Sediame S, Herigault R, et al. Hemodynamic and Gas Exchange Responses to Infusion of Acetylcholine and Inhalation of Nitric Oxide in Patients with Chronic Obstructive Lung Disease and Pulmonary Hypertension. Am Rev Respir Dis. 1993;148:310–6. doi:10.1164/ajrccm/148.2.310.

115. Boeck L, Tamm M, Grendelmeier P, Stolz D. Acute Effects of Aerosolized Iloprost in COPD Related Pulmonary Hypertension - A Randomized Controlled Crossover Trial. PLoS One. 2012;7:e52248. doi:10.1371/journal.pone.0052248.

116. Hegewald MJ, Elliott CG. Sustained Improvement With Iloprost in a COPD Patient With Severe Pulmonary Hypertension. Chest. 2009;135:536–7. doi:10.1378/chest.08-1515.

117. Dernaika TA, Beavin M, Kinasewitz GT. Iloprost Improves Gas Exchange and Exercise Tolerance in Patients with Pulmonary Hypertension and Chronic Obstructive Pulmonary Disease. Respiration. 2010;79:377–82. doi:10.1159/000242498.

118. Ghofrani H-A, D'Armini AM, Grimminger F, Hoeper MM, Jansa P, Kim NH, et al. Riociguat for the Treatment of Chronic Thromboembolic Pulmonary Hypertension. N Engl J Med. 2013;369:319–29. doi:10.1056/NEJMoa1209657.

119. Ghofrani H-A, Galiè N, Grimminger F, Grünig E, Humbert M, Jing Z-C, et al. Riociguat for the Treatment of Pulmonary Arterial Hypertension. N Engl J Med. 2013;369:330–40. doi:10.1056/NEJMoa1209655.

120. Ghofrani HA, Staehler G, Grünig E, Halank M, Mitrovic V, Unger S, et al. Acute Effects of Riociguat in Borderline or Manifest Pulmonary Hypertension Associated with Chronic Obstructive Pulmonary Disease. Pulm Circ. 2015;5:296–304. doi:10.1086/680214.

121. Atkins PJ. Dry powder inhalers: an overview. Respir Care. 2005;50:1304–12; discussion 1312. http://www.ncbi.nlm.nih.gov/pubmed/16185366.

122. Wright J. Inhaler devices for the treatment of asthma and chronic obstructive airways disease (COPD). Qual Saf Heal Care. 2002;11:376–82. doi:10.1136/qhc.11.4.376.

123. Druckmann S, Banitt Y, Gidon A, Schürmann F, Markram H, Segev I. A novel multiple objective optimization framework for constraining conductance-based neuron models by experimental data. Front Neurosci. 2007;1:7–18. doi:10.3389/neuro.01.1.1.001.2007.

124. Ho W-H, Chang C-S. Genetic-algorithm-based artificial neural network modeling for platelet transfusion requirements on acute myeloblastic leukemia patients. Expert Syst Appl. 2011;38:6319–23. doi:10.1016/j.eswa.2010.11.110.

125. Goldberg DE. Genetic Algorithms in search, optimization, and machine learning. 1st edition. Boston, MA, USA: Addison-Wesley Longman Publishing Co., Inc.; 1989.

126. Pellegrino R, Sterk PJ, Sont JK, Brusasco V. Assessing the effect of deep inhalation on airway calibre: a novel approach to lung function in bronchial asthma and COPD. Eur Respir J. 1998;12:1219–27. doi:10.1183/0903.1936.98.12051219.

127. Thorpe CW, Salome CM, Berend N, King GG. Modeling airway resistance dynamics after tidal and deep inspirations. J Appl Physiol. 2004;97:1643–53. doi:10.1152/japplphysiol.01300.2003.

128. Mathur RS, Revill SM, Vara DD, Walton R, Morgan MD. Comparison of peak oxygen consumption during cycle and treadmill exercise in severe chronic obstructive pulmonary disease. Thorax. 1995;50:829–33. doi:10.1136/thx.50.8.829.

129. Corriveau ML, Rosen BJ, Dolan GF. Oxygen transport and oxygen consumption during supplemental oxygen administration in patients with chronic obstructive pulmonary disease. Am J Med. 1989;87:633–7. doi:10.1016/S0002-9343(89)80395-X.

130. Cloutier MM. Respiratory Physiology. Mosby; 2007. https://books.google.co.uk/books?id=jRdmQgAACAAJ.

131. Naranjo J. A nomogram for assessment of breathing patterns during treadmill exercise. Br J Sports Med. 2005;39:80–3. doi:10.1136/bjsm.2003.009316.

132. Kovacs G, Olschewski A, Berghold A, Olschewski H. Pulmonary vascular resistances during exercise in normal subjects: a systematic review. Eur Respir J. 2012;39:319–28. doi:10.1183/09031936.00008611.

133. Ashbaugh D, Boyd Bigelow D, Petty T, Levine B. Acute respiratory distress in adults. Lancet. 1967;290:319–23. doi:http://dx.doi.org/10.1016/S0140-6736(67)90168-7.

134. Bernard GR, Artigas A, Brigham KL, Cat-let J, Falke K, Hudson L, et al. Report of the American-European Consensus conference on acute respiratory distress syndrome: definitions, mechanisms, relevant outcomes, and clinical trial coordination. Consensus Committee. J Crit Care. 1994;9:72–81. doi:10.1164/ajrccm.149.3.7509706.

135. ARDS Definition Task Force, Ranieri VM, Rubenfeld GD, Thompson BT, Ferguson ND, Caldwell E, et al. Acute respiratory distress syndrome: the Berlin Definition. JAMA. 2012;307:2526–33. doi:10.1001/jama.2012.5669.

136. Pediatric Acute Respiratory Distress Syndrome: Consensus Recommendations From the Pediatric Acute Lung Injury Consensus Conference. Pediatr Crit Care Med. 2015;:1–12. doi:10.1097/PCC.0000000000000350.

137. Khemani RG, Smith L, Lopez-Fernandez YM, Kwok J, Morzov R, Klein MJ, et al. Paediatric acute respiratory distress syndrome incidence and epidemiology (PARDIE): an international, observational study. Lancet Respir Med. 2019;7:115–28. doi:10.1016/S2213-2600(18)30344-8.

138. De Luca D, Piastra M, Chidini G, Tissieres P, Calderini E, Essouri S, et al. The use

of the Berlin definition for acute respiratory distress syndrome during infancy and early childhood: multicenter evaluation and expert consensus. Intensive Care Med. 2013;39:2083–91. doi:10.1007/s00134-013-3110-x.

139. Kneyber MCJ, de Luca D, Calderini E, Jarreau PH, Javouhey E, Lopez-Herce J, et al. Recommendations for mechanical ventilation of critically ill children from the Paediatric Mechanical Ventilation Consensus Conference (PEMVECC). Intensive Care Med. 2017;43:1764–80.

140. Eichacker PQ, Gerstenberger EP, Banks SM, Cui X, Natanson C. Meta-analysis of acute lung injury and acute respiratory distress syndrome trials testing low tidal volumes. Am J Respir Crit Care Med. 2002;166:1510–4. doi:10.1164/rccm.200208-956OC.

141. Amato MBP, Meade MO, Slutsky AS, Brochard L, Costa ELV, Schoenfeld DA, et al. Driving Pressure and Survival in the Acute Respiratory Distress Syndrome. N Engl J Med. 2015;372:747–55. doi:10.1056/NEJMsa1410639.

142. Gattinoni L, Tonetti T, Cressoni M, Cadringher P, Herrmann P, Moerer O, et al. Ventilator-related causes of lung injury: the mechanical power. Intensive Care Med. 2016;42:1567–75. doi:10.1007/s00134-016-4505-2.

143. Serpa Neto A, Deliberato RO, Johnson AEW, Bos LD, Amorim P, Pereira SM, et al. Mechanical power of ventilation is associated with mortality in critically ill patients: an analysis of patients in two observational cohorts. Intensive Care Med. 2018. doi:10.1007/s00134-018-5375-6.

144. Vasques F, Duscio E, Pasticci I, Romitti F, Vassalli F, Quintel M, et al. Is the mechanical power the final word on ventilator-induced lung injury?—we are not sure. Ann Transl Med. 2018;6:395–395. doi:10.21037/atm.2018.08.17.

145. de Jager P, Burgerhof JGM, van Heerde M, Albers MJIJ, Markhorst DG, Kneyber MCJ. Tidal Volume and Mortality in Mechanically Ventilated Children. Crit Care Med. 2014;42:2461–72. doi:10.1097/CCM.0000000000000546.

146. Albuali WH, Singh RN, Fraser DD, Seabrook JA, Kavanagh BP, Parshuram CS, et al. Have changes in ventilation practice improved outcome in children with acute lung injury?*. Pediatr Crit Care Med. 2007;PAP. doi:10.1097/01.PCC.0000269390.48450.AF.

147. Khemani RG, Conti D, Alonzo TA, Bart RD, Newth CJL. Effect of tidal volume in children with acute hypoxemic respiratory failure. Intensive Care Med. 2009;35:1428–37. doi:10.1007/s00134-009-1527-z.

148. Erickson S, Schibler A, Numa A, Nuthall G, Yung M, Pascoe E, et al. Acute lung injury in pediatric intensive care in Australia and New Zealand–A prospective, multicenter, observational study*. Pediatr Crit Care Med. 2007;PAP:317–23. doi:10.1097/01.PCC.0000269408.64179.FF.

149. Yehya N, Servaes S, Thomas NJ. Characterizing degree of lung injury in pediatric acute respiratory distress syndrome. Crit Care Med. 2015;43:937–46. doi:10.1097/CCM.0000000000000867.

150. Winkler T, Krause A, Kaiser S. Simulation of mechanical respiration using a

multicompartment model for ventilation mechanics and gas exchange. Int J Clin Monit Comput. 1995;12:231–9. doi:10.1007/bf01207204.

151. Yem JS, Tang Y, Turner MJ, Baker AB. Sources of error in noninvasive pulmonary blood flow measurements by partial rebreathing: a computer model study. Anesthesiology. 2003;98:881–7. doi:00000542-200304000-00014 [pii].

152. de Simone G, Devereux RB, Daniels SR, Mureddu G, Roman MJ, Kimball TR, et al. Stroke Volume and Cardiac Output in Normotensive Children and Adults. Circulation. 1997;95.

153. Thorsteinsson A, Jonmarker C, Larsson A, Vilstrup C, Werner O. Functional residual capacity in anesthetized children: Normal values and values in children with cardiac anomalies. Anesthesiology. 1990;73:876–81. doi:10.1097/00000542-199011000-00014.

154. Kirkby J, Stanojevic S, Welsh L, Lum S, Badier M, Beardsmore C, et al. Reference equations for specific airway resistance in children: The Asthma UK initiative. Eur Respir J. 2010;36:622–9.

155. Lentner C. Geigy scientific tables Vol. 5. Basle, Switzerland: CIBA-GEIGY; 1990.

156. Brower RG, Lanken PN, MacIntyre N, Matthay MA, Morris A, Ancukiewicz M, et al. Higher versus lower positive end-expiratory pressures in patients with the acute respiratory distress syndrome. N Engl J Med. 2004;351:327–36. doi:10.1056/NEJMoa032193.

157. Nuckton TJ, Alonso JA, Kallet RH, Daniel BM, Pittet J-F, Eisner MD, et al. Pulmonary Dead-Space Fraction as a Risk Factor for Death in the Acute Respiratory Distress Syndrome. N Engl J Med. 2002;346:1281–6. doi:10.1056/NEJMoa012835.

158. Beitler JR, Thompson BT, Matthay MA, Talmor D, Liu KD, Zhuo H, et al. Estimating Dead-Space Fraction for Secondary Analyses of Acute Respiratory Distress Syndrome Clinical Trials. Crit Care Med. 2015;43:1026–35. doi:10.1097/CCM.0000000000000921.

159. Yehya N, Bhalla AK, Thomas NJ, Khemani RG. Alveolar Dead Space Fraction Discriminates Mortality in Pediatric Acute Respiratory Distress Syndrome. Pediatr Crit Care Med. 2015;17:1. doi:10.1097/PCC.0000000000000613.

160. Cordioli RL, Park M, Costa ELV, Gomes S, Brochard L, Amato MBP, et al. Moderately high frequency ventilation with a conventional ventilator allows reduction of tidal volume without increasing mean airway pressure. Intensive Care Med Exp. 2014;2:13. doi:10.1186/2197-425X-2-13.

161. Protti A, Votta E, Gattinoni L. Which is the most important strain in the pathogenesis of ventilator-induced lung injury. Curr Opin Crit Care. 2014;20:33–8. doi:10.1097/MCC.0000000000000047.

162. Protti A, Maraffi T, Milesi M, Votta E, Santini A, Pugni P, et al. Role of Strain Rate in the Pathogenesis of Ventilator-Induced Lung Edema*. Crit Care Med. 2016;44:e838–45. doi:10.1097/CCM.0000000000001718.

163. García-Prieto E, López-Aguilar J, Parra-Ruiz D, Amado-Rodríguez L, López-Alonso I, Blázquez-Prieto J, et al. Impact of Recruitment on Static and Dynamic Lung Strain in Acute Respiratory Distress Syndrome. Anesthesiology. 2016;124:443–52. doi:10.1097/ALN.0000000000000946.

164. Retamal J, Borges JB, Bruhn A, Feinstein R, Hedenstierna G. Open lung approach ventilation abolishes the negative effects of respiratory rate in experimental lung injury. 2016;60:1131–41.

165. Retamal J, Borges JB, Bruhn A, Cao X, Feinstein R, Hedenstierna G, et al. High respiratory rate is associated with early reduction of lung edema clearance in an experimental model of ARDS. 2016;60:79–92.

166. Zimmerman JJ, Akhtar SR, Caldwell E, Rubenfeld GD. Incidence and Outcomes of Pediatric Acute Lung Injury. Pediatrics. 2009;124:87–95. doi:10.1542/peds.2007-2462.

167. Zhu Y feng, Xu F, Lu X lan, Wang Y, Chen J li, Chao J xin, et al. Mortality and morbidity of acute hypoxemic respiratory failure and acute respiratory distress syndrome in infants and young children. Chin Med J (Engl). 2012;125:2265–71. doi:10.3760/cma.j.issn.0366-6999.2012.13.005.

168. Santschi M, Randolph AG, Rimensberger PC, Jouvet P. Mechanical ventilation strategies in children with acute lung injury: a survey on stated practice pattern*. Pediatr Crit Care Med. 2013;14:e332-7. doi:10.1097/PCC.0b013e31828a89a2.

169. Ward SL, Quinn CM, Valentine SL, Sapru A, Curley MAQ, Willson DF, et al. Poor Adherence to Lung-Protective Mechanical Ventilation in Pediatric Acute Respiratory Distress Syndrome. Pediatr Crit Care Med. 2016;17:917–23. doi:10.1097/PCC.0000000000000903.

170. Laffey JG, Bellani G, Pham T, Fan E, Madotto F, Bajwa EK, et al. Potentially modifiable factors contributing to outcome from acute respiratory distress syndrome: the LUNG SAFE study. Intensive Care Med. 2016;42:1865–76.

171. De Luca D. Personalising care of acute respiratory distress syndrome according to patients' age. Lancet Respir Med. 2019;7:100–1. doi:10.1016/S2213-2600(18)30429-6.

172. Yehya N, Thomas NJ. Disassociating Lung Mechanics and Oxygenation in Pediatric Acute Respiratory Distress Syndrome*. Crit Care Med. 2017;45:1232–9. doi:10.1097/CCM.0000000000002406.

173. Yehya N, Keim G, Thomas NJ. Subtypes of pediatric acute respiratory distress syndrome have different predictors of mortality. Intensive Care Med. 2018;44:1230–9. doi:10.1007/s00134-018-5286-6.

174. Huhle R, Serpa Neto A, Schultz MJ, Gama de Abreu M. Is mechanical power the final word on ventilator-induced lung injury?—no. Ann Transl Med. 2018;6:394–394.

175. Khemani RG, Markovitz BP, Curley MAQ. Characteristics of Children Intubated and Mechanically Ventilated in 16 PICUs. Chest. 2009;136:765–71. doi:10.1378/chest.09-0207.

176. Santschi M, Jouvet P, Leclerc F, Gauvin F, Newth CJL, Carroll CL, et al. Acute lung injury in children: therapeutic practice and feasibility of international clinical trials. Pediatr Crit Care Med. 2010;11:681–9. doi:10.1097/PCC.0b013e3181d904c0.

177. De Durante G, Del Turco M, Rustichini L, Cosimini P, Giunta F, Hudson LD, et al. ARDSNet lower tidal volume ventilatory strategy may generate intrinsic positive end-expiratory pressure in patients with acute respiratory distress syndrome. Am J Respir Crit Care Med. 2002;165:1271–4. doi:10.1164/rccm.2105050.

178. Writing Group for the Alveolar Recruitment for Acute Respiratory Distress Syndrome Trial (ART) Investigators, Cavalcanti AB, Suzumura ÉA, Laranjeira LN, Paisani D de M, Damiani LP, et al. Effect of Lung Recruitment and Titrated Positive End-Expiratory Pressure (PEEP) vs Low PEEP on Mortality in Patients With Acute Respiratory Distress Syndrome: A Randomized Clinical Trial. JAMA. 2017;318:1335–45. doi:10.1001/jama.2017.14171.

179. Meade MO, Cook DJ, Guyatt GH, Slutsky AS, Arabi YM, Cooper DJ, et al. Ventilation Strategy Using Low Tidal Volumes, Recruitment Maneuvers, and High Positive End-Expiratory Pressure for Acute Lung Injury and Acute Respiratory Distress Syndrome. JAMA. 2008;299:637. doi:10.1001/jama.299.6.637.

180. Mercat A, Richard JM, Vielle B. Positive End-Expiratory Pressure Setting in Adults With Acute Lung Injury. 2008;299:646–55.

181. Bellani G, Laffey JG, Pham T, Fan E, Brochard L, Esteban A, et al. Epidemiology, patterns of care, and mortality for patients with acute respiratory distress syndrome in intensive care units in 50 countries. JAMA - J Am Med Assoc. 2016;315:788–800. doi:10.1001/jama.2016.0291.

182. Retamal J, Bugedo G, Larsson A, Bruhn A. High PEEP levels are associated with overdistension and tidal recruitment/derecruitment in ARDS patients. Acta Anaesthesiol Scand. 2015;59:1161–9. doi:10.1111/aas.12563.

183. Cavalcanti AB, Suzumura ÉA, Laranjeira LN, De Moraes Paisani D, Damiani LP, Guimarães HP, et al. Effect of lung recruitment and titrated Positive End-Expiratory Pressure (PEEP) vs low PEEP on mortality in patients with acute respiratory distress syndrome - A randomized clinical trial. JAMA - J Am Med Assoc. 2017;318:1335–45. doi:10.1001/jama.2017.14171.

184. Moraes L, Silva PL, Thompson A, Santos CL, Santos RS, Fernandes MVS, et al. Impact of different tidal volume levels at low mechanical power on ventilator-induced lung injury in rats. Front Physiol. 2018;9 APR:318. doi:10.3389/fphys.2018.00318.

185. Santos RS, Maia L de A, Oliveira M V., Santos CL, Moraes L, Pinto EF, et al. Biologic Impact of Mechanical Power at High and Low Tidal Volumes in Experimental Mild Acute Respiratory Distress Syndrome. Anesthesiology. 2018;128:1193–206. doi:10.1097/ALN.0000000000002143.

186. Network SSG of the EKSNNR. Early CPAP versus Surfactant in Extremely Preterm Infants. N Engl J Med. 2010;362:1970–9. doi:10.1056/NEJMoa0911783.

187. National Neonatal Audit Programme 2017 Annual Report on 2016 data. London; 2017.

188. Groups TB-IA and UKC. Outcomes of Two Trials of Oxygen-Saturation Targets in Preterm Infants. N Engl J Med. 2016;374:749–60. doi:10.1056/NEJMoa1514212.

189. Hagadorn JI, Furey AM, Nghiem T-H, Schmid CH, Phelps DL, Pillers D-AM, et al. Achieved Versus Intended Pulse Oximeter Saturation in Infants Born Less Than 28 Weeks' Gestation: The AVIOx Study. Pediatrics. 2006;118:1574–82. doi:10.1542/peds.2005-0413.

190. Clavieras N, Wysocki M, Coisel Y, Galia F, Conseil M, Chanques G, et al. Prospective randomized crossover study of a new closed-loop control system versus pressure support during weaning from mechanical ventilation. Anesthesiology. 2013;119:631–41. doi:10.1097/ALN.0b013e3182952608.

191. Arnal J-M, Wysocki M, Novotni D, Demory D, Lopez R, Donati S, et al. Safety and efficacy of a fully closed-loop control ventilation (IntelliVent-ASV®) in sedated ICU patients with acute respiratory failure: a prospective randomized crossover study. Intensive Care Med. 2012;38:781–7. doi:10.1007/s00134-012-2548-6.

192. Arnal J-M, Garnero A, Novonti D, Demory D, Ducros L, Berric A, et al. Feasibility study on full closed-loop control ventilation (IntelliVent-ASV™) in ICU patients with acute respiratory failure: a prospective observational comparative study. Crit Care. 2013;17:R196. doi:10.1186/cc12890.

193. Jouvet P, Eddington A, Payen V, Bourdessoule A, Emeriaud G, Lopez Gasco R, et al. A pilot prospective study on closed loop controlled ventilation and oxygenation in ventilated children during the weaning phase. Crit Care. 2012;16:R85. doi:10.1186/cc11343.

194. Thomas NJ, Jouvet P, Willson D. Acute Lung Injury in Children—Kids Really Aren't Just "Little Adults." Pediatr Crit Care Med. 2013;14:429–32. doi:10.1097/PCC.0b013e31827456aa.

195. De Luca D, van Kaam AH, Tingay DG, Courtney SE, Danhaive O, Carnielli VP, et al. The Montreux definition of neonatal ARDS: biological and clinical background behind the description of a new entity. The Lancet Respiratory Medicine. 2017;5:657–66. doi:10.1016/S2213-2600(17)30214-X.

196. Sweet DG, Carnielli V, Greisen G, Hallman M, Ozek E, Plavka R, et al. European Consensus Guidelines on the Management of Respiratory Distress Syndrome - 2016 Update. Neonatology. 2017;111:107–25. doi:10.1159/000448985.

197. Kambarami R, Chidede O, Chirisa M. Neonatal intensive care in a developing country: Outcome and factors associated with mortality. Cent Afr J Med. 2000;46:205–7.

198. Lee A, Cheung YSL, Joynt GM, Leung CCH, Wong W-T, Gomersall CD. Are high nurse workload/staffing ratios associated with decreased survival in critically ill patients? A cohort study. Ann Intensive Care. 2017;7:46. doi:10.1186/s13613-017-0269-2.

199. Drews FA, Musters A, Markham B, Samore MH. Error Producing Conditions in the Intensive Care Unit. Proc Hum Factors Ergon Soc Annu Meet. 2007;51:702–6. doi:10.1177/154193120705101121.

200. Harrison W, Goodman D. Epidemiologic Trends in Neonatal Intensive Care, 2007-2012. JAMA Pediatr. 2015;169:855. doi:10.1001/jamapediatrics.2015.1305.

201. Walther FJ, Siassi B, Ramadan NA, Ananda AK, Wu PY. Pulsed Doppler determinations of cardiac output in neonates: normal standards for clinical use. Pediatrics. 1985;76:829–33. http://www.ncbi.nlm.nih.gov/pubmed/2932675.

202. Gerhardt T, Reifenberg L, Hehre D, Feller R, Bancalari E. Functional residual capacity in normal neonates and children up to 5 years of age determined by a N2washout method. Pediatr Res. 1986;20:668–71.

203. Rudolf AM. The Changes in the Circulation After Birth: Their Importance in Congenital Heart Disease. Circulation. 1970;41:343–59. doi:10.1161/01.CIR.41.2.343.

204. Numa AH, Newth CJ. Anatomic dead space in infants and children. J Appl Physiol. 1996;80:1485–9. doi:10.1152/jappl.1996.80.5.1485.

205. Dassios T, Dixon P, Hickey A, Fouzas S, Greenough A. Physiological and anatomical dead space in mechanically ventilated newborn infants. Pediatr Pulmonol. 2018;53:57–63. doi:10.1002/ppul.23918.

206. Linderkamp O, Zilow EP, Zilow G. The critical hemoglobin value in newborn infants, infants and children. Beitr Infusionsther. 1992;30:235–46; discussion 247-64.

207. Kates EH, Kates JS. Anemia and polycythemia in the newborn. Pediatr Rev. 2007;28:33–4. doi:10.1542/PIR.28-1-33.

208. Rozé JC, Liet JM, Gournay V, Debillon T, Gaultier C. Oxygen cost of breathing and weaning process in newborn infants. Eur Respir J. 1997;10:2583–5. doi:10.1183/09031936.97.10112583.

209. Scopes JW, Ahmed I. Minimal Rates of Oxygen Consumption in Sick and Premature Newborn Infants. Arch Dis Childh. 1966;:407. doi:10.1136/adc.41.218.407.